DIGITAL IMAGE PROCESSING FOR GROUNDWATER IN CARBONATE TERRAIN - A CASE STUDY IN CENTRAL CHHATTISGARH BASIN, M. P., INDIA

A Thesis Submitted
In Partial Fulfilment of the Requirements
for the Degree of

DOCTOR OF PHILOSOPHY

by

CHADA DAKSHINAMURTY

to the

DEPARTMENT OF CIVIL ENGINEERING
INDIAN INSTITUTE OF TECHNOLOGY, KANPUR

JUNE, 1988

DEDICATED

TO

MY PARENTS

7 NOV 1989

CENTRAL LIBRARY
I.I.T. KANPUR
Acc. No. A106222

106222

DEDICATED

TO

MY PARENTS

CERTIFICATE

Certified that the work presented in this thesis entitled "DIGITAL IMAGE PROCESSING FOR GROUNDWATER IN CARBONATE TERRAIN - A CASE STUDY IN CENTRAL CHHATTISGARH BASIN, M.P., INDIA" has been carried out by Shri Chada Dakshinamurty under my supervision and has not been submitted elsewhere for a degree.

June 10, 1988

K.V.G.K.GOKHALE
Professor
Department of Civil Engineering
Indian Institute of Technology
Kanpur - 208016

ACKNOWLEDGEMENTS

The author feels pleasure in expressing his most sincere gratitude to Prof. K.V.G.K. Gokhale of Engineering Geology section, Civil engineering Department for his continued valuable guidance. It was a pleasure to have been associated with him on this research. The author is grateful to Prof. K.K. Rampal of Remote Sensing section for several discussions and suggestions and also appreciates the constant encouragement and suggestions received from Prof. B.C. Raymahashay, Prof. S.Surya Rao and Dr.R.P. Singh.

The author is indebted to Dr.A.K.Roy, Director, and Dr. D.P. Rao, Manager, Water resources division, of India Institute of Remote Sensing, Dehradun for giving valuable suggestions and providing the computer facility, in the initial stages of the work, in their Institute. Special mention has to be given to Prof. Dave, Geology Department Raipur University and Shri G.B.Singh, Director Project No III, Geological Survey of India, Raipur Division for several discussions during the course of the study. The author is thankful to the Director General, GSI for giving the permission to use the aerial photographs. The author appreciates the help of Jaiswal, senior hydrogeologist Groundwater division, Raipur and Shri D.P.Madhuria, senior hydrogeologist, CGWB, Bhopal for providing the facilities for pumptests.

The author is indebted to Prof. M.U. Siddique c the Advanced Centre of Electronic Systems and Prof. S.G Dhande of the CAD centre at IIT, Kanpur for providing th computer facilities. Help received from Shri K.Ananthakrish nan, Research engineer of ACES and A.V.N.S. Prakash Rao c CAD centre is gratefully acknowledged.

Pleasant company and constant help given at variou stages of work by Shri V.Devaraj and Shri M.V.R.L. Murthy n a special mention.

Mr. K. Venugopal, Mr. Doji Samson, Mr. V.Somasekha and Mr.P. Srinivas have been of help during the final stag in arranging the typed material. The author is thankful all of them.

A neat execution of drawings by Shri Verma a photographs by Shri S.N.Shukla deserve much appreciatio Shri M.L. Srivastava and Shri S.D. Dubey both of t Engineering Geology laboratory were helpful at various stag of this work.

DAKSHINAMURTY

CONTENTS

LIST OF FIGURES

LIST OF TABLES

DIGITAL IMAGE PROCESSING FOR GROUNDWATER IN CARBONATE TERRAIN - A CASE STUDY IN CENTRAL CHATTISGARH BASIN, M.P, INDIA

A Thesis Submitted
In Partial Fulfilment of the Requirements
For the Degree of
DOCTOR OF PHILOSOPHY

by
CHADA DAKSHINAMURTY
to the
Department of Civil Engineering
Indian Institute of Technology, Kanpur
June 1988

SYNOPSIS

The topic of the study has been chosen from several considerations. In hard rock areas in India there is a need for systematic investigations for groundwater development. Several of the drought-prone areas are situated in limestone terrain which if properly studied offers a potential source of groundwater. Limestone terrains contain typical features such as fractures, collapsed zones and solution cavities. Remote sensing offers a good scope for the identification and delineation of such features. Although studies on remote sensing for groundwater exploration have been carried out in India during last 10 years, most of them have been based on the visual interpretation of the imageries and the false colour composites that are directly obtained from National Remote Sensing Agency. There is a need for image processing of digital data and selective techniques for further

enhancement of features that are of interest in groundwater exploration. To date, no such attempt has been made on a systematic basis for the carbonate terrains in India.

Thus in the present work, both the aspects are dealt with. Methodology and the sequence of operation for digital image processing are presented. Enhancement techniques such as band ratioing, histogram equalization, and edge enhancement as developed by the author and software for all the steps involved are provided. As a case study for the application of this methodology, central part of the Chhattisgarh basin in Madhya Pradesh has been chosen. This region supplies limestone to the Bhilai steel plant and many other industries. With increasing mining and industrial activity, demand for water has stepped up considerably in recent years. Groundwater is the major source of supply. Regional field mapping has been undertaken by governmental agencies during the last six years. Work on digital image processing and interpretation techniques contained in the study on the basin are reported for the first time. The methodology developed here is applicable to other drought-prone limestone regions such as the formations of Cuddapah and Vindhyan supergroups in India.

The study area covers around 2500 sq.kms. The geological and drainage maps have been prepared on the basis of field work, aerial photographs and processed imageries. In addition, measurements of static water levels for the pre-

monsoon and post-monsoon periods have been made in large number of wells within the period pertaining to the analyzed satellite data, on the basis of which water level contour maps have been prepared. In the terrain delineated for good aquifer zones on the basis of digital image processing in the present work, pumptests were conducted on few selected wells and aquifer parameters were estimated. A few pumptests were also conducted on wells located outside the delineated zones for comparison with the productive aquifers. For making the groundwater picture complete, chemical analyses for limited number of samples of groundwater have been carried out.

The work contained in the thesis is organized into 6 chapters. In chapter 1, the topic has been introduced and the details of the study area are given. The preview of the Chhattisgarh basin with the significant contributions of all earlier workers is presented. The geology and characteristics of limestone and shale members within the study area are given in detail. In chapter 2 mathematical background of image processing techniques along with the methodology are dealt in detail. Several steps are involved in the pre-processing, image enhancement and image classification stages. The pre-processing stage contains all geometric corrections and data transfer for the study area. Conical orthomorphic projection has been used in the present study for geometric corrections as it is appropriate for a country

like India with prominent north-south elongation. Utilizing the line numbers and pixel numbers generated, the study area has been windowed from the tape and processed for further image processing work. The image enhancement includes several enhancement techniques in a sequence. Band ratioing forms the first step to achieve tonal contrast in the valley regions. Stretching forms the next step involving both the linear and selective stretching. The histograms initially plotted over the range of reflectance values (1.0 to 2.5) have been subsequently stretched to the entire medium which has resulted in considerable improvement of the resolution of the area. The lithological differences in limestone and shale members have been clearly brought out. Pseudocolouring technique was used to improve the morphological characteristics of three limestone members. Histogram equalization developed by the author has been used in combination with stretching to enhance vegetational areas that indicate the proximity of groundwater. A 5 by 5 filter as developed in the present work has been used for edge enhancement to clearly bring out the edges of features like sinkholes and collapsed zones within the limestone members. The entire area has been classified on the basis of training sets with the help of Bayes' classifier. All the computational steps involved and the software developed for all these techniques are presented in this chapter.

The lithological identification of the formations

is given in chapter 3. On the basis of image enhancement techniques the area has been classified into three lithological units namely limestone, shale and alluvial tract. Within the limestone tract, three members have been demarcated based on the reflectance values, tonal characteristics and the soluble nature of the members. The details of the characteristics of all these formations relevant to groundwater are provided.

In the fourth chapter, various morphological features, structural details and drainage patterns in the study area along with the land use classification are presented. The study area was classified into three distinct morphological units- upland tract, valley tract and moisture-stress tract. Areas with fractures and solutions features have been delineated using the techniques presented in the previous chapter. The drainage behaviour in the cavernous zones has been worked out. Classification of the study area into land use and land cover types has been carried out and a line printer map has been prepared. The accuracy involved has been justified on the basis of statistical analyses. The groundwater situation in general and the evaluation of the delineated aquifer zones in particular form the theme for chapter 5. The groundwater level contour maps for both pre-monsoon and post-monsoon periods are prepared and the areas of recharge as well as the possible directions of the

groundwater flow in the study area are identified. The cavernous zone in the central part of the area acts as a sink for groundwater flow. Of the productive aquifer zones identified within the three limestone members namely the Nipania, Pendri and Newari members, the Pendri member is identified as the most productive one with the transmissivity (T) at places ranging to 1150 m^2/day. The productive zones in the Newari member registered a maximum T value of 700 m^2/day while the Nipania limestone has a range of 100 to 124 m^2/day for the same. Estimates of T from pumptest data conducted on wells outside the productive zones in all the three limestone members have revealed the T values to be of the order of 50 to 60 m^2/day. The details of the aquifer evaluation of the productive aquifer zones in the study area delineated on the basis of image processing have been presented. The variation of the groundwater quality as related to groundwater flow direction is also discussed in this chapter. The summary of the findings in terms of a comprehensive hydrogeological picture and the applicability of remote sensing for groundwater are presented in chapter 6.

CHAPTER 1

INTRODUCTION

1.1 GENERAL

The central region of the Chhattisgarh basin, chosen for the present work, has been a center of mining activity for the last three decades as it constitutes an important source of supply of dolomitic limestone to the Bhilai steel plant and also limestone for few cement factories. Groundwater is the principal source of water supply. Demand for water has been on the increasing trend with the increasing industrial activity in this region. Although sporadic attempts have been made to develop groundwater at certain chosen locations, no systematic effort has been made to locate favourable zones within this carbonate terrain. The terrain is flat with gently undulating topography. Areas with considerable groundwater storage exist in the region due to the recharge from surface drainage and the formation of solution cavities through selective dissolution of limestone.

In the present work, delineation of such potential aquifer zones has been carried out through digital image processing techniques. To date, digital interpretation of imageries has not been attempted for formations in this

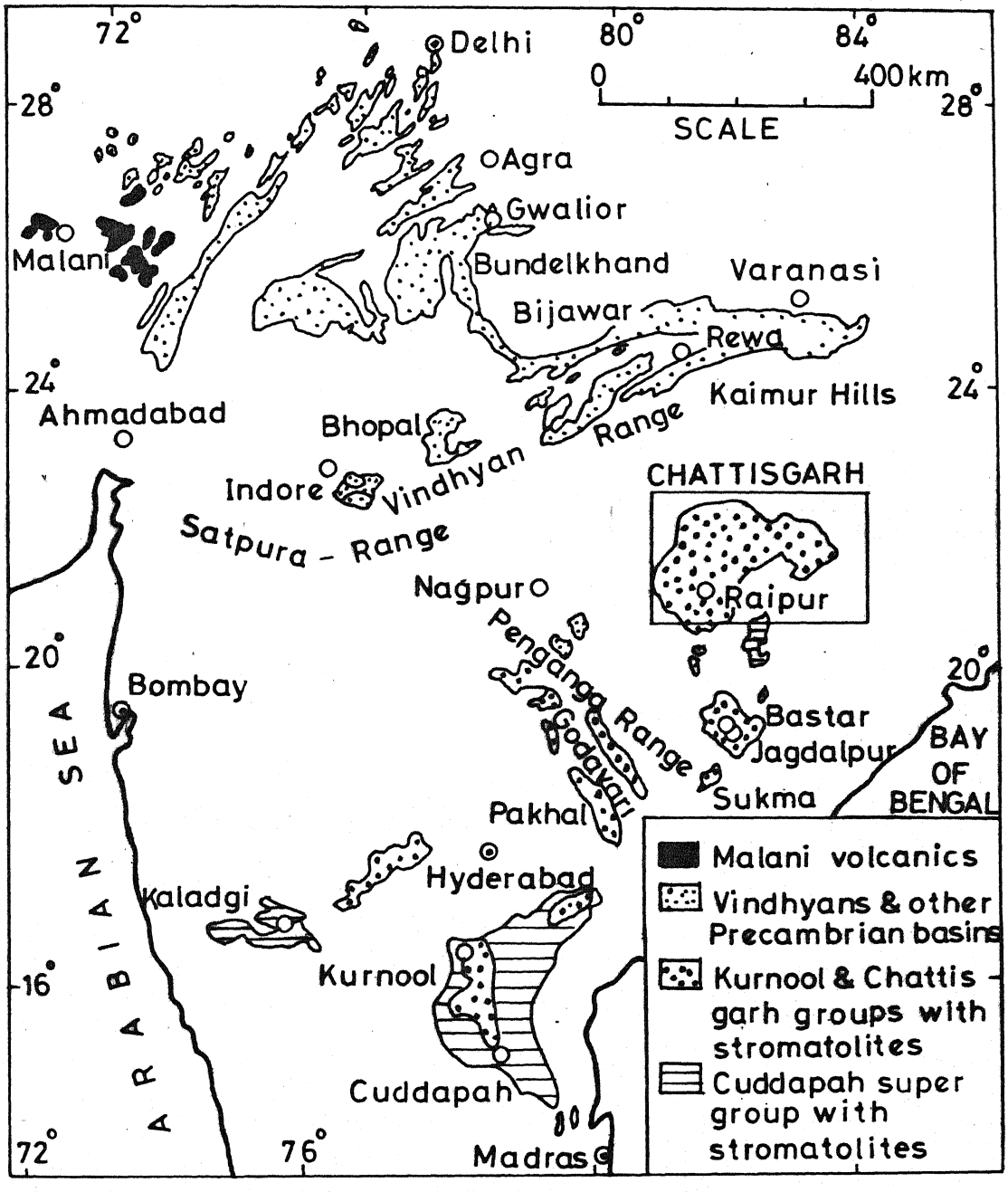

FIG. 1·1 DISTRIBUTION OF PRECAMBRIAN BASINS

region by any of the earlier workers. The author, for the first time, has adopted an approach to the problem of the location of aquifer zones within the carbonate terrain through filtering and edge enhancement techniques. The software used in this work at different stages of operation has been developed during the present study. Systematic pumptests conducted in the delineated zones have confirmed the presence of such potential aquifer zones.

1.2 CHHATTISGARH BASIN -A PREVIEW

1.2.1 General

The Chhattisgarh basin, one of the major sedimentary basins in India, is a crescent shaped intra-cratonic basin. It occupies an area about 33000 sq.kms. between the latitudes 20°30'-22°20'N and longitudes 80°46'-83°46'E, within Durg, Raipur and Bilaspur districts of Madhya Pradesh and adjoining areas in Orissa (Figs.1.1 and 1.2) and has an annual rainfall of 110-132 cms. The climate is tropical with temperatures fluctuating between 11°C and 47.5°C.

The sediments mainly comprise of arenaceous and calcareous sequence attaining a total thickness of 550-600 m and unconformably overlying the Archean basement of granites, gneisses and metasediments. The formations exhibit varying strikes with gentle centripetal dips, except along the western and northern fringes where the basin has faulted margins against metavolcanics and granites. Part of the

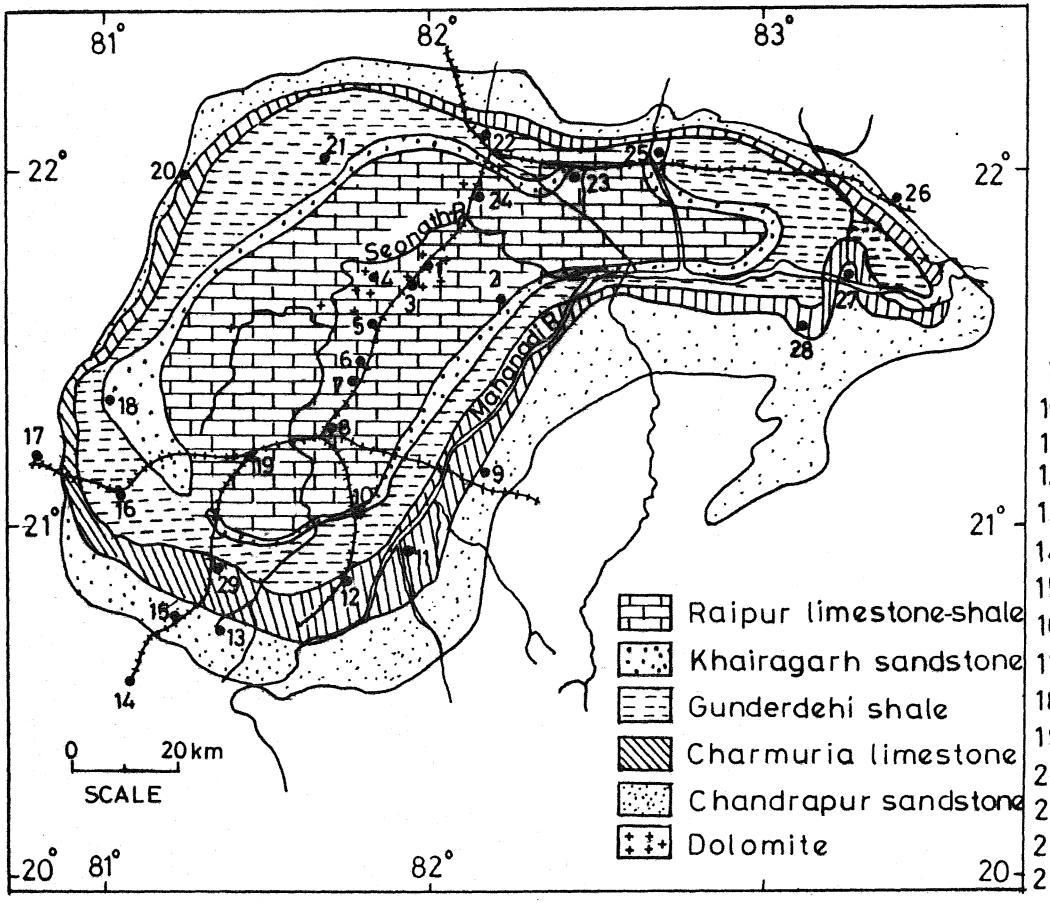

FIG. 1·2 GEOLOGICAL MAP OF CHHATTISGARH BASIN
(AFTER D.G. & M, M.P.)

southern boundary is also gneissic. Outliers of Gondwana formations represented by sandstones with basal conglomerate, occur in the eastern part. These formations are intensely folded and faulted. Disturbances along the northern margin are also evidenced from the occurrence of faulted ridge of Chandarpur sandstone near Karsia. In general, the shales and limestones exhibit flat topography with intermittent sandstone ridges. The southern and southwestern margins of the basin do not exhibit any signs of disturbances.

The earliest reports on the geology of different areas in the basin date back to over a century (Meddlicot, 1867; Blanford, 1870; King, 1885; Ball; 1897, Fermor; 1936). These investigations in general consisted of descriptions of field features and lithology. Due to the paucity of detailed information, the age correlations with other stratigraphic sequences as reported by these authors were not accurate. Pascoe (1950) subdivided the sediments in the basin into two broad categories, the quartzo-conglomeratic Chandarpur series and overlying calcareous, clayey and marly Raipur series, of essentially a shale-limestone sequence, with the Kurnool group and Vindhyan supergroup of formations.

Dutt (1964) on the basis of detailed field mapping in southern part of the basin has reported the first comprehensive stratigraphic succession of Chhattisgarh series (Table 1.1) and also indicated the possibility of correlating the same with sediments of adjoining Kurnool and Bastar

TABLE 1.1

STRATIGRAPHIC SUCCESSION OF CHHATTISGARH BASIN

(After Dutt, 1964)

Raipur Shale - limestone	450 m
Khairagarh sandstone	Variable thickness
Gunderdehi Shale	180 m
Charmuria limestone	300 m
Chandarpur sandstone	300 m

groups. In the study area located in the central part of the Chhattisgarh basin, the formations belong to the Raipur series.

1.2.2 Raipur Series

Schnitzer (1974) has subdivided the Raipur series on the basis of detailed investigations. He has reported the cyclic nature of the sedimentation within the same. The series has been divided into five cycles (Table 1.2). The formations within each cycle have been demarcated on the basis of occurrence of ripple marks and stromatolites as also the Ca and Mg contents of limestones. The formations of the first cycle are well exposed between Sarangarh and Seorinarayan while the second cycle formations occur to the west of this area. The Akaltara-Lilagar region is the type area for third cycle of formation. The area between Raipur and Bilaspur has fourth cycle of formations with the occurrence of fifth cycle of formations in the locations S and SW of Bilaspur.

Based on the oligomictic conglomerate, coarse grained nature of the sandstone and ubiquitous cross-bedding (Fig.1.3) the Chandarpur series underlying the Raipur series have been relegated to beach environment of deposition (Murti,1987). The dominance of limestone and shales in the sequence of Raipur series is an indication of increase the depth of the basin during its deposition. The even lamination

Series	Cycles	Stages	(m)	Lithology
RAIPUR SERIES	5	Maniari	100	
		Hirri-kharkhena	50	D
				Nandhghat
			100	Torwa-D
	4c	Belha	80	Ch D
	4b	Patharia-Umaria	50	Ch
	4a	Nandini	80	L L D
			100	D D L
		Bhatapara	50	L D
	3	Lilagar	50	Shl l
		Akaltara	40	L D
	2	Karuid II	100	SL Shl
			150	SL
		Karuid I	50	SL BL
	1	Seorinarayan	100	Shl
		Sarangarh	30	SL
			50	BL
		Chandarpur quartzite and conglomerate	150	
			200	

L
D
Shl
Ch
SL
BL

TABLE 1·2 CYCLES OF SEDIMENTATION IN CHHATTISGARH BASIN (After Schnitzer, 1976)

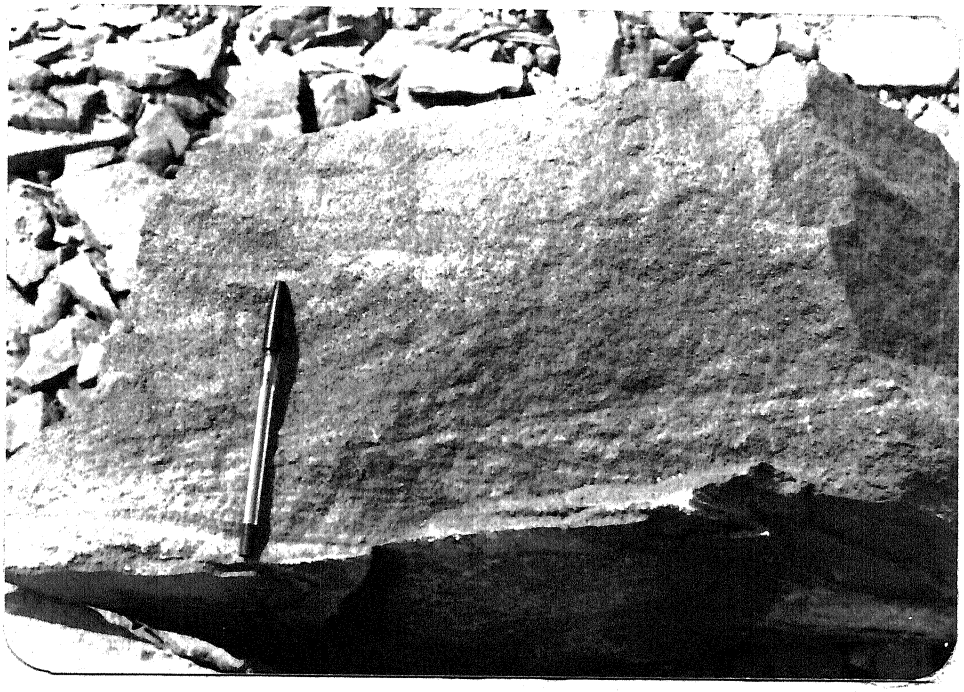

Fig.1.3 Coarse-Grained Sandstone with Cross Bedding

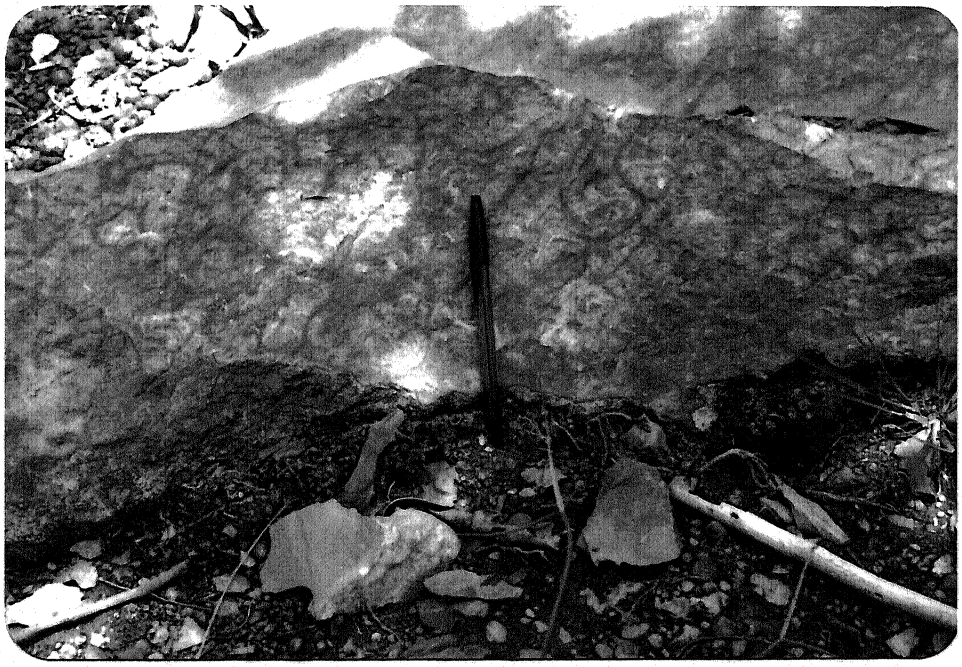

of bedded chert suggests its deposition in quiet water conditions. The existence of fine laminations in the limestone points to the lack of strong currents which is to be expected in a subtidal environment or sheltered lagoon (Murti,1987). According to Murti, the micritic nature, thinness of laminations and general absence of sedimentary structures show that the limestone was formed under quiet water and low-energy conditions below wave base. The overall paucity of clastics is indicative of the peneplain nature for the provenance. Schnitzer (1974) inferred that the formations of Raipur series have been deposited in sub-tidal to tidal environments as each of the cycles starts with limestone and ends with shale. Minor uplift of the landmass by the epirogenic forces possibly released fine mud which ultimately resulted in the formation of shale. Dominance of carbonates in the sequence reflects prevalance of warm temperatures, absence of clastic supply, chemical weathering in the provenance and removal of CO_2 from sea water. Extensive occurrence of dolomites and dolomitic limestones indicates adequate availability of Mg in sea water. The pink shale of Gunderdehi formation shows that it was formed in an oxidizing environment. Dominance of the pink shale (Gunderdehi formation) reflects the humid and warm climate (oxidizing environment) that has prevailed in the region. The frequent interbedding of shale with the Pendri and Nipania limestones

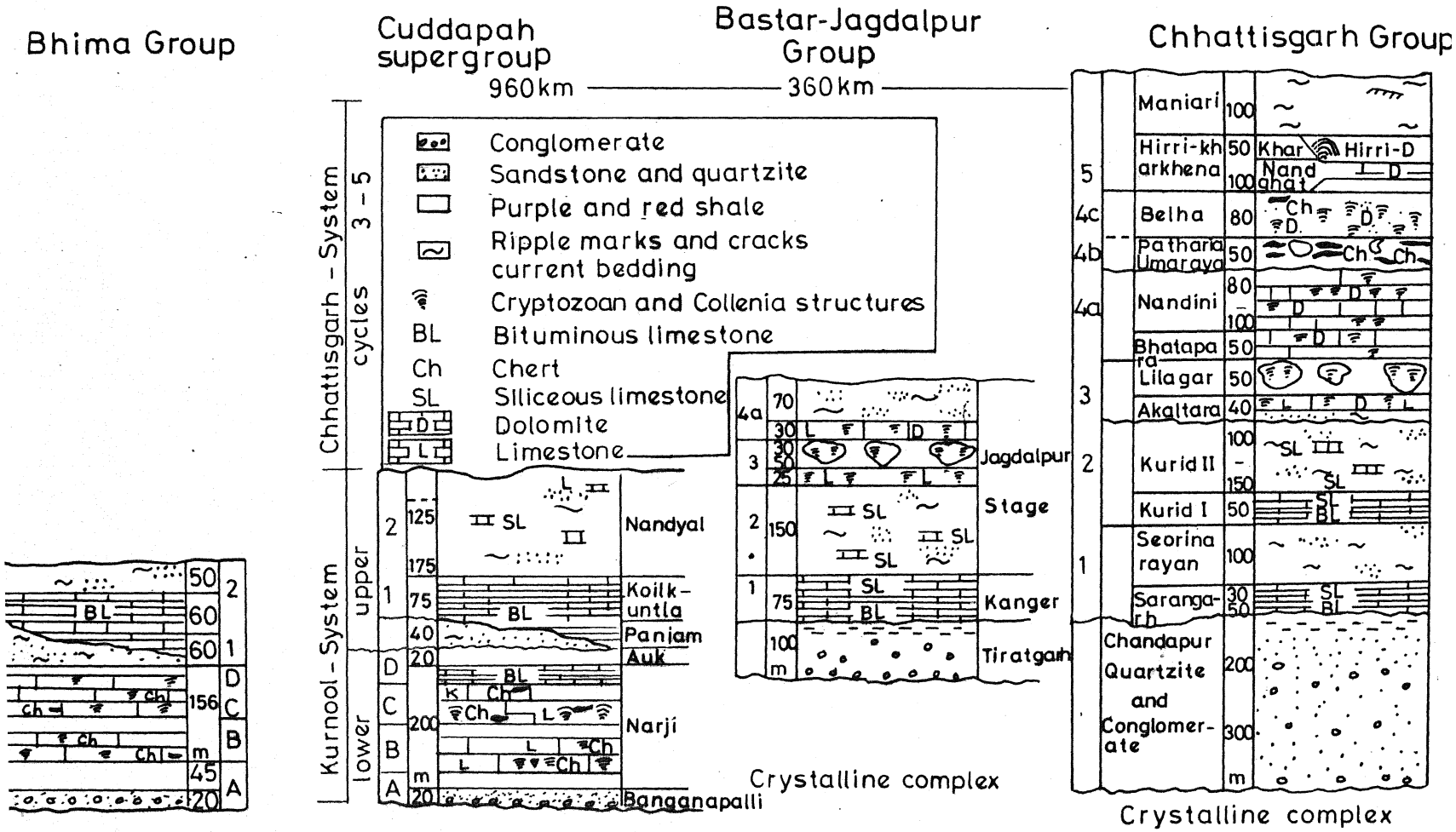

Schnitzer (1971)

Schnitzer (1969a) King (1872) Schnitzer (1969a) Dutt (1962) Schnitzer (1968)

FIG·1·4 REGIONAL CORRELATION ON THE BASIS OF CYCLIC SEDIMENTATION

is of interest. The former is interbedded with olive green shale which is indicative of the deposition in a subtidal or oxygen-poor environment. Olive green and purple shale interbedded with purple limestone of Nipania reveals the nonuniformity of the conditions of the deposition. Purple shale intercalations reflect an oxidizing environment. Further, the basin might have fluctuated between oxidizing and reducing environments in the Nipania times.

The regional correlation of the formations in the northern Chhattisgarh basin with the corresponding ones in Bastar, Jagadalpur and Bhima groups as also with the Kurnool group of the Cuddapah supergroup is presented in Fig.1.4. Murti (1987) considered the formations in the Chhattisgarh basin to be equivalent to the formations of Rewa and Bhander series of Vindhyan supergroup (Table 1.3). Murti has given a comprehensive correlation of the stratigraphy of the entire chhattisgarh basin (Fig.1.5). The dominance in the eastern and western margins of the basin with shale-limestone sequence in the central and southern regions is indicative of shallow nature of the basin towards the margins. The dominance of sandstone in the eastern and western margins of the basin with shale-limestone sequence in the central and southern regions is indicative of shallow nature of the basin towards the margins.

Estimation of the age of the formations in the Chhattisgarh basin has been carried out by several workers.

STRATIGRAPHIC CORRELATION OF THE KURNOOL, CHHATTISGARH GROUPS AND VINDHYAN SUPERGROUP

Kurnool group	Chhattisgarh group	Vindhyan supergroup
	5	Upper Vindhyan Succession: Bhander series: Upper Bhander Sandstones; Sirbu Shales; Lower Bhander Sandstones; Bhander Limestone (Nagode); Ganurgarh Shales
	Cycles 4c	
	4b	
	4a	
	Cycles	
	3	Diamond-bearing Conglomerate
	Cycles 1+2	Rewa series: Upper Rewa Sandstones; Jhiri Shales; Lower Rewa Sandstones; Panna Shales
Kundair	Chandarpur Series	
Paniam	700 - 750 m.y.	Diamond-bearing Conglomerate
D Jammalamadugu		Kaimur Series Upper: Dandhraul Quartzite; Scarp Sandstone & Conglomerate 890 ± 40 m.y.
C		
B		Kaimur Series Lower: Bijaigarh Shales; Upper Quartzites and Sandstones; Susnai Breccia; Lower Quartzites and Shales
A Banganapalle		
Cuddapah System		Lower Vindhyans: Semri Series mainly calcareous 1080 ± 40 m.y.
1500 - 1100 m.y.		

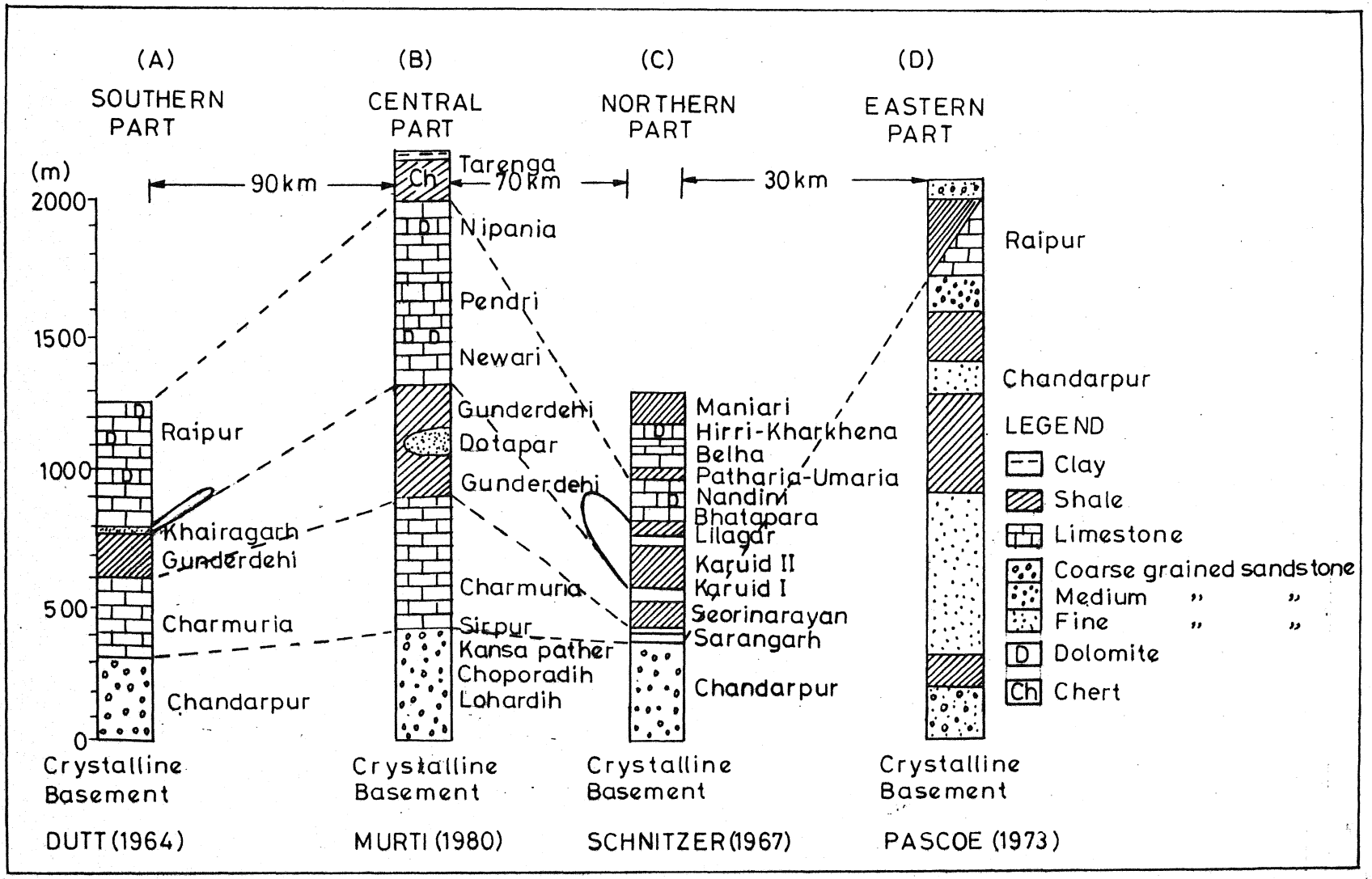

FIG. 1·5 STRATIGRAPHIC CORRELATION IN THE CHHATTISGARH BASIN

While Dutt (1964) reported the sediment to be younger than 1400 m.y, Schnitzer (1971) estimated the age to be between 1000-600 m.y. Sarkar (1972) conceived the Chhattisgarh sediments to be younger than 600 m.y. Krenzer and co-workers (1977) assigned 700-750 m.y. for Chandarpur sandstone on the basis of K-Ar dating of the authigenic glauconite. Verma and co-workers (1977) on the basis of paleomagnetic studies have concluded that the pole position for pink shale of Gunderdehi is intermediate between Rewa and Cuddapah sandstones. Since the age of Rewa formations is reported to be 800-900 m.y (Crawford,1960) and that of Cuddapah is 1220-1600 m.y (Crawford and Compston,1973), the age of Gunderdehi formation on the basis of pole position is likely to be close to 1250-1300 m.y.

1.2.3 Drainage

The drainage network in the basin is a part of the Mahanadi system. The Mahanadi river has its course from SW to NE and drains through northeastern part of the basin (Fig.1.2). Several of its tributaries, ephemeral and perennial in nature, drain across the basin. The prominent one is the Seonath river which is a result of the confluence of Tandula and Kharun in the central part of the basin. The Jamunia river joins Seonath at Rajpur. Contribution of surface drainage to groundwater is significant in limestone terrain in the study area.

1.3 GEOLOGICAL SETUP OF THE STUDY AREA

1.3.1 General

Present work covers an area of around 2500 sq.kms. within the Raipur, Baloda Bazar, and Bilaspur districts in the central part of the basin. The formations in the study area (Fig.1.6) pertain to Raipur series. Only members belonging to the Chandi and Tarenga groups are present. These formations correspond to the 3rd and 4th cycles in the sequence (Schnitzer, 1969). The stratigraphic succession and the geological map for the same are presented the Table 1.4 and Fig.1.6 respectively.

The Raipur group of sediments overlies the Chandarpur group with an erosional disconformity. The disconformable nature of the contact is very clear between Birkoni and Tumgaon, where limestone has been deposited on the eroded surface of the sandstone.

1.3.2 Chandi Formation

The Gunderdehi formation is succeeded conformably by Chandi formation (comprising limestone members) with gradational contact. The formation is characterized by prolific growth of stromatolites (Fig.1.7) occurring as extensive reef complexes in the area. Within the Chandi formation, sandstone pockets of localized occurrence have been reported by Dutt(1964). This sandstone, designated as Raipur sandstone at the base of Akaltara limestone sequence,

Chhattisgarh Group	Raipur Series	Tarenga Formation (+180m)		Pink and Purp shale
		Chandi Formation (670m)	Nipania Member (300m)	Purple limestone
			Pendri Member (215m)	Grey limestone
			Newari Member (155m)	Pink limestone

TABLE 1·4 STRATIGRAPHIC SUCCESSION OF THE STUDY AREA

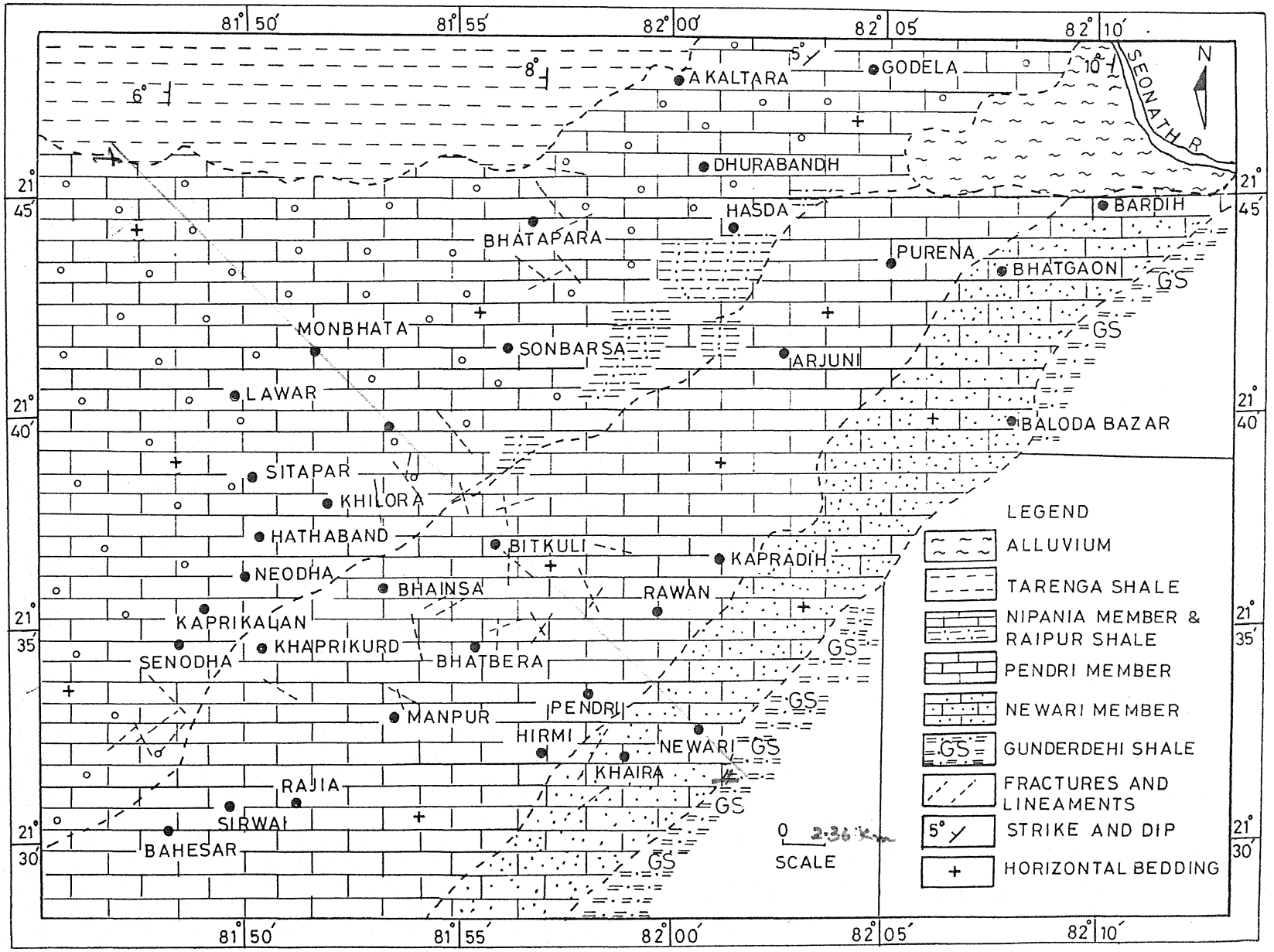

FIG·1·6 GEOLOGICAL MAP OF THE STUDY AREA

exhibits cross bedding with reversal of current directions (Fig.1.8), indicative of an agitated environment. The Chandi formation can be broadly divided into three members (1) Newari (2) Pendri and (3) Nipania on the basis of lithological considerations.

1.3.2.1 Newari Member

The pink and purple coloured medium-grained limestone representing the Newari member conformably overlies the Gunderdehi formation with a gradational contact. In the vicinity of its contact with shale, the limestone is friable. Dolomitization is noticed along the joints within the same. Except in its proximity to the Gunderdehi formation, this limestone member is very massive and compact with indistinct bedding. Stromatolites and stylolites are quite common. The stromatolite columns are separated by calcareous mud and stand out prominently on weathering.

1.3.2.2 Pendri Member

The limestone member is gray in colour, fine-grained and is stromatolitic. The limestone is characterized by frequent lithological variation to a greenish flaggy type and often with intercalations of shale. There is preferential dolomitization in this algal limestone. Stromatolites tend to be stunted, show branching and are ill-preserved because of the extremely fine lamination. The Pendri member corresponds to Bhatapara limestone of Schnitzer(1969).

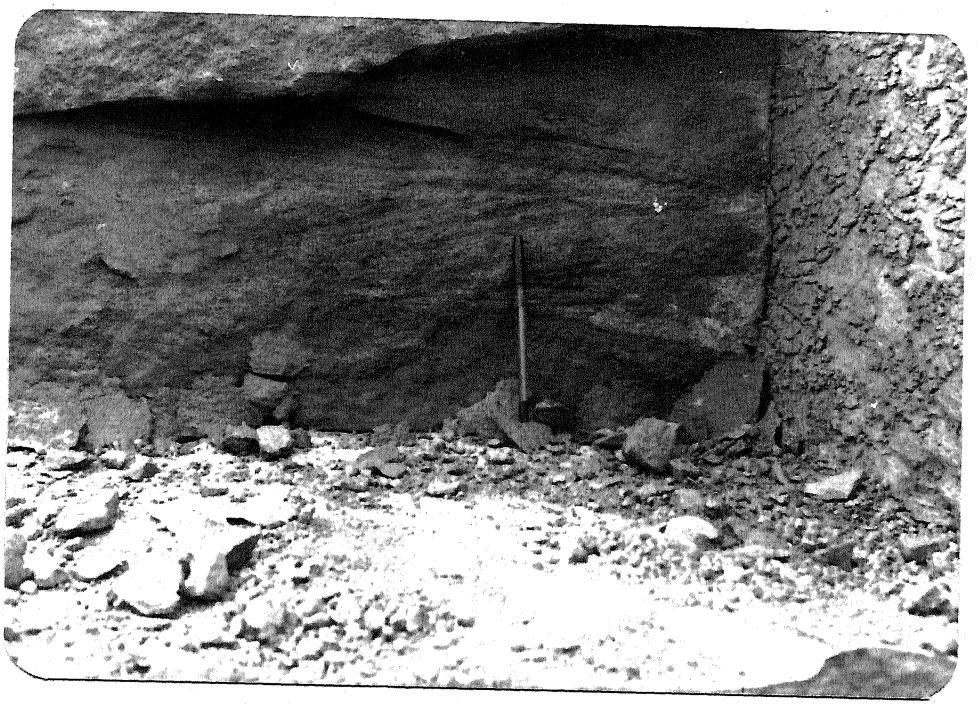

Fig.1.8 Reversal of current directions in the Raipur Sandstone

0 30 Cms

Fig.1.10 Surface feature of a sinkhole

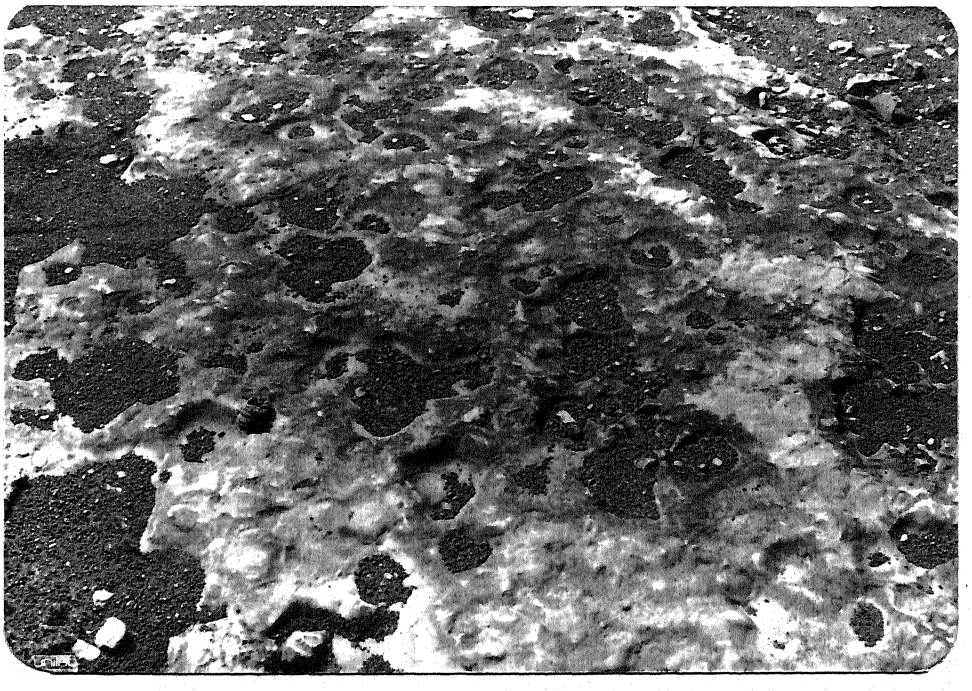

0 30 Cms

1.3.2.3 Nipania Member

Coarse to medium grained, this limestone member is purple with mottled appearance on the surface. Stromatolites with variety of species are abundant in the limestone. This member corresponds to Nandini limestone of Schnitzer (1969). The nature of stromatolites reveals the depositional conditions. The random orientation of the individual colonies of stromatolites is indicative of an agitational environment. Presence of coarser laminae in the stromatolites (Fig.1.9) further confirms such an inference. The gradation of the stromatolites to finer laminae in the sequence is indicative of transition to a relatively quiet depositional environment.

The members of the Chandi formation exhibit typical karst topography in the field. Differential weathering and structure has controlled the development of the landforms in the area. The collapsed zones (Fig.1.10) on the surface in the field reveal the presence of sinkholes underneath. Karst morphology (Fig.1.11) has a typical appearance of its own with a very thin and remarkably smooth patina of siliceous material on the karstic surface resulting in a relict fossil appearance on the karstic surface.

Karstification is structurally controlled. On the surface of an extensively exposed bed of limestone as in Kesili area, initially the swallow holes (Figs.1.12 and 1.13) that have resulted from solution phenomena have rapidly coalesced giving rise to small channels which expand deeper

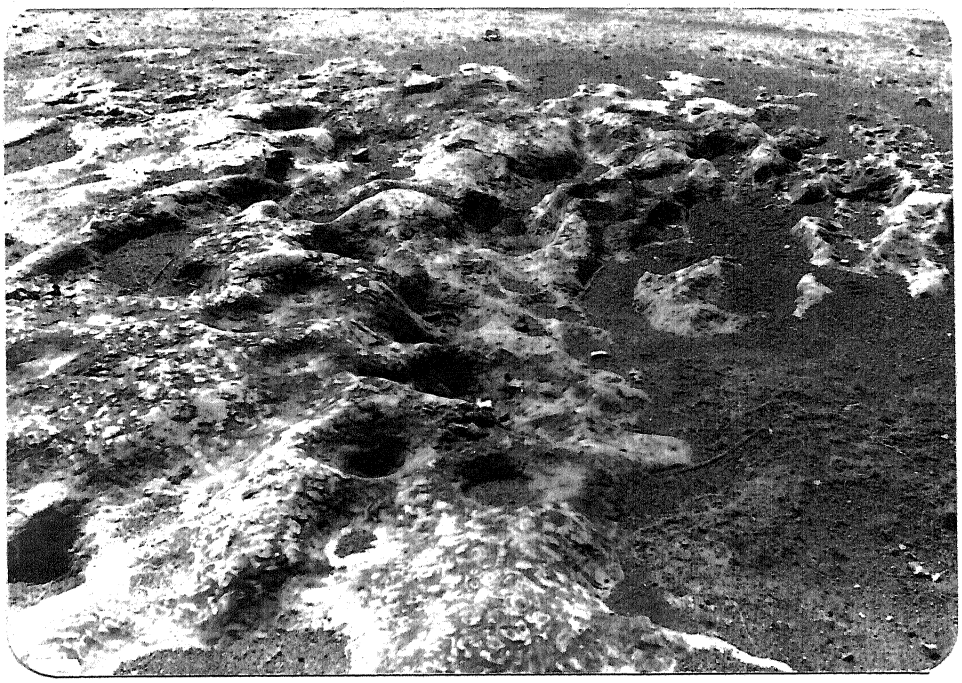

Fig.1.12 Swallow holes of Pendri limestone

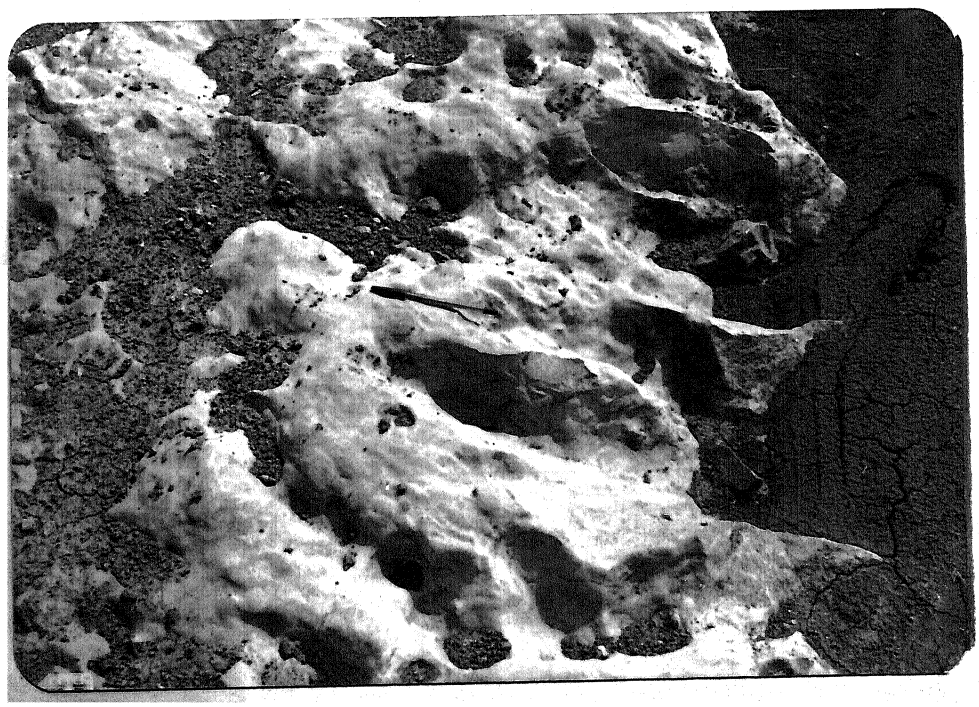

Fig.1.14 Channelised clints in Nipania limestone

Fig.1.15 Solution cavities in Pendri limestone on the banks of Jamunia river

to form clints (Fig.1.14). In the Raipur stromatolitic limestone (Fig.1.9), karstification is developed along the contacts between the individual stromatolites as also along the contact of stromatolite with cement material, justifying thereby more prominent vertical karstification. Solution cavities (Fig.1.15) are also noticed along the banks of rivers Jamunia and Seonath. Typical karst landforms are noticed in the study area in different forms, such as the sinkholes, lapies (Figs.1.16 and 1.17) and caverns (Fig.1.18). The sinkholes occur in different sizes with the depression varying between 0.5m and 8m . Sinkholes noticed in the study area are formed due to down-hole reaction. Widespread outcrops of limestone occur having lapies with characteristic rugged, grooved, pitted, faulted and etched surface as around the Nawapara and Kesili villages. Cavities of different shapes and sizes are common along the banks of Jamunia (Fig.1.15) and these act as conduits for groundwater movement.

1.3.3 Tarenga Formation

This formation is represented by a pink shale with interbedded chert. In the field, the occurrence of intraformational conglomerate is observed around Tarenga village. This formation corresponds to Patharia Umaria series of Schnitzer(1969).

Fig.1.16 Karst landform-Lapies in Pendri limestone

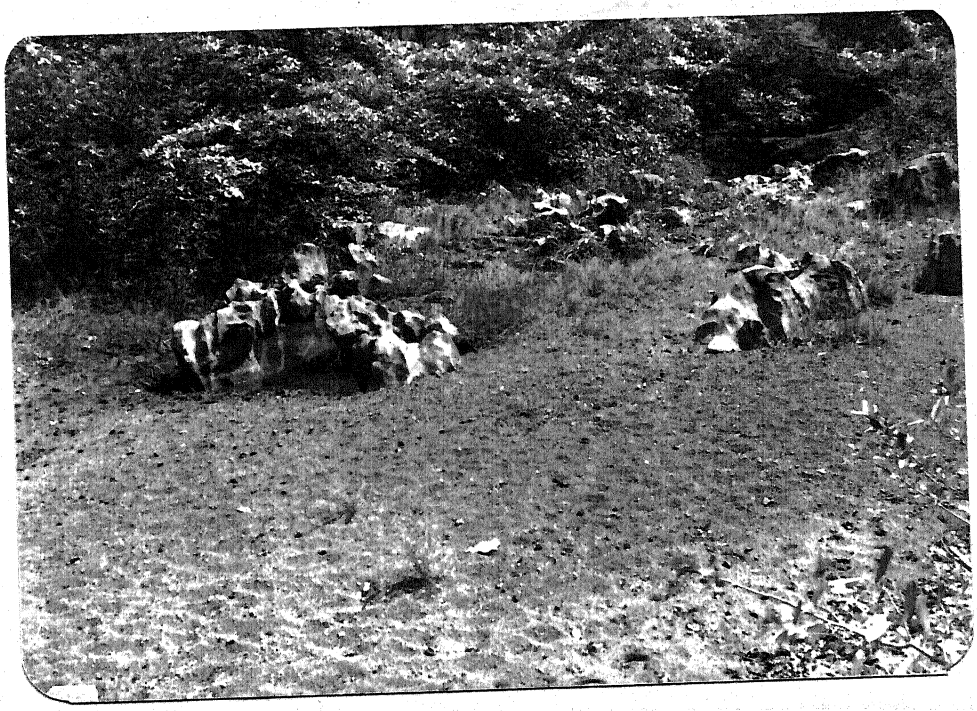

Fig.1.17 Karst landform-Lapies in Newari limestone

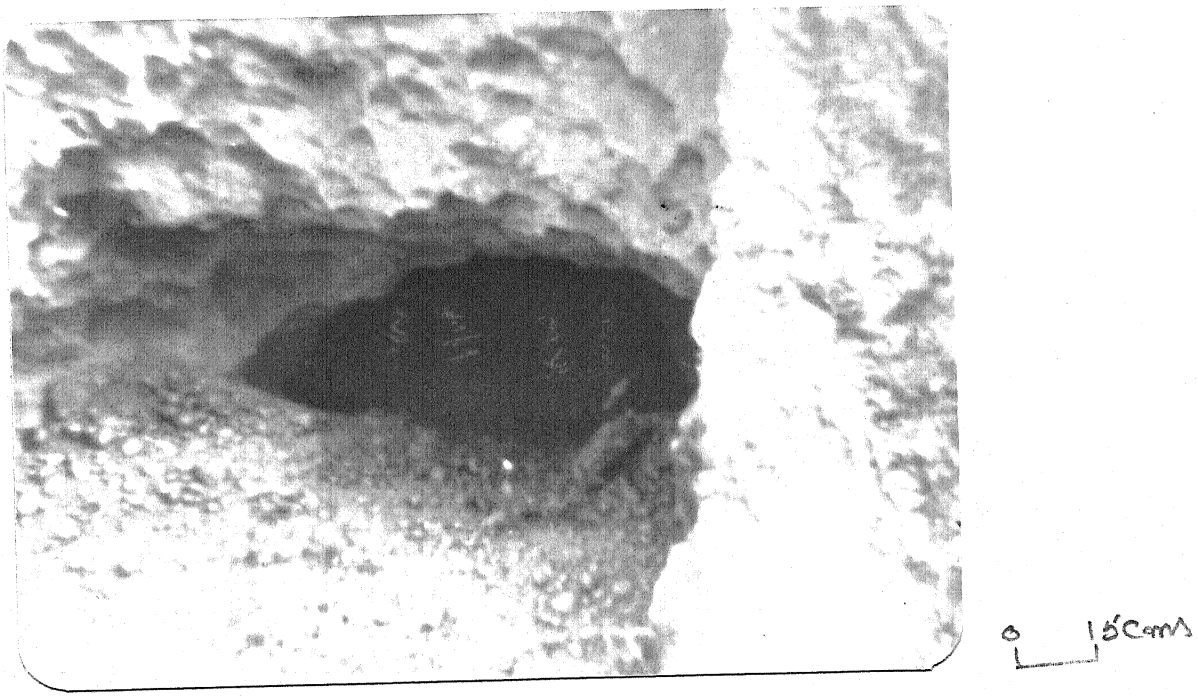

Fig.1.18 Solution channels in Newari limestone

1.3.4 Hydrogeology

The karstic limestones in the present area constitute potential aquifers. Although the limestone by itself possesses negligible primary porosity, with hardly any permeability when fresh and thus making it to be very poor aquifer. Karstification due to potential dissolution with water has rendered the same into permeable complex having interconnected simple or complex conduit systems which facilitate free movement of groundwater in both confined and unconfined conditions. On the basis of field investigations in the shallow unconfined groundwater body of Raipur limestones, the open wells of moderate diameter with well developed cavities and interconnected conduit flow are capable of yielding 500-1000 m_3/day with drawdown of 5 to 8 m. In such zones the individual wells have a specific capacity of 100 to 300 lpm/m of drawdown and the cavernous aquifers with specific yield of 5 to 15 percent and hydraulic conductivity of 5 to 14 m/d.

Published work on the hydrogeological and the aquifer characteristics of the Raipur limestone is scant in literature. Adyalkar and co-workers (1975) have reported the values of transmissivity (T) to be between 40 m^2/day and 600 m^2 while permeability variations are in the range of 0.9 m/day to 5 m/day. Chowdhary (1973) has discussed in general the ground water provenances in Madhya Pradesh. However, no published reports are available on the aquifer

characteristics and the well performance in the different formations in the Chhattisgarh basin.

1.4 SCOPE OF THE PRESENT STUDY AND ITS ORGANIZATION

Digital image processing of satellite data plays an important role in the groundwater exploration and development in carbonate terrains. In India, as evident from scanty published literature, no attempt has been made for detailed study in this direction. The work reported herein deals with the development of the methodology and related software for identification of collapsed and cavernous zones and also sinkhole-prone areas that are potential zones of groundwater storage within carbonate terrain. The region from the central part of the Chhattisgarh basin is chosen as a case study for investigations. The demand for groundwater is ever increasing in this area with increase in mining and industrial activity. There is a need for systematic location of potential aquifer zones in the limestone terrain in this region and no work has been undertaken so far in this direction. Thus, the present study, an attempt for the first time in India, is undertaken to evolve suitable methodology and software for digital image processing for use in location of aquifer zones in carbonate terrain. Inferences arrived at, on the basis of digital image interpretation, in the study area have been confirmed by extensive ground checks through detailed field work.

The material contained in the thesis is organized

and presented under several chapters. In chapter 1, the topic is introduced with review of existing information pertaining to the Chhattisgarh basin in general and the study area in particular. The scope of the present study also outlined. In chapter 2, the methodology adopted in the present study is detailed with all the relevant mathematical background. Edge enhancement techniques developed in the present work are presented in detail. In chapter 3, the lithological identification within the limestone members and shale through enhancement techniques have been described. The morphology, structural features of limestone and their role in the formation of the caverns and collapsed zones together with the classification results of various landuse are given in chapter 4. Chapter 5 deals with the groundwater situation in general and the evaluation of the cavernous limestone aquifers in particular. In this chapter, analyses of the time-drawdown and time-recovery data for the pumptests conducted in the productive areas delineated on the basis of image processing interpretation are presented. The aquifer parameters of the limestone aquifers in the study area are estimated. Summary and conclusions are presented in chapter 6.

CHAPTER 2

IMAGE PROCESSING TECHNIQUES FOR HYDROGEOLOGIC INVESTIGATIONS

2.1 GENERAL

Remote sensing is the use of reflected and emitted energy to measure the physical properties of distant objects and their surroundings. The sensors in the range 0.4μm-1.1μm of the electromagnetic spectrum (Fig.2.1) are considered here.

Photographic sensors still remain the primary tool of hydrogeologists. Black and white aerial photography is used to determine some of the parameters such as boundaries of the rock types and drainage pattern. Thermal sensors (8-14μm) have been used for several hydrological studies in the past. Stephenson (1971) and Coker (1970) are two of many who found thermal imagery as a valuable tool in geohydrological studies, particularly with respect to the groundwater movement.

In the present work, multispectral data have been used to delineate sinkholes and fracture zones which act as avenues for groundwater in carbonate rocks. Recourse has also been taken to aerial photographs for checking the drainage and moisture-saturation zones. Robinove (1965, 1966, 1968) has periodically reported the progress of remote sensing in the field of hydrology and hydrogeology. His evaluation of

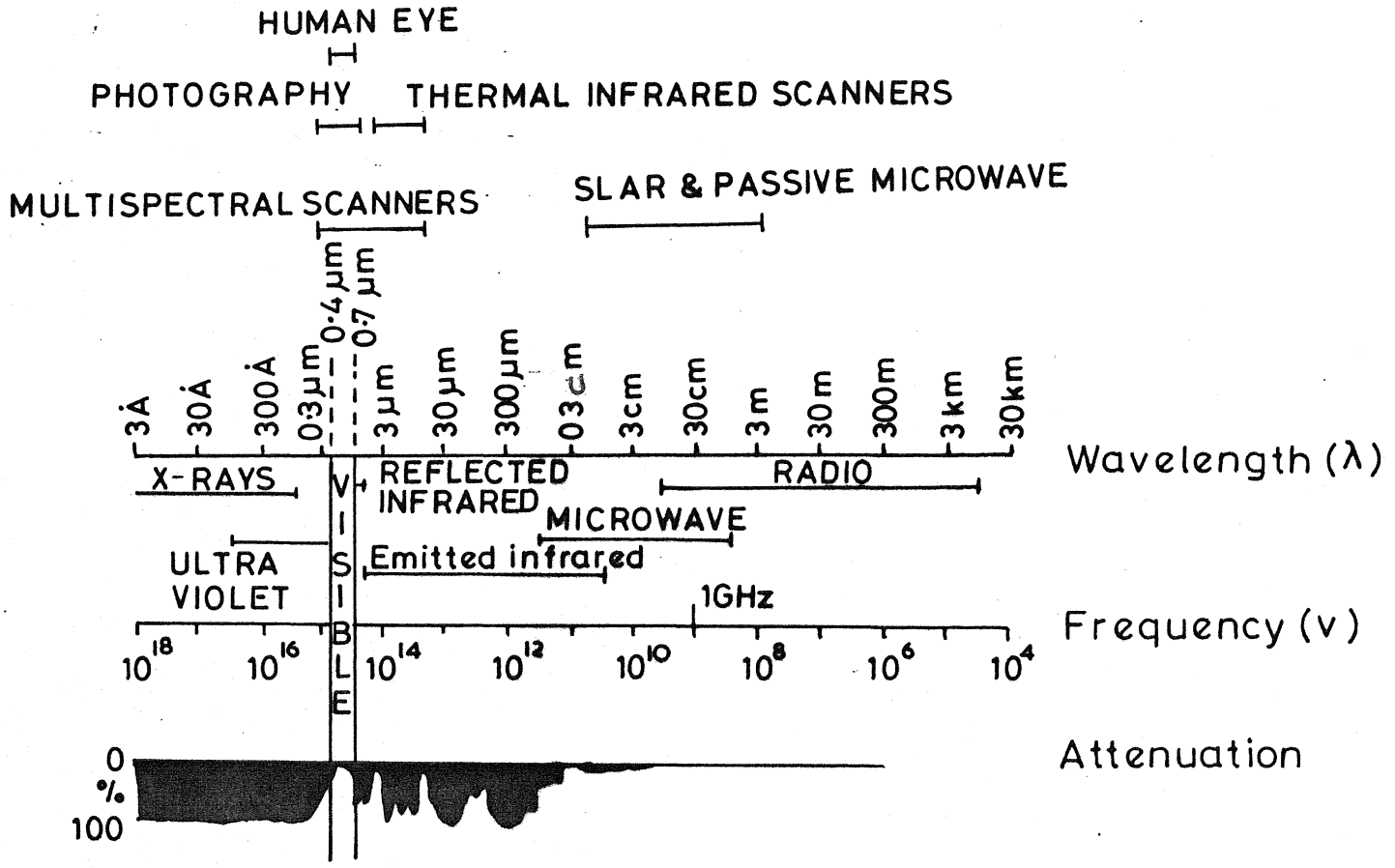

FIG. 2·1 ELECTROMAGNETIC SPECTRUM

remote sensors as hydrologic tools is presented in Appendix-I

Information derived from these techniques is valuable in the study of carbonate terrains. Moreover, because large areas can be examined in a very short period of time, remote sensing technology can be viewed as a time saving tool.

LaMoreaux and Wilson (1980) have reported the following uses of multispectral data connected with hydrological studies in carbonate terrains:

1.Inventory of sinkholes.

2.Monitoring the sinkhole development.

3.Mapping sinkhole alignments.

4.Investigating the relationship among the sinkhole development, fracture traces, lineaments, and groundwater.

5.Delineating collapsed zones.

6.Mapping the surface karst springs.

7.Locating potential water well sites.

8.Mapping the regional geological structures.

Moore (1980) has presented the various steps involved in the aquifer mapping using remote sensors. Details of the same are provided in the Appendix-II.

In India, studies on remote sensing have been reported since last 10 years covering agriculture, forestry, land use and mineral surveys. However, the work pertaining to groundwater investigations was limited and largely based on the visual interpretation of imageries. Santosh Kumar and

Tiruvengadachari (1981) have presented an integrated approach for groundwater studies in parts of central and southern India on the basis of geomorphology and hydrology information in relation to groundwater occurrence and movement. Chaturvedi and co-workers (1983) have evaluated the groundwater potential for the terrain in the Bundelkhand region of Uttar Pradesh based on Landsat imageries. Tillaigovindarajan et.al (1983) have evaluated the hydrogeological conditions in the Madurai, Tirunelvelli, Ramanathapuram and Kanya Kumari districts of Tamil Nadu. The hydrogeological and lineament maps were prepared on the basis of the Landsat imageries (bands 4,5,6, and 7) and false colour composites. Studies have also been reported on the application of Landsat imageries for groundwater exploration in the state of Gujarat (Baldev Sahai and co-workers,1983). The hydrogeological maps for the semi-arid hard rock region have been presented using Landsat imageries. Balakrishnan (1986) reported in detail the different aspects of the water resources development and management and has presented a summary of work done through remote sensing. As already indicated, in all these cases visual interpretation of imageries has been reported. Working with Landsat and M^2S in the Tirupati area of Andhra Pradesh. for the groundwater exploration, Sharma and co-workers (1985) have concluded that the band ratio images of Landsat and M^2S as well as density-

sliced and thermal pictures have better interpretation capabilities over the other remote sensing formats. They have delineated level-I and level-II land use and land cover categories for the Tirupati region. Rampal (1985) has given procedures for estimation of water table depths using digital reflectance data. Data for Kanpur region was used for classification in terms of the groundwater table depth and land use. A line printer map was also presented. During the last 5 years in India, efforts are concentrated on the study of groundwater conditions in limestone terrains, since initial invesigations have indicated a good potential for the same in extensive carbonate terrains particularly in the drought-prone areas in various states. No work has been reported to date in India on the digital image processing for aquifer delineation in limestones.

It is easily seen from the material presented above that there is a wide scope for remote sensing applications in hydrogeology. In order to be able to utilize or even propose a proper remote sensing system as a hydrogeological tool, one has to not only have a complete understanding of the physics of the electromagnetic spectrum but also of its interaction with hydrologic features. The ultimate objective of this study is to explore the use of remote sensing system to identify the source areas.

2.2 ACQUISITION OF REMOTE SENSING DATA

Space remote sensing began in earnest during the

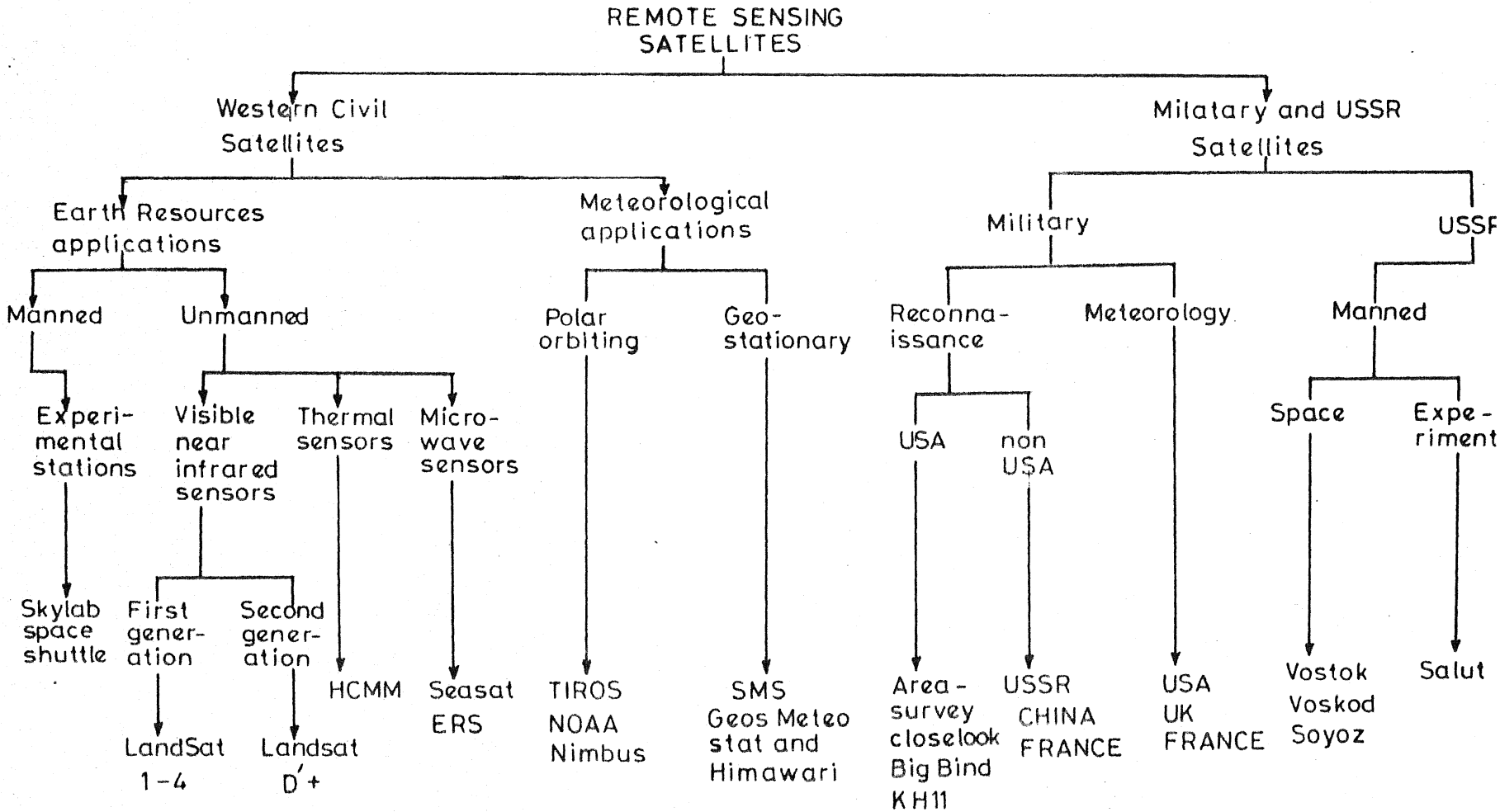

FIG. 2·2 TAXONOMY OF REMOTE SENSING SATELLITES

period 1946 to 1950. The taxonomy of remote sensing satellites is shown in Fig.2.1. On July 23 of 1972, NASA launched Earth Resources Satellite (ERTS), which produced moderately high resolution imagery of the cloud-free Earth. Just prior to the launch of ERTS-B on January 25 in 1975, the ERTS program has been officially redesignated by NASA as the "Landsat Program".

In the present work, data from Landsat-4 have been used. The Landsat-4 moving in a Sun-synchronous orbit at an altitude of 705 kms with 16 days repetitive coverage having a field of view of 14.93° carries a four channel multispectral scanner and Thematic Mapper. On the NASA Landsat-4 coverage index map, the study area is located by path number and row number as 142-045. The Landsat data corresponding to the aforesaid scene was obtained in the form of CCT (1600 BPI) containing reflectance values.

2.2.1 Multispectral Scanner System (MSS)

The multispectral scanner system records four images for a scene in green, red and two near-infrared wavelength bands (Table.2.1) which are identified by the channels they occupied in the satellite telemetry system as 1,2,3 and 4. Each frame of the imagery covers an area of about 185 by 185 sq.km. on a scale of 1:1000,000 and has a ground resolution of 79m by 79m. Due to the 10 percent overlap, the pixels of the MSS image are rectangular instead of square in shape

TABLE: 2·1

Landsat MSS bands

Landsat 1,2 & 3	Landsat 4 & 5	Bandwidth (μm)	Waveband name
4	1	0·5 - 0·6	Green
5	2	0·6 - 0·7	Red
6	3	0·7 - 0·8	Near Infrared
7	4	0·8 - 1·0	Near Infrared

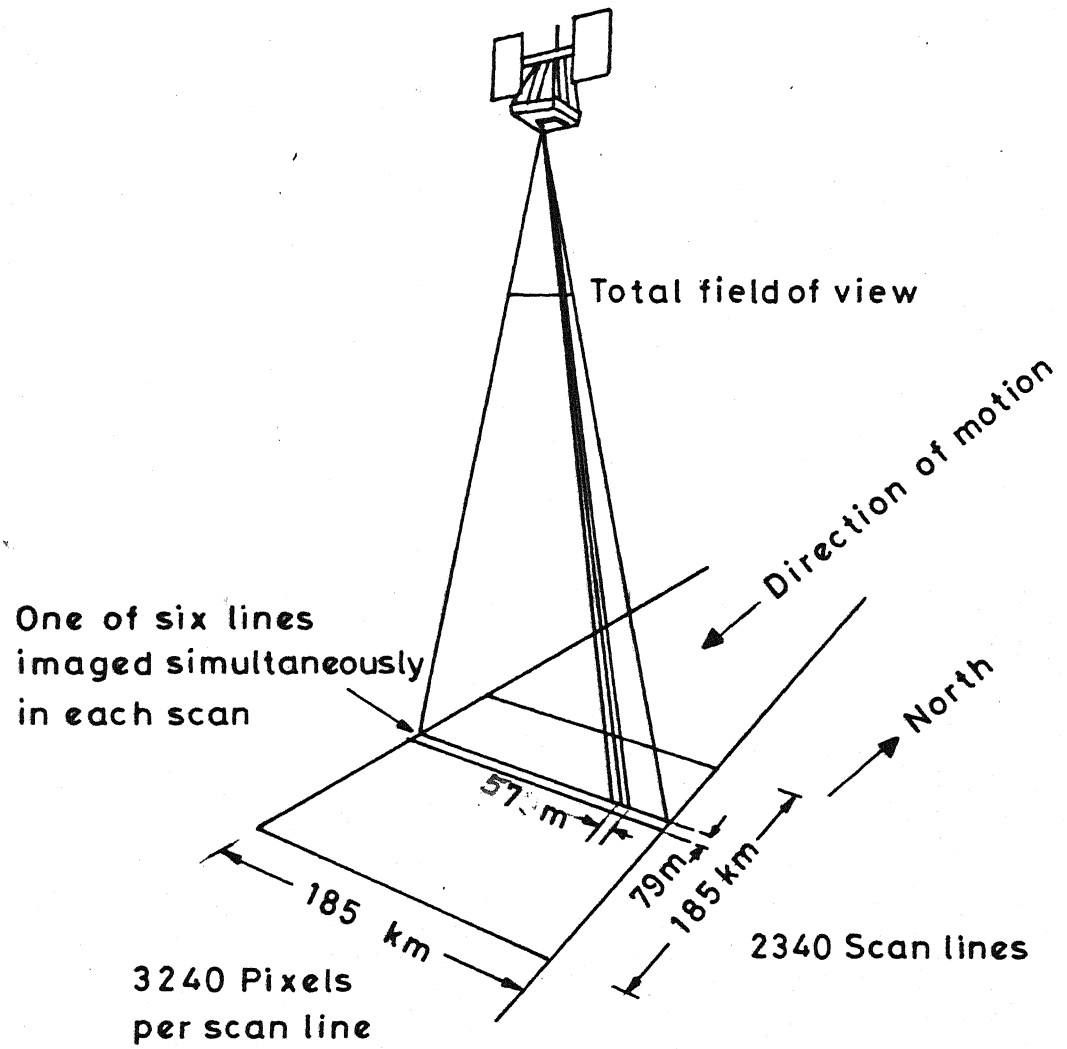

FIG. 2·3 CONFIGURATION OF LANDSAT MSS

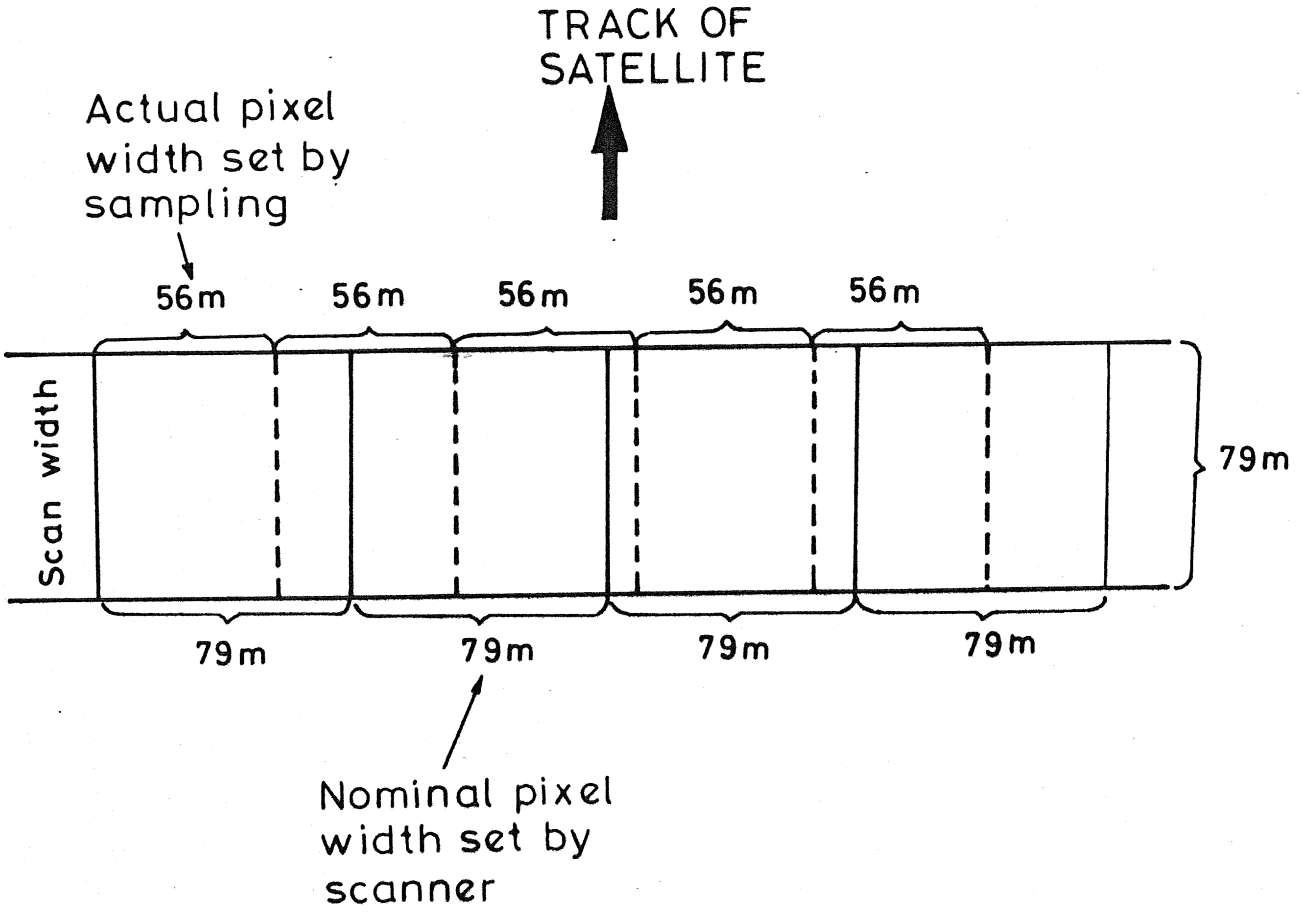

FIG. 2·4 THE SAMPLING PATTERN OF THE LANDSAT MULTISPECTRAL SCANNING SYSTEM (Modified from NASA 1976)

(Slater, 1979), consequently the ground coverage of each pixel being 56m by 79m (Fig.2.3 and 2.4).

A complete channel of Landsat MSS imagery contains 2340 scanlines and 3240 pixels per line with a total of around 7.5 million pixels per scene of 4 channels and the entire data recorded was recorded on computer compatible tapes (CCT).

2.2.2 Thematic Mapper (TM)

The Landsat 4 and 5 carried Thematic Mapper, which has higher resolution than that of MSS. It records 256 radiance levels in 7 wave bands with a spatial resolution of 30m in 6 of them and 120m in the seventh one, in contrast to MSS that records 64 radiance levels in four wave bands with spectral resolution of 79m. The details of wave bands are indicated in Table 2.2. The Landsat-4 TM data was not available at the Indian Landsat Earth Station(ILES), located 60 Km from Hyderabad, due to the failure of the X band radio channel (in Feb 1983) that is responsible for the transmission of TM data directly to ground stations. However, the MSS data from Landsat-4 is not affected since a separate S-band radio channel is involved.

Along with the satellite MSS digital data, the Survey of India toposheets of the study area on 1:250,000 and 1:50,000 scale were also used.

The wave bands of Thematic Mapper

Band number	Band name	Band width (μm)	Points
1	Blue/Green	0·45 - 0·52	Good water penetration, strong vegetation absorbance
2	Green	0·52 - 0·60	Strong vegetation reflectance
3	Red	0·63 - 0·69	Very strong vegetation absorbance
4	Near Infrared	0·76 - 0·90	High land/water contrasts, very strong vegetation reflectance
5	Near-middle Infrared	1·55 - 1·75	Very moisture sensitive
6	Thermal Infrared	10·4 - 12·5	Very sensitive to soil moisture and vegetation
7	Middle Infrared	2·08 - 2·35	Good geological discrimination

TABLE: 2·3

Coordinates of the Imagery

Latitude	Longitude	Line no.	Pixel no.
20° 43′ 05·25432″	83° 03′ 59·72472″	2340	3240
22° 19′ 31·7172″	83° 26′ 18·033″	1	3240
22° 39′ 20·5416″	81° 43′ 57·1206″	1	1
21° 02′ 41·6364″	81° 22′ 42·1140″	2340	1

2.3 PRE-PROCESSING OF LANDSAT MSS DATA

The digital data of Landsat-4 MSS obtained on a CCT was processed on fourth generation computer system to delineate and map the land use. The CCT was recorded on a 32-bit computer system, which is not compatible to the DEC-1090 system (existing at the Computer Center of I.I.T, Kanpur) as the latter is a 36-bit configuration and hence necessitates conversion of the original CCT. When the original tape is run on DEC-1090 system, it was reading 4 bytes and 4 bits of the next word, thus tampering the data. This problem was overcome by converting the original data tape to DEC compatible mode, keeping dummy bytes after each computer word and copied on another tape. For this work OMEGA computer system of CAD Center of I.I.T, Kanpur has been used. Subsequently, the original tape data was used in other computer system, PDP 11/24 (which has an image processor) for the image processing work. The software involved for use on all these systems was developed by the author during the present study and has been used for processing the data.

2.3.1 Band Separation

The CCT (of 27th Dec 1984) used in the present study was in BIL format (Fig.2.5). The data for each image were band separated and kept in different files. This operation has been carried out on the OMEGA system using software in C-language as developed by the author.

2.3.2 Windowing

The CCT of one Landsat MSS scene represents over 34,000 sq.km of the Earth's surface. In the first stage of operation, the area of interest was extracted, pertaining to bands 1,2,3 and 4, from the complete scene with the help of line and pixel number addresses as calculated from the knowledge of scene corners. The data on the test site covering 480 scan lines and 715 pixels have been windowed. The boundaries of the windowed data are as follows :

Starting scan line	--1036	480 scan lines
Ending scan line	--1516	
Starting pixel	-- 644	715 pixels
Ending pixel	--1358	

The precise demarcation of the study area has been confirmed with the help of the Survey of India toposheets. The coordinates and the respective constants of the entire scene are presented in Table 2.3

2.3.3 Histograms

Histograms reveal the frequency of various digital numbers present in the data. Each digital number (DN) represents the reflectance of each pixel area, on a pre-assigned gray level scale. The gray level scale may be on 0-63 (six bit number), 0-127 (7 bit number) or 0-255 (8 bit number). The frequency distribution is of immense use in the image enhancement process as it aids in understanding the

spectral contrast.

2.3.4 Cartographic Projection for Mapping Landsat MSS Data

The Landsat series of satellites map geodal surface of the Earth on to plane. These images therefore show various geometric distortions. All satellite motion-related errors have been corrected at the time of generating the Landsat imagery itself. However, errors due to non-linearity of ground track of satellite are not corrected and these produce images which cannot be compared directly with cartographic maps. In order to bring Landsat images on par with cartographic maps, it is necessary to transform the line number and pixel number of digital images into Cartesian coordinate system of latitude and longitude. Landsat orbit is inclined at an angle of approximately 81° to the equatorial plane of the Earth. The MSS aboard Landsat scene has a long strip of 185 km width which is oblique to meridional plane. It is therefore desirable to use a conformal map projection based on North-South strips. Conical orthomorphic projection has been adopted in the present work as it is appropriate for countries like India with prominent north-south elongation.

2.3.5 Conversion of Geographical Coordinates to Conical Orthomorphic Coordinates

This requires the availability of accurate maps of the image area and image identifiable ground control points such as highway intersections and small water bodies.

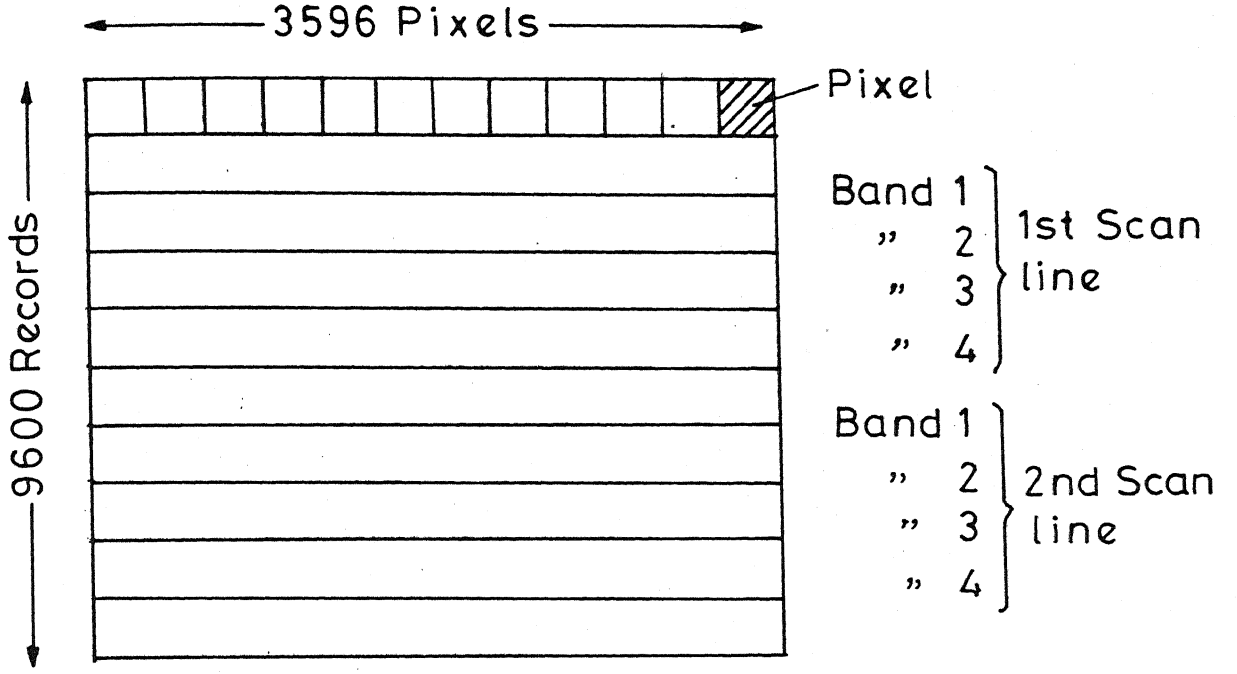

FIG.2·5 MSS FULL SCENE BAND INTERLEAVED RECORD FORMAT

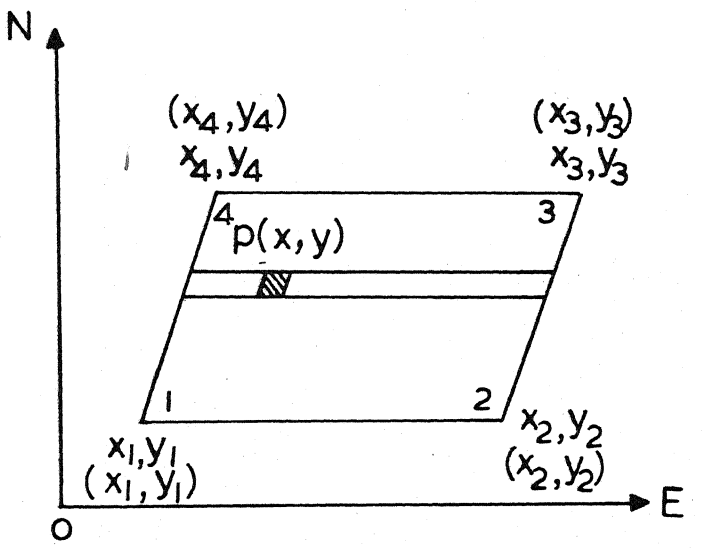

FIG.2·6 CORNER CO-ORDINATES OF THE IMAGE AND CONVERSION TO LINE NUMBER AND PIXEL NUMBER

For conversion, the precise longitudes and latitudes of the four corners of the imagery (Table 2.3) are obtained from Survey of India toposheets on 1:250,000 scale. The procedure involved is as follows :

The origin 'O'(Fig.2.6), chosen just outside the imagery edges, (Fig.2.6) has geographical coordinates (B_0, L_0), where 'B_0'is the latitude and 'L_0' is the longitude. Let (B_p, L_p) be geographical coordinates of any point on the imagery. The conical orthomorphic coordinates are

$$X = (P - m')\sin\tau \qquad .....(2.1)$$

$$Y = m' + X \tan(\tau/2) \qquad .....(2.2)$$

where

$$\tau = L \sin B_0$$

where $L = L_p - L_0$

i.e. the difference between the longitudes at any point 'p' on the imagery and the origin 'O'

$$m' = m + \frac{m^3}{6R_0 N_0} + \frac{m^4 \tan B_0}{24 R_0 N_0^2} + \frac{m^5(5+3\tan^2 B_0)}{120 R_0 N_0^3} \qquad .... (2.3)$$

R_0 = Radius of the curvature of the Earth spheriod at P (meridional)

$$R_0 = \frac{a(1 - e^2)}{\sqrt{(1 - e^2 \sin^2 B_0)}} \qquad ..... (2.4)$$

a = major axis of the reference ellipsoid (6377277.6m for Everest ellipsoid)

b = minor axis of the reference ellipsoid (6356075.0m, for India)

e^2 = eccentricity

$e^2 = (1 - b^2/a^2) = 1/300.8$ ..... (2.5)

N_0 = Normal to the surface at B_0 (radius of curvature in the direction perpendicular to the meridian)

$$N_0 = \frac{a}{(1 - e^2 \sin^2 B_0)^{1/2}} \quad \text{..... (2.6)}$$

R_m = mean radius of the Earth at mean latitude

$m = R_m (B_p - B_0)$ ..... (2.7)

$p = N_0 \cot B_0$ ..... (2.8)

Using the above equations, the orthomorphic coordinates (X,Y) are calculated.

2.3.6 Transformations

The conical orthomorphic coordinates (X,Y) can be transformed to the Landsat imagery coordinates (x,y) using the equations :-

$X = A_1 x + B_1 y + C_1$ ..... (2.9)

$Y = A_2 x + B_2 y + C_2$ ..... (2.10)

where

x = Line number

y = Pixel number

and

$A_1, A_2, A_3, A_4, A_5, A_6$ are constants of transformations.

The values for the six constants can be determined from a minimum of 3 ground points which are the three

corners of the imagery, whose coordinates (x,y) are computed from the earlier equations for their geographical coordinates. The values of X,Y obtained are presented in Table 2.4 The line number and pixel number of these three points are also known since they are corners of the imagery. For evaluating the six unknown constants we need to solve six simultaneous equations (Eqns.2.11 to 2.16).

$$X_1 = A_1 x_1 + B_1 y_1 + C_1 \quad \ldots\ldots (2.11)$$

$$Y_1 = A_2 x_2 + B_2 y_2 + C_2 \quad \ldots\ldots (2.12)$$

$$X_2 = A_1 x_2 + B_1 y_2 + C_1 \quad \ldots\ldots (2.13)$$

$$Y_2 = A_2 x_2 + B_2 y_2 + C_2 \quad \ldots\ldots (2.14)$$

$$X_3 = A_1 x_3 + B_1 y_3 + C_1 \quad \ldots\ldots (2.15)$$

$$Y_3 = A_2 x_3 + B_2 y_3 + C_2 \quad \ldots\ldots (2.16)$$

These six simultaneous equations were solved using Gauss elimination method and the constants A_1, A_2, B_1, B_2, C_1, C_2 were determined.

The validity of the solutions was checked at 4th corner using the equations

$$X_4 = A_1 x_4 + B_1 y_4 + C_1 \quad \ldots\ldots (2.17)$$

$$Y_4 = A_2 x_4 + B_2 y_4 + C_2 \quad \ldots\ldots (2.18)$$

The line number and pixel number (x_p, y_p) of any point on the imagery can be determined by solving equations 2.19-2.20 using the values of six constants already obtained (Rampal,1978).

TABLE 2.4

COORDINATES AND ORHTOMORPHIC COORDINATES FOR THE LANDSAT-4 IMAGERY OF CHHATTISGARH AREA,M.P

20.718126	83.066590	X = 215142.585862787705	Y = -29983.33940945559
22.325477	83.438342	X = 251112.531892367146	Y = 149459.03199593853
22.655706	81.732534	X = 75274.108094912138	Y = 184484.91900469838
21.044899	81.378365	X = 39304.712218415477	Y = 5043.94876056306

CENTRAL LIBRARY
106222

$$X_p = A_1 x_p + B_1 y_p + C_1 \quad \ldots\ldots (2.19)$$

$$Y_p = A_2 x_p + B_2 y_p + C_2 \quad \ldots\ldots (2.20)$$

The six constants of the imagery of Chhattisgarh Basin are presented in Table 2.5.

2.4 COMPUTER PROCESSING OF THE LANDSAT-4 DATA

Through computer processing of digital data,valuable information is obtained. The three properties of Landsat data which are important for computer processing are the multispectral nature of the sensors,the presentation of the data in the image format and multitemporal coverage of the orbits. Number of steps are involved in the computer processing of remotely sensed data.

The methodology of the image processing techniques used in the present study is presented in the subsequent pages within this section.

2.4.1 Image Restoration

This is the first stage in any image processing sequence. It was used to restore distorted image data to a more meaningful representation. It includes both radiometric correction and geometric restoration and correction. The radiometric corrections are done while preparing the computer compatible tape where as the geometric corrections are to be done to make it conformal with base maps.

2.4.1.1 Geometric Restoration and correction

The aim of the geometric restoration and correction

TABLE 2.5

CONSTANTS OF TRANSFORMATION FOR THE LANDSAT-4 IMAGERY OF CHHATTISGARH AREA,M.P

A1	=	- 15.37834371515483
B1	=	54.28787394037448
C1	=	75235.19856468876090
A2	=	- 76.71755874202162
B2	=	- 10.81379684548759
C2	=	184572.45036062989400

is to make an image conform to a prearranged scheme. It can be done through resampling. Image resampling involves the reformation of an image onto a new base. This is achieved by using features that are common both in the image and the new base (Bernstein, 1976). These features which are termed ground control points (GCPs), are chosen to be in sharp contrast to their surroundings such as the edges of water bodies and airport runways (Bernstein, 1976; Benny, 1983). The ground control points are located on the image by their 'x' and 'y' coordinates and on the new base by their latitude and longitude. The functional relationship (f_1 and f_2) between image 'x' and 'y' and latitude and longitude are determined by least squares regression as follows :

$$x = f_1 \text{ (latitude and longitude)} \quad .....(2.21)$$

$$y = f_2 \text{ (latitude and longitude)} \quad .....(2.22)$$

where

(x,y) = Image coordinates (column,row)

and f_1 , f_2 = transformation relationships.

Four stages are involved in the use of these two equations to geometrically transform an image :

(1) A geometrically correct geographical grid is defined in terms of latitude and longitude.

(2) The computer proceeds through each cell in this geographical grid and transforms the latitude and

longitude values into values of x,y (Eqs.2.21 and 2.22), which become new address in the image pixel.

(3) The appropriate pixel value is transferred from the image data set to its new location in the geographical grid .

(4) This process is repeated until the geographical grid is full at which point the image has been geometrically corrected usually to an accuracy of +1 pixel (Bernstein, 1976). In the present study +2 to +3 pixels accuracy maintained There are three methods available for this resampling procedure.

(1) Nearest neighbour method.

(2) Bilenear interpolation.

(3) Cubic convolution.

In the present study, nearest neighbour method is adopted as it is computationally simple and avoids altering pixel values.

$$f(x) = f(x_i) \quad \text{for the } x_i \text{ closest to } x$$

2.4.2 Image Enhancement

Image enhancement aids in highlighting the features of interest by improving the visual appearance of the image,as also the interpretability of an image by increasing apparent contrast between the features in the scene.Several steps involved in achieving the image enhancement are as follows :

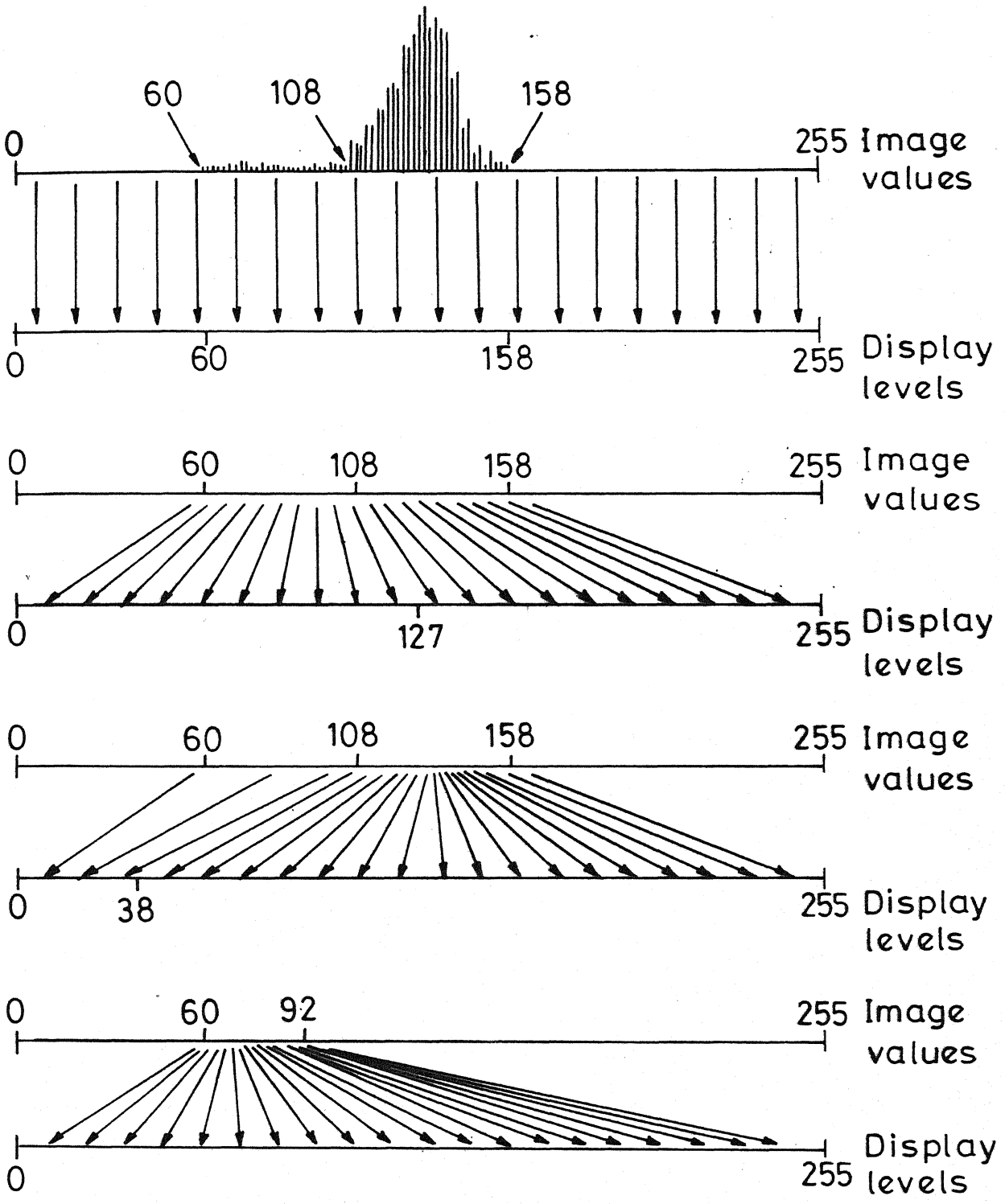

FIG·2·7 PRINCIPLE OF CONTRAST STRETCH ENHANCEMENT

2.4.2.1 Contrast Stretching

Contrast stretching is one of the most widely used enhancement techniques in image processing for lithological mapping.Since the Landsat MSS is designed to accommodate a wide range of scene illumination conditions,from poorly lit arctic regions to high reflectance desert regions,the pixel values in the majority of the scenes occupy a relatively small portion of the possible range of image values. If the pixel values are displayed in their original form, only a small range of gray values will be used,resulting in a low contrast display on which similar features might be indistinguishable. Contrast stretching is the process of redistributing the brightness levels in a picture to utilize the entire dynamic range of the display device (Fig.2.7). Several linear and non-linear algorithms are available which can be used for this technique.Depending upon the probability density function of the scene and identifying the areas of interest, a suitable algorithm can be chosen to maximize the contrast between those areas (Siegal and Gillespe, 1979). A linear stretch is generated by mapping each gray level encountered in the image, pixel by pixel, and then separating the pixel gray level as much as possible to fill the complete dynamic range of the display medium. The contrast stretch algorithm (Arlington,1979) utilized in the present work is as follows :

$$G'_{ij} = \frac{G_{ij} - Min}{Max - Min} \times 255 \qquad \ldots\ldots (2.23)$$

where

G_{ij} = input pixel values line 'i'and sample 'j'

G'_{ij} = corresponding output pixel value after the contrast stretch.

(Min,Max) = The range of Min-Max brightness of a particular image

2.4.2.2 Histogram Equalization

A technique for obtaining uniform histogram is known as histogram equalization (Gonzalez and Wintz,1977). In the case of digital image processing, the gray levels are discrete values. Since original image is rescaled, this type of technique is useful to know in detail the darker regions of the image. Mathematically, it can be explained as follows:

Let 'r' represent the gray level of the pixels in the image to be enhanced. The pixel values have been normalized so that they lie in the range

$$0 \leq r \leq 1$$

with r = 0 representing black and r= 1 representing white in gray scale. For any 'r' in the interval [0,1], attention is focused on transformations of the form

$$s = T(r) \qquad \ldots (2.24)$$

which produces a level 's' for every pixel value 'r' in the

original image. It is assumed that the transformation function given in Eqn.2.24 satisfies the conditions

(a) T(r) is a single value monotonically increasing in the interval $0 \leq r \leq 1$, and

(b) $0 \leq T(r) \leq 1$ for $0 \leq r \leq 1$

While the first condition preserves the order from black to white in gray scale, the second one generates mapping that is consistent with allowed range of the pixel values. Keeping these conditions in mind, a transform function has been considered in the present study which is represented as

$$s = T(r) = \int_0^r p_r(w)\, dw \qquad 0 \leq r \leq 1 \qquad \ldots\ldots(2.25)$$

where 'w' is a dummy variable of integration. The extreme right side of the equation is recognized as cumulative distribution function(CDF) of 'r'. The above concept has been formulated in discrete form for digital image processing.

For gray levels which assume discrete values, we deal with probabilities given by the relation

$$p_r(r_k) = \frac{n_k}{n} \qquad 0 < r < 1$$

$$k = 0, 1, \ldots\ldots\ldots \quad l-1$$

$$\ldots\ldots (2.26)$$

where L is the number of levels, $p_r(r_k)$ is the probability of the k th gray level, n is the number of times this gray level appears in the image, and 'n' is the total number of pixels in the image.

The discrete form of Eqn.(2.25) is given as

$$s_k = T(r_k) = \sum_{j=0}^{k} \frac{n_i}{n}$$

$$= \sum_{j=0}^{k} p_r(r_j) \qquad 0 \leq r_k \leq 1$$

$$k = 0,1 \ldots L-1$$

.....(2.27)

Software for this has been developed by the author which has been used in the detailed study of densely vegetated collapsed zones.Some system routines (PDP 11/24) have been used to make it interactive.Results of the same are presented in the subsequent chapter.

2.4.2.3 Band Ratioing

Band ratioing is useful in enhancing minor differences between geological formations. Ratio images minimize the first order effects due to variations in the brightness arising from the slopes of the formations.Ratio images display the differences between reflectance spectra of bands in one image. Band ratioing is a processing technique in which two spatially registered spectral images are divided,pixel by pixel. The resultant data are rescaled to use the full dynamic range of display using contrast enhancement techniques.

Mathematically,

$$DN' = \frac{DN_1}{DN_2} \times DN_1 \qquad \ldots\ldots (2.28)$$

where

DN' is the ratio of digital number from channel 1 and channel 2.

The DN is bright when $DN_2 > DN_1$ and dark if $DN_2 < DN_1$. The ratio pictures have the effect of suppressing the details of features like the topographic effects or vegetational effects while emphasizing colour boundaries. This property has made ratio pictures quite useful in geological applications as they exaggerate subtle colour differences in a scene.

2.4.2.4 Edge Enhancement

Edge enhancement filters are high-pass filters and their effect is to enhance or boost edges. This technique enables enhancement of subtle gray scale variations. When the values of adjacent pixels vary by a more than predetermined threshold value, the interface is marked on the image display with a contour. It is achieved through spatial filtering. Spatial filtering is of two types. In one, the procedure is undertaken on the transformed image frequency data in what is known as "frequency domain" and the other one is known as the "spatial domain". In the present work, spatial domain filtering is adopted. The filtering in spatial domain involves passing a filter of N X N pixels over an image and converting the pixel of this so called "kernel" to some measurement of the total array. As this technique involves the rolling together of all DN within the pixel array, it is

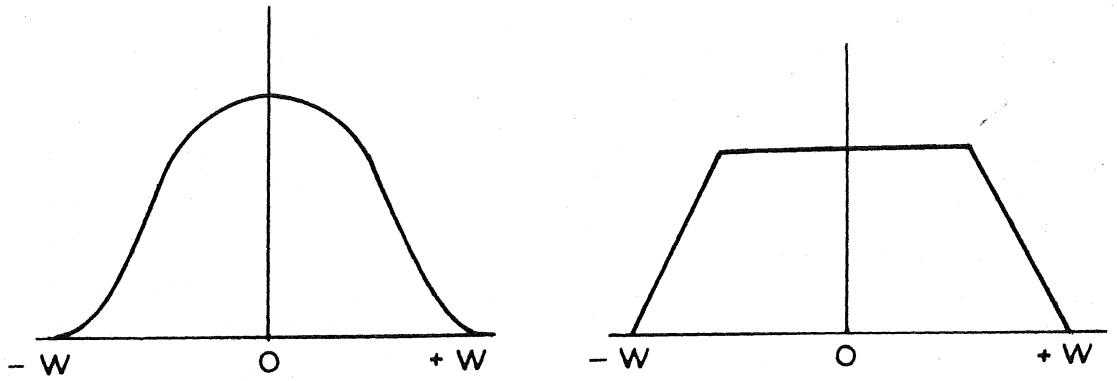

FIG. 2·8 A TYPICAL POINT SPREAD FUNCTION h(t)

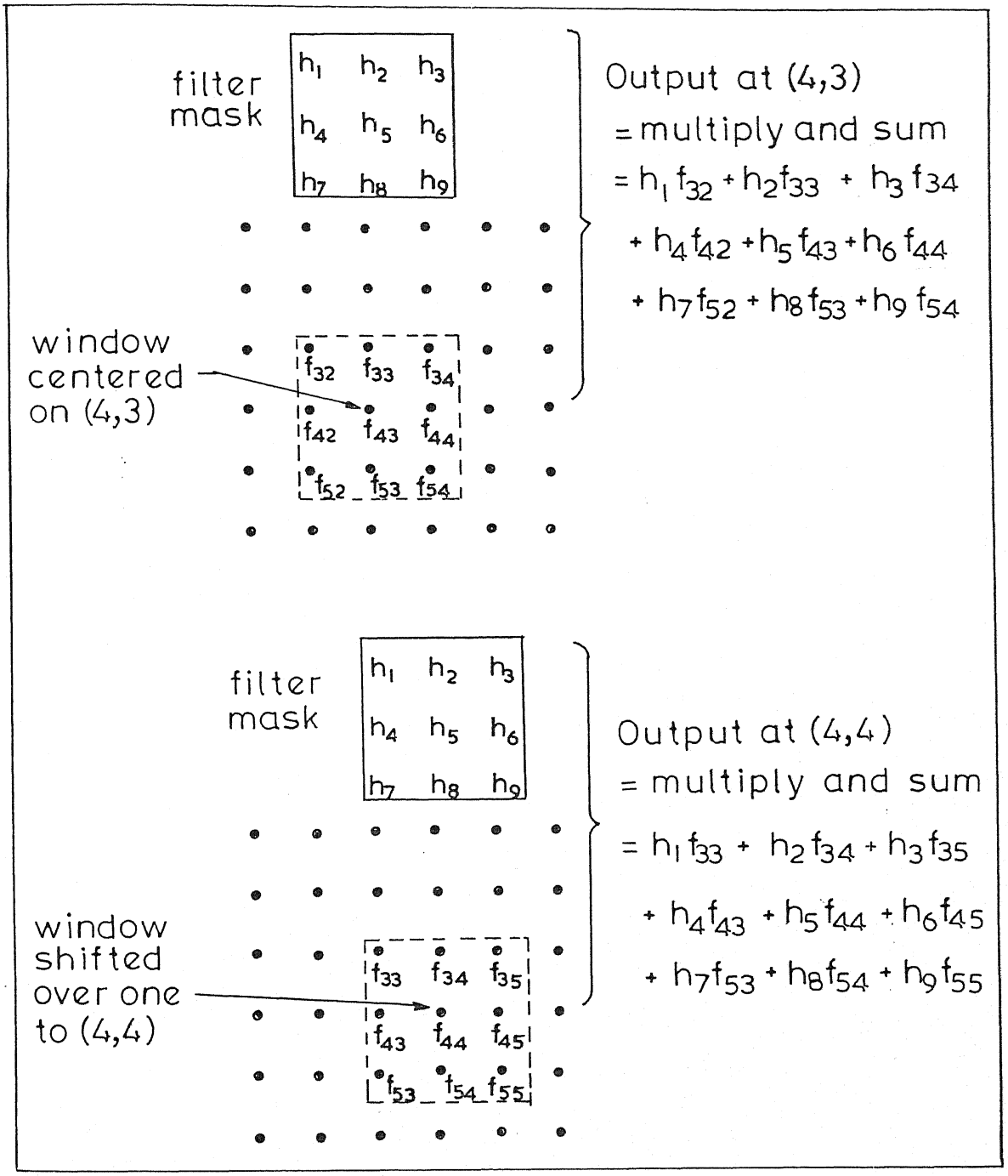

FIG.2·9 DIGITAL CONVOLUTION

often known by a descriptive term as "Convolution'(Kim and Strintzis,1980). The convolution is the movement (pixel by pixel and line by line) of a filter window through an image.

Mathematical representation of the convolution is as follows:

A system 'S' is considered a black box with an input f(x) and output g(x) = S(f(x)).

$$f(x) \text{ -----> } S \text{ -----> } g(x) \qquad \ldots\ (2.29)$$

In this case,'f(x)'is the original image,represented in one dimension for simplicity,'g(x)' is the filtered output image, and 'S' the filtering operation.Then the output of the filter can be expressed as

$$g(x) = \int f(t)\, h(x - t)\, dt \qquad \ldots\ (2.30)$$

where h(f) is the point spread function or impulse response.In digital case,the integral becomes summation :

$$g(i) = \sum_{-\infty}^{+\infty} f(k)\, h(i-k) \qquad \ldots\ (2.31)$$

and, although the limits of the summation are infinite, the function 'h' is usually zero outside some range as indicated in Fig.2.8. If the range over which 'h' is non-zero is (-w to +w), the equation (2.31) may be written as

$$g(i,j) = \sum_{k=i-w}^{i+w} \sum_{l=j-v}^{j+w} f(k,l)\, h\ (i-k, j-l) \qquad \ldots(2.32)$$

Thus the output g(i,j) at a point i,j is given by a weighted sum of input pixels surrounding i,j where the weights are

given by h(k). To create the output at the next pixel i+1 the function h(k) is shifted by one, and the weighted sum is recomputed. The full output is created by a series of shift-multiply-sum operations (termed as digital convolution) shown in Fig.2.9. The values of 'h'are referred to as the filter weights, the filter kernel, or filter mask.

The high-pass filtering is of two types-(1) gradient filters and (2) laplacian filters.These are defined for a continuous function f(x,y) of two variables as

Gradient

$$\nabla f = \frac{\delta f}{\delta x} i + \frac{\delta f}{\delta y} j \qquad \ldots\ldots (2.33)$$

Laplacian

$$\nabla^2 f = \frac{\delta^2 f}{\delta x^2} + \frac{\delta^2 f}{\delta y^2} \qquad \ldots\ldots (2.34)$$

where i and j are unit vectors in the x and y directions.

(a) Gradient

The gradient operator applied to a continuous function produces a vector at each point whose direction gives the direction of maximum change of the function at that point and whose magnitude gives the magnitude of this maximum change. Generally Sobel operators are used for Landsat data in this type. Few typical gradient operators are presented in Fig.2.10. The summation of the elements in each filter equals to '0'.

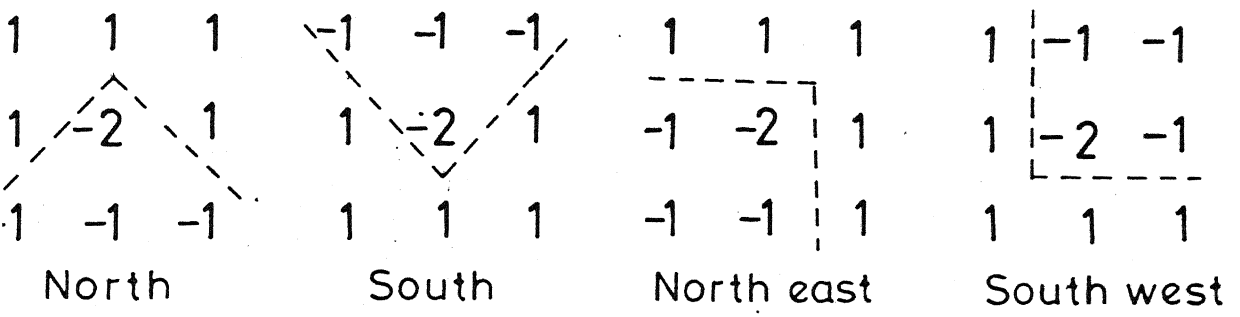

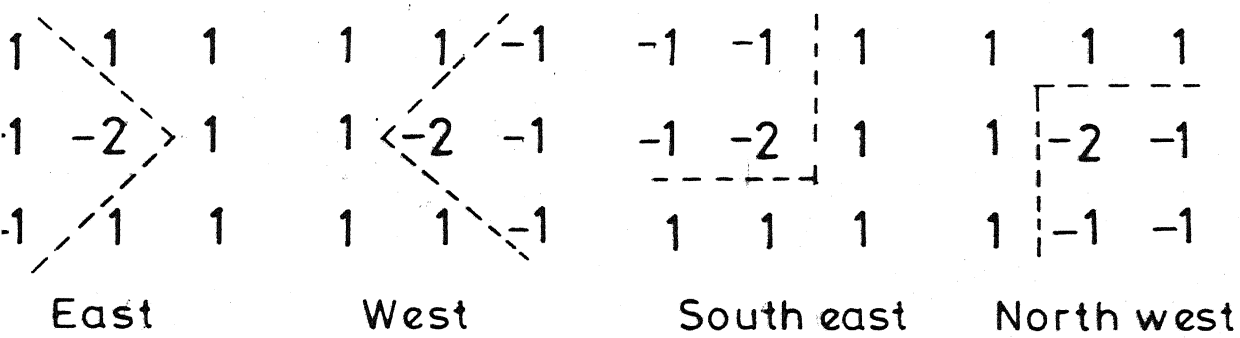

FIG. 2·10 GRADIENT FILTERS

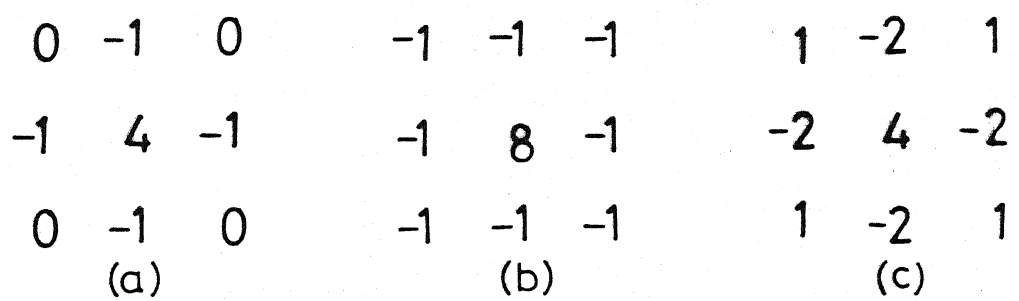

FIG. 2·11 LAPLACIAN FILTERS

(b)Laplacian filter :

This filter has been used in the present work to enhance the sinkhole and collapse prone areas in the study area. This filter is also computed by convolving the image. A sharpened edge without regard to edge direction is obtained through this process.

Mathematically the filter can be derived as

Continuous	Digital
$f(x)$	$v(i)$
$f'(x)$	$v'(i) = v(i-1)$
$f''(x) = \nabla^2 f(x)$	$v''(i) = v'(i) - v'(i-1)$
	$= [v(i)-v(i-1)]-[v(i-1)-v(i-2)]$
	$= v(i-2)-2v(i-1)+v(i)$
	$= (1\ -2\ 1)\ (v(i-2)\ \ v(i-1)\ \ v(i))$

..... (2.35)

giving the convolution mask (1 -2 1).In this form the laplacian at 'i' is computed from the values centered about 'i-1'. To keep the laplacian symmetric, it is normally shifted and given at 'i' as :

(1 -2 1) v(i-1) v(i) v(i+1)

This is a one-dimensional digital laplacian filter. Based on the same principle, in the present work a two-dimensional filter has been used. Few examples of the two-dimensional laplacian filters have been presented in Fig.2.11.

Though the digital image processing technique gives more details in recognizing the source areas,it is restricted to a spatial constraint of the processor window. Due to this reason a line printer map has also been presented to represent the moisture-stress areas for which image

classification techniques were also presented in this chapter.

Application of the above techniques to limestone region in the present work is detailed in the succeeding pages.

2.4.3 Image Classification

2.4.3.1 General

The terrain has been classified based on the image analysis. In the present study, three channel data has been used for interactive classification to make a thematic map of the terrain. All the four channel data have been used to classify the moisture-stress areas and produce a line printer map based on the classification. In the present work, supervised classification has been used. Spectral signatures have been studied in detail for the limestones and morphological features of limestones.

2.4.3.2 Supervised Classification

It involves user in selecting some pixels from each possible class. From these, the classification algorithm determines what each class "looks like", and then assigns each pixel of the image to one of the classes. In the present study Bayesian maximum likelihood classifier has been used.

Bayesian Maximum Likelihood Classifier

It is a well developed method from statistical decision theory which performs a decision-making function on

a data vector by assigning it to one of a given set of possible classes (Swain,1972). The data vector can be derived from any set of mesurements and in the case of multispectral scanner data, the measurements are the levels of reflected or emitted electromagnetic energy.

Estimation of probability with this technique involves two weighted factors. The a priori probability is to be determined first followed by a weight associated with the cost of misclassification being applied for each class.

The mathematical formulation involves several steps. The probability function is assumed and the parameters of that distribution are estimated. Let x_i .....x_n be random variables where x_i is the noise measurement of the feature. Let $P(x/G_i)$ be the conditional probability density function of class i and $P(G_i)$ is a priori probability of class G_i. The task of the classifier is to assign the input sample such that the probability of misrecognition is minimized.

The Bayes' decision is that

$$x \approx G_i$$

that is if there are G groups then Bayes' rule is to assign the feature to group i where :

$$P(G_i/x) > P(G_j/x) \quad \text{for all } j \neq i \quad \ldots.(2.36)$$

Although it is easy 'in principle' to obtain $P(x/G_i)$, the probability that we are interested in is $P(G_i/x)$. Fortunately there is a connection between the two, known as 'Bayes'

theorm' :

$$P(G_i/x) = \frac{P(x/G_i)\ P(G_i)}{\Sigma\ P(x/G_i)\ P(G_i)} \qquad \ldots.(2.37)$$

All the items on the right hand side of the equation can be found by sampling. The conditional probability $P(x/G_i)$, the probability of a particular set of measurements 'x' given that the feature comes from group i, $P(G_i)$ is the a priori probability.

Putting the Bayes' theorm into Bayes' rule gives :

assign to group i if

$$\frac{P(x/G_i)\ P(G_i)}{\underset{\text{all k}}{\Sigma}\ P(x/G_k)\ P(G_k)} > \frac{P(x/G_j)\ P(G_j)}{\underset{\text{all k}}{\Sigma}\ P(x/G_k)\ P(G_k)} \qquad \ldots.(2.38)$$

for all $J \neq i$

or, as the bottom lines on both sides of the inequality are the same, they can be cancelled out to give i, if

$$P(x/G_i)\ P(G_i) > P(x/G_j)\ P(G_j) \text{ for all } J \neq i \qquad \ldots(2.39)$$

This is the form of Bayes' rule. The following steps are neccessary to classify an image:

(1) Training areas for each class are selected. These areas are known (or assumed) to contain numberof pixels in the class. In general the more training data per class, the better the accuracy, since it should give a truer representation of the class.

(2) The most common choice of functional representation of

$P(x/G_i)$ is a Gaussian distribution in which for one dimensional case, the parameters to be estimated are mean and standard deviation of the distribution. The general form of a one- dimensional Gaussian with mean m, standard deviation σ, and normalized to have area is :

$$\frac{1}{\sqrt{2\pi}\sigma} \; e^{-1/2\left((x-m)^2/\sigma^2\right)} \qquad \ldots\ldots (2.40)$$

In the present case, it can be expressed in the form

$$P(x/G_i) = \frac{1}{\sqrt{2\pi}\sigma_i} \; e^{-(x-m_i)^2/2\sigma^2} \qquad \ldots\ldots (2.41)$$

Where m_i and σ_i are the mean and standard deviation of the i-th class. For a multivariate n band problem, the m_i becomes an 'n' dimensional vector of means, σ_i becomes an nXn covariance matrix Σ_i, and the scaling factor becomes $(2\pi)^{n/2}$.

To perform the classification of an image using the parametric forms, the trainig data are used to compute 'n' dimensional vector mean and nXn covariance matrix Σ_i for each class. However if within each group the variables that make up the mesurement vector x have a multivariate normal distribution, then the form of $P(x/G_i)$ is known. Hence

$$P(x/G_i) = \frac{1}{(2\pi)^{n/2}|\Sigma_i|^{1/2}} \exp\left[-\tfrac{1}{2}(x-m_i)^T \; \Sigma_i^{-1} \; (x-m_i)\right] \qquad (2.42)$$

In this case, estimating $P(x/G_i)$ comes down to estimating two parameters for each group m_i, the group mean vector and Σ_i the group covariance matrix.

Using the normal form of $P(x/G_i)$ in Bayes' rule gives:

assign x to G_i if

$$\frac{P(G_i)}{(2\pi)^{n/2}|\Sigma_i|^{1/2}} \exp[-1/2(x-m_i)^T \Sigma_i^{-1} (x-m_i)] > \frac{P(G_j)}{(2\pi)^{n/2}|\Sigma_j|^{1/2}} \exp[-1/2(x-m_j)^T \Sigma_j^{-1} (x-m_j)]$$

for all $j \neq i$ ..... (2.43)

Taking the natural log(ln) on both sides of the inequality gives:

assign x to G_i if

$$-1/2 \ln(2\pi) -1/2 \ln|\Sigma_i| -1/2(x-m_i)^T \Sigma_i^{-1} (x-m_i) + \ln(P(G_i)) > -1/2 \ln(2\pi) -1/2 \ln|\Sigma_j| -1/2(x-m_j)^T \Sigma_j^{-1} (x-m_j) + \ln(P(G_j))$$

for all $j \neq i$ .....(2.44)

Cancelling both the terms that are common to both sides gives

$$-1/2\ln|\Sigma_i| -1/2(x-m_i)^T \Sigma_i^{-1} (x-m_i) + \ln(P(G_i)) > -1/2\ln|\Sigma_j| -1/2(x-m_j)^T \Sigma_j^{-1} (x-m_j) + \ln(P(G_j))$$

for all $j \neq i$ ....(2.45)

This expression has one difficulty in that the cancellation of all the common terms has resulted in a quantity that is negative. This can be corrected by multiplying both sides of the inequality by -1 and changing the greater than sign to less than sign giving:

assign x to G_i if

$$\ln|\Sigma_i| + \tfrac{1}{2}(x-m_i)^T \Sigma_i^{-1} (x-m_i) - \ln(P(G_i)) <$$
$$-\ln|\Sigma_j| + \tfrac{1}{2}(x-m_j)^T \Sigma_j^{-1} (x-m_j) - \ln(P(G_j))$$
$$\text{for all } j \neq i \qquad \ldots.(2.46)$$

Although matrix operations are involved in working out the above expressions, the final result is number for which each group depends on x. That is

$$P(G_i/x) = \ln|\Sigma_i| + \tfrac{1}{2}(x-m_i)^T \Sigma_i^{-1} (x-m_i) - \ln(P(G_i)) \ldots.(2.47)$$

This is the form we use normally in the computational work, and in this case, p is assigned to the class for which $P(G_i/x)$ is minimum.

Numerical Separability of the Classes

A good classification can be obtained only if the classes are numerically separated. If there is extensive overlap in their distributions, even a high likelihood value for a pixel does not give us confidence in its correct classification. So we need some measure of class separability in order to assess the accuracy we can expect from a classification.

Divergence is one of the first measures of statistical separability used in the machine processing of remote sensor data, and it is still widely used as a method of feature selection. It addresses the basic problem of diciding what is the best q-band subset for use in the

supervised classification process. The number of combinations, c, of n bands taken q at a time is

$$C \frac{n}{q} = \frac{n!}{q!\ (n - q)!} \qquad \ldots\ldots (2.48)$$

The degree of divergence or "separability" between two classes c and d, $divergence_{cd}$, is computed according to the formula -

$$Diverg_{cd} = 1/2\ T_r\ (V_c - V_d)\ (V_d^{-1} - V_c^{-1}) + 0.5\ T_r\ (V_c^{-1} + V_d^{-1})\ (M_c - M_d)\ (M_c - M_d)^T \qquad \ldots\ldots (2.49)$$

Where $T_r[.]$ is the trace of a matrix (i.e, the sum of diagonal elements, V_c and V_d are the covariance matrix for two classes, c and d, under investigation, M_c and M_d are mean vectors for classes c and d.

If there are more than two classes, the average divergence, $Diverg_{avg}$, is computed over all possible pairs of classes c and d while holding the subset of bands, q constant, as follows :

$$Diverg_{cd}^T = \frac{1}{C} \sum_{c=1}^{m-1} \sum_{d=c+1}^{m} Diverg_{cd} \qquad \ldots\ldots (2.50)$$

It is possible to take the divergence logic one step further and the computed transformed divergence, expressed as

$$Diverge_{cd}^T = 2000\ [\ (\ 1 - \exp \frac{(1 - Diverg_{cd})}{8}\ )\ ] \qquad ..(2.51)$$

This statistics gives an exponentially decreasing weight to increasing distance between the class. It also scales the divergence value to lie between 0 and 2000.

A transformed divergence value of 2000 suggests an excellent class separation. Above 1900 provides good separation, while below 1700 is a poor separation.* For divergence values less than 1500, we get spectrally similar classes. * Kumar and Silva (1972)

CHAPTER 3

DIGITAL IMAGE PROCESSING FOR LITHOLOGICAL IDENTIFICATION

3.1 GENERAL

The principal objective of enhancement techniques is to process a given image so that the result is more suitable than the original image for specific application. In the present work, spatial domain approach based on gray level mapping has been adopted.

Enhancement procedures are carried out through pseudocolour concepts with superimposition procedure as well as through contrast stretching, histogram modification and edge enhancement techniques. While former procedures have enabled distinct demarcation of lithological variations, the latter have enhanced the structural features such as fracture zones, lineaments as well as the associated sinkhole features.The interpretations have been correlated with hydrogeological field data to confirm the compatibility of the techniques in detecting these features. Software has been developed interactively for all these techniques by the author. Few areas were selected, for enhancement, which apparently represented dense vegetation under moisture-stress conditions, thought to have been induced by sinkhole collapsed formation. Using enhancement techniques, various

lithological units have been delineated for further hydrogeologic evaluation. Extensive field observations were undertaken as ground checks.

3.2 LITHOLOGIC IDENTIFICATION

For this purpose, enhancement procedures such as contrast stretching, pseudocolouring and superimposition have been used. Compactness of the limestone, its tonal contrast, erosional features, and the drainage pattern are the parameters which aid in the terrain differentiation. Based on these parameters, it is possible to demarcate the lithologic units. Distinct lithological differences within the limestones have been recognized in the present study. In addition to these variations in the limestones, structural features of hydrogeological significance have also been delineated through enhancement techniques. The study area can be broadly divided into three lithological units :

(i) Limestones.

(ii) Shale.

(iii) Alluvial tract.

To distinguish them distinctly the enhancement techniques used are ratioing, histogramming, histogram equalization, contrast stretching and edge enhancement.

3.2.1 Limestone

This unit, designated as the Chandi formation within Raipur group, occurs in the central part of the Chhattisgarh

basin. The Chandi formation has been subdivided into Nipania, Pendri and Newari limestone members. Distinct differences within these members have been recognized on the basis of the above mentioned enhancement procedures. For this purpose, pseudocoloured superimposed method and ratioing and contrast enhancement techniques have been used. The Nipania member is characterized by its light tonal contrast (indicated by 'N' in Figs.3.8 and 3.11) in pseudocoloured photographs. It could be noticed that the oval features such as sinkholes are very scant in the limestone due to its compactness. This member is located on the N-W side of the Jamunia river between Hathbandh and Bhatapara areas. On the other hand, on the eastern side of the same river in the region south of Tilda, the Pendri and Newari members were identified by their dark tonal contrast and soluble nature of the limestone. For a distinct identification, ratioing and contrast stretching methods have been utilized.

In the ratioing process, two spatially registered spectral images are divided pixel by pixel (Siegal, 1980). Ratioing can be thought of enhancing minor differences between formations (between Pendri member and Nipania member in the present case). The Pendri member can be clearly identified by its dark gray tonal contrast with the dominant occurrence of oval and irregular features (indicating 'P' in Figs.3.9 and 3.12) revealing the soluble nature of the member.

To confirm that all the dark irregular features in Fig.3.4 do not represent the sinkholes, contrast enhancement has been done on the ratioed (2/4) picture. For obtaining the contrast enhancement, the probability density function of the reflectance values of the area of interest should be known. For this purpose,a histogram was plotted for the area (indicated by 'I' in Fig.3.14). It has been observed that most of the reflectance values in the histogram were distributed between 1.0 to 2.5. These values were later subjected to stretching for the entire medium to improve the contrast of the area. Through this enhancement, the actual sinkholes were identified clearly by their dark tone (Fig.3.17). The gray tone linear feature (indicated by 'LV' in Figs.3.14 and 3.17) is a recent active zone along which the solution action is prominent. The rest of the areas with light gray tone in the vicinity reveal dense vegetation along the fracture zone indicating the proximity of groundwater. The exposed surface of the Pendri member has been identified by its light tonal contrast (shown by 'P' in Figs.3.11 and 3.12). Compared to the Newari member, this member has greater solubility. The Jamunia river follows the contact of Nipania and Pendri members. This area was later subjected to selective stretching to enhance the subdued caverns under thick vegetational growth (indicated by 'CV'in Fig.3.20). The red patches indicate the vegetational growth

and distribution pointing to the proximity of the groundwater.

The third member has been identified by its light and gray coloured irregular shape (indicated by 'NE'in Figs.3.9, 3.12, and 3.16). The river Banjari has its initial course in the Newari member and the remaining part is along the contact of Pendri and Newari members. The Newari member (indicated by 'NE' in Fig.3.9) is also a soluble limestone. In this member, several collapsed zones and sinkholes have been identified. To distinguish this member clearly, ratioing and contrast stretching have been used. The exposed portion of this member is restricted, which can be identified by its light tonal contrast with irregular shape (Figs.3.9 and 3.12). The ratio of bands 2 and 4 was used to detect the sinkhole and collapsed zone areas. They have been located with irregular and oval shape features in the northern part of the area. A histogram has been plotted for these areas to know the probability distribution function of the reflectance values and it has been observed that most of the values have been in the 2 to 3.5 range. This range has later been stretched to entire medium to enhance clearly the collapsed zones and sinkholes. These were represented by 'CZ' in Figs.3.15 and 3.18. Edge enhancement has enabled identification of the actual collapsed zones filled with sediments and with dense vegetation zone from within the dark tonal contrast zone, the entire portion which apparently

looks other wise like a collapsed zone. The oval collapsed zone with a storage tank is a recent one located on eastern border of the Newari member and has been identified by its gray tonal contrast. Within this limestone member, it has been observed in the present study that the groundwater is under unconfined conditions in the sediment filled area of the collapsed zone, while in the deeper regions, where intercalations of Gunderdehi shale occurs, the confined conditions exist. The surface of the limestone terrain is characterized by discontinuous drainage system in the vicinity of the oval features.

3.2.2 Shales

Two shale members, the Raipur and Tarenga, have been identified in the imageries and were later confirmed by field checks. The Raipur shales are recognized in the contrast stretched window (indicated by 'Sh' in Figs.3.9,3.12 and 3.18) along the Jamunia river. These shales, interbedded with Pendri limestones and Nipania limestones, are poorly visible in bands 2 and 4 due to paucity of their exposure and extensive vegetation. Checks around Murpar and Diggi villages have enabled the confirmation of these shales (Figs.3.29 and 3.30). To enhance these areas to the maximum extent, selective stretching procedure was applied by choosing the suitable stretch parameters. The Raipur shales are characterized by the dark tonal contrast (indicated by 'Sh'

in Fig.3.18) due to their fine-grained nature with presence of moisture.

The Tarenga shale occurs in the region north-west and north of Tilda-Bhatapara line (indicated by 'Tsh' in Figs.3.2 and 3.8) . Although, in general this shale is also of fine texture, it exhibits relatively lesser tonal contrast due to the absence of moisture as compared to the Raipur shales.

3.2.3 Alluvium

The major alluvial tract of the terrain has been identified in the north-western part of the image near Rajpur where the river Jamunia has its confluence with Seonath river (indicated by 'Al' in Figs.3.4, 3.7, 3.10 and 3.13). To demarcate the area clearly, it has been subjected to ratioing and selective stretching. The fine-textured gray coloured tonal contrast, as indicated by 'Al' in Figs.3.16 and 3.19 aids in the interpretation of this tract. For the alluvial tract, reflectance is a sensitive indicator of the terrain along with the vegetational growth. Variation in reflectance values is related to the compositional variations of the sub-surface in the alluvial regions. The alluvial patches are potential sources for groundwater in the region and are extensively developed.

Edge enhancement procedure has been utilized to demarcate the structural features such as fracture zones and

lineaments and to demarcate perfect boundaries of sinkholes and collapsed zones. It is mainly based on high-pass filtering through which sudden reflectance changes can be delineated and edged. This would facilitate the demarcation of various structural features. The software for the edge enhancement has been developed by the author during the present study.

Laplacian 3 X 3 and 5 X 5 filters have been used in the present work for a convolutional operation. The edge of a sinkhole or a collapsed zone represents some kind of irregularity with respect to the surrounding pixels. Due to this change, the sharp edges of the limestones (Fig.3.21) were delineated. The measure of the magnitude of the irregularity at a specific point, is the difference between the actual value for that point minus an interpolated value based on the remaining pixels. The actual sharp edges of the sinkholes and caverns were edged and assigned a black colour to differentiate from the surrounding areas (indicated by 'CZ and SK' in Fig.3.21) within the region covering Tilda, Hathbandh and Nawapara villages. This area has been inferred as active solution action zone which was later confirmed by ground checks.

The present investigations have revealed the maximum occurrence of the collapse features in the area between Pendri and Arjuni villages. All the collapsed and filled zones and sinkholes were edged due to sharp differences in

reflectance values and were assigned a black colour for these areas (Fig.3.21) to represent the structurally -controlled moisture zones. Dense vegetational growth has been identified along the fracture zones indicating the proximity of the groundwater (demarcated by 'V'). Vegetation has been assigned red colour for easy identification. The shaded red areas indicate the slopes of the limestone areas with vegetation. The major fracture zone with NE-SW trend along which the Jamunia river flows, has been edged due to sharp change in reflectance and was identified by its linear nature (indicated by L-L in Figs.3.23). To obtain clarity of information about the boundaries of limestone edges, the edge enhancement procedure is performed on original band-4 windowed data. The white coloured curved edges represent the boundaries(B) of the limestones and straight lines represent lineaments and fracture zones (indicated by L-L in Fig.3.23). These weak zones have been confirmed through field checks. Pumptests in the present work have revealed that such areas are potential areas of groundwater yield with high transmissivity values.

ig.3.1 Enhanced window indicating the fractured limestone

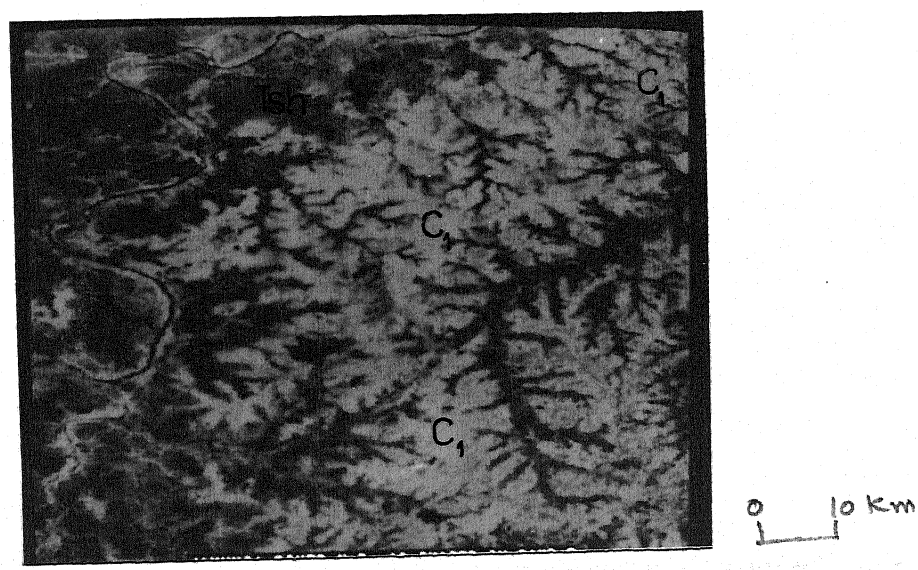

ig.3.2 Enhanced window of band 2 (Bhatapara-Tilda region)

C_1 = Upland tract; Tsh = Tarenga Shale

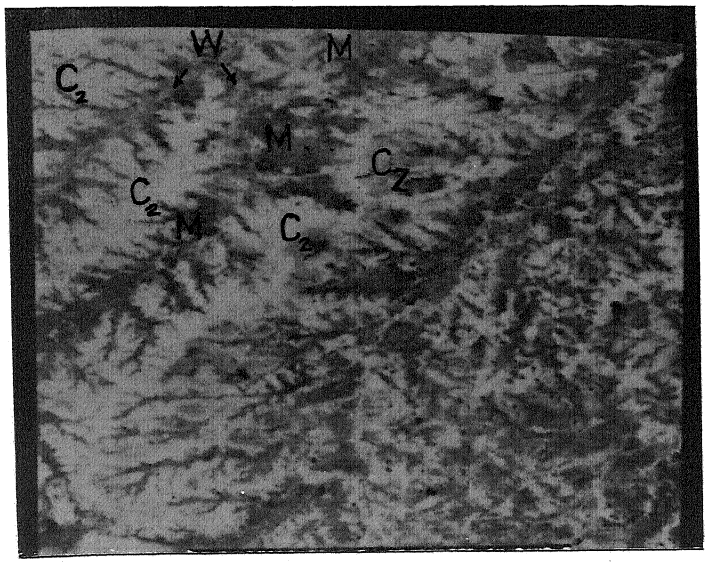

Fig.3.3 Enhanced window of band 2 (Arjuni-Pendri region)

C_2 = Upland tract; M = Moisture zone; W = Water;
Cz = Collapsed zone; NE = Newari limestone

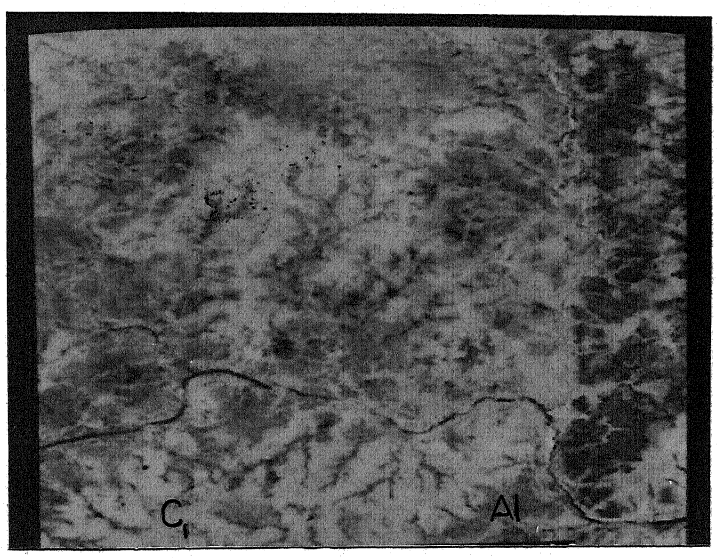

Fig.3.4 Enhanced window of band 2 (Rajpur region).

C_1 = Upland tract; Al = Alluvial tract

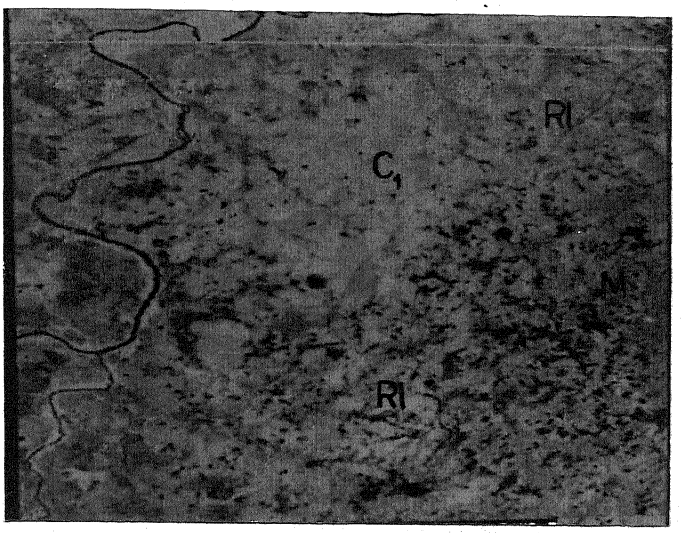

Fig.3.5 Enhanced window of band 4 (Bhatapara-Tilda region)

C_1 = Upland tract; M = Moisture zone;
Rl = Railway line

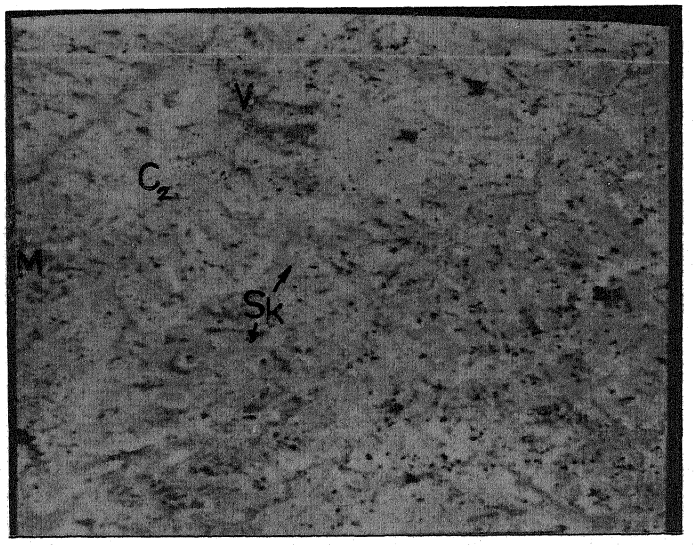

ig.3.6 Enhanced window of band 4 (Arjuni-Pendri region)

C_2 = Upland tract; V = Vegetation; Sk = Sinkholes
M = Moisture zone

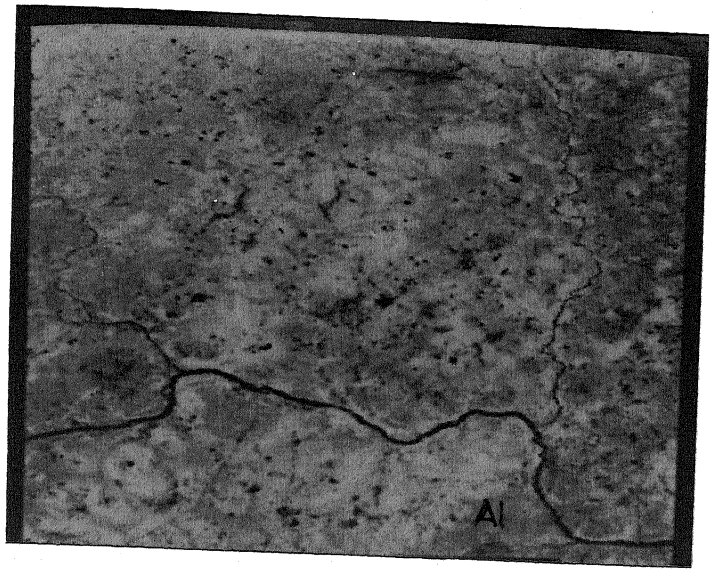

Fig.3.7 Enhanced window of band 4 (Rajpur region)
Al = Alluvial tract

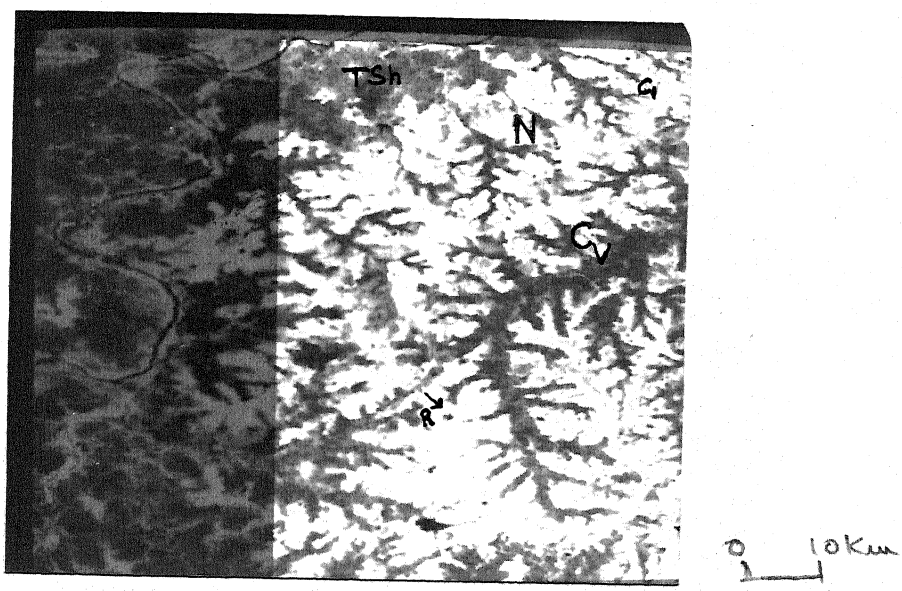

3.8 Pseudocoloured and superimposed section of band 2 (Bhatapara-Tilda region); C_1 = Upland tract; Vl = Valley tract; Cv = Caverns; N = Nipania limestone; R = Runway (arrow indicates aircraft);

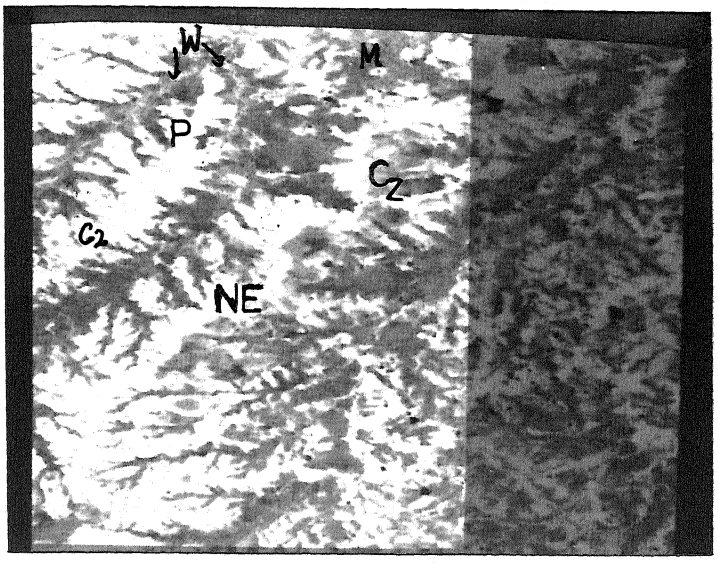

3.9 Pseudocoloured and superimposed section of band 2 (Arjuni-Pendri region). C_2 = Upland tract; M = Moisture zone; NE = Newari limestone; P = Pendri limestone; Cz = Collapsed zone; W = Water

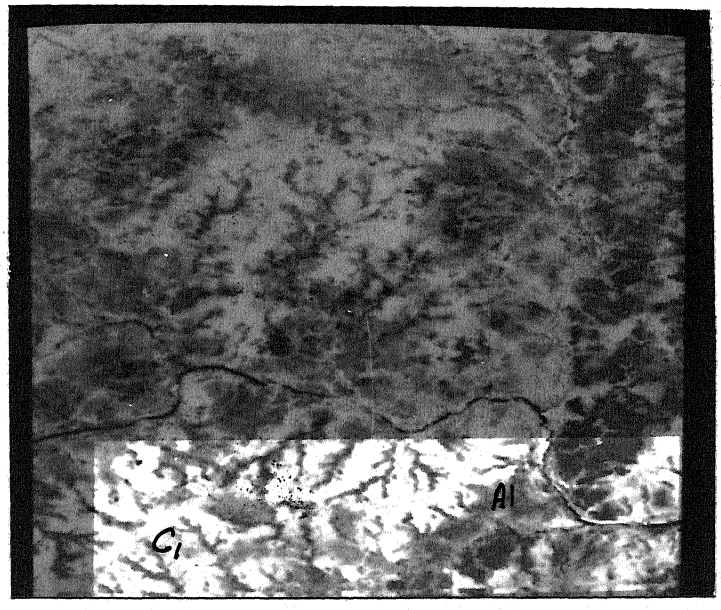

.10 Pseudocoloured and superimposed section of band 2 (Rajpur region). C_1 = Upland tract; Al = Alluvial tract

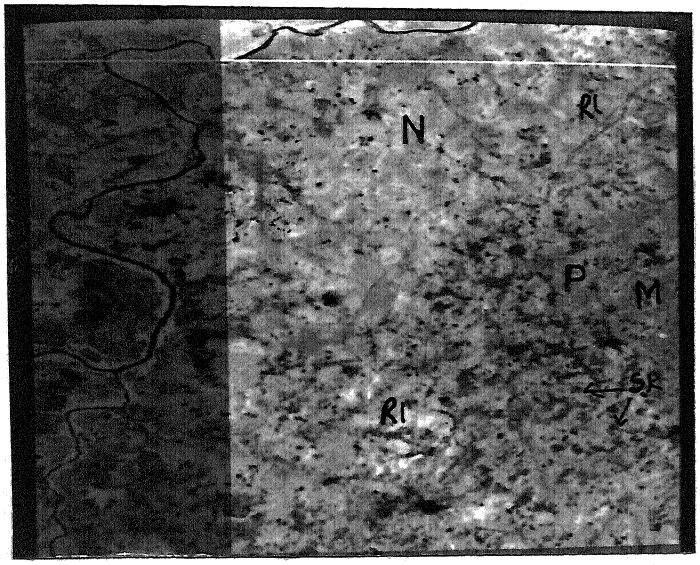

3.11 Pseudocoloured and superimposed section of band 4 (Bhatapara - Tilda region). M = Moisture zone; N = Nipania limestone; Sk = Sinkhole; Rl = Railway line P = Pendri limestone

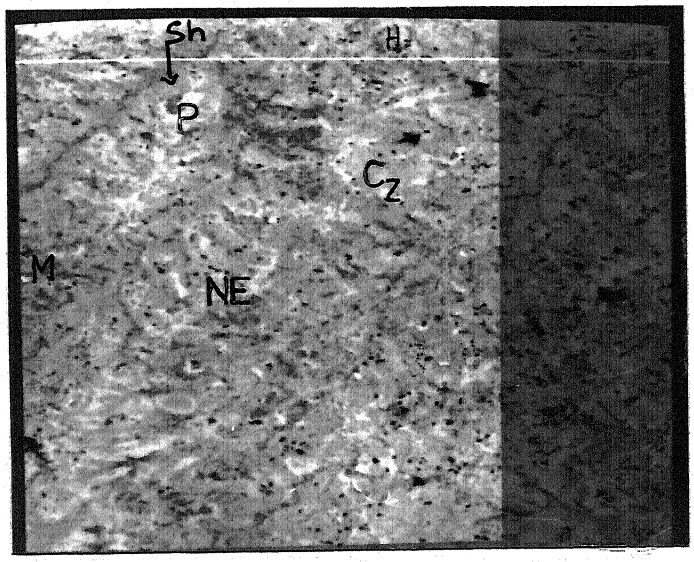

Fig.3.12 Pseudocoloured and superimposed section of band 4 (Arjuni-Pendri region). M = Moisture zone; NE = Newari limestone; P = Pendri limestone; Sh = Raipur Shale; Cz = Collapsed zone;

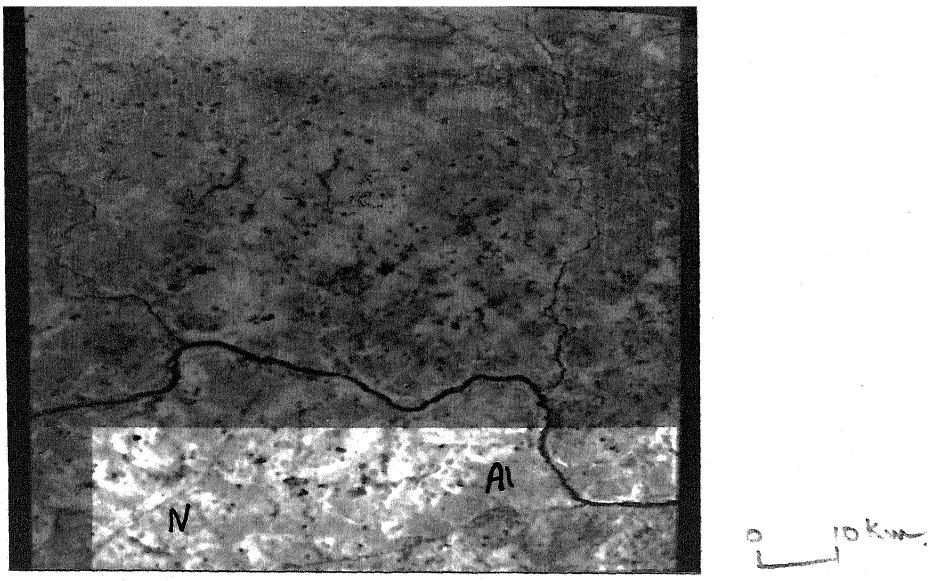

3.13 Pseudocoloured and superimposed section of band 4 (Rajpur region). Al = Alluvial tract; N = Nipania limestone

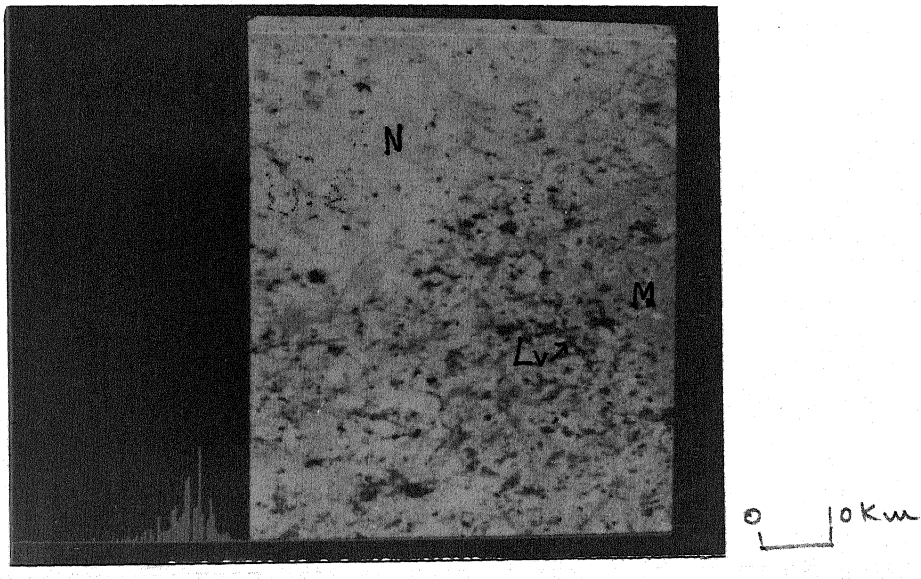

3.14 Band ratio (2/4) with histogram (Bhatapara-Tilda region). M = Moisture zone; N = Nipania limestone; Lv = Linear feature with vegetation

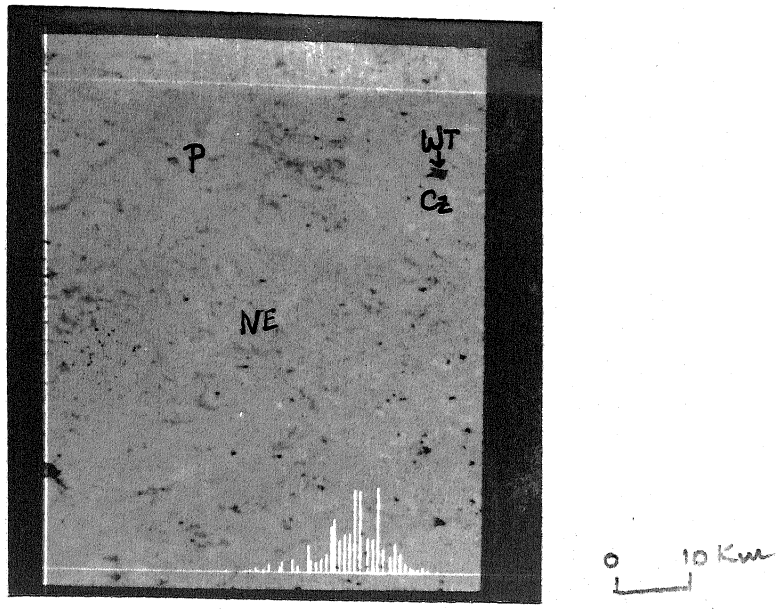

Fig.3.15 Band ratio (2/4) with histogram (Arjuni-Pendri region).
NE = Newari limestone; P = Pendri limestone;
WT = Surface water tank within the collapsed zone(Cz)

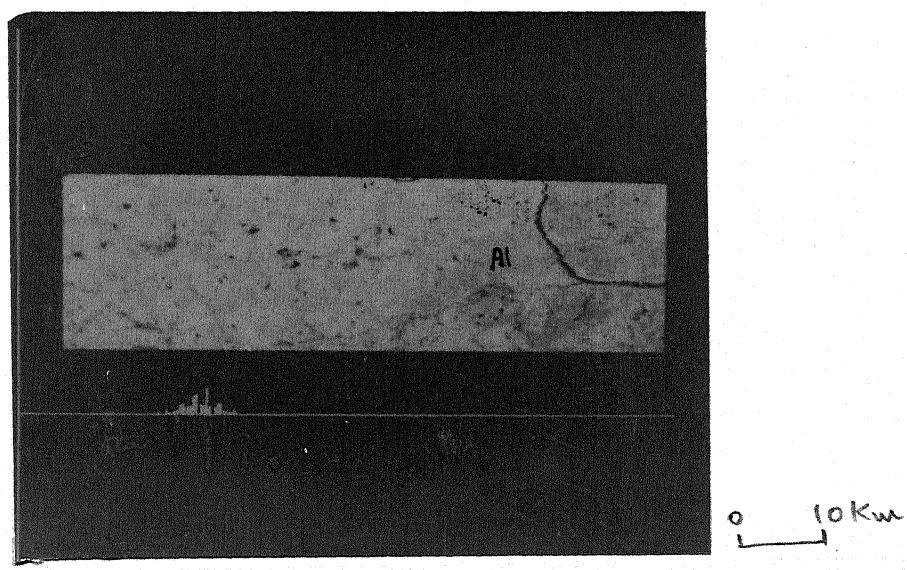

Fig.3.16 Band ratio (2/4) with histogram (Rajpur region).
Al = Alluvial tract

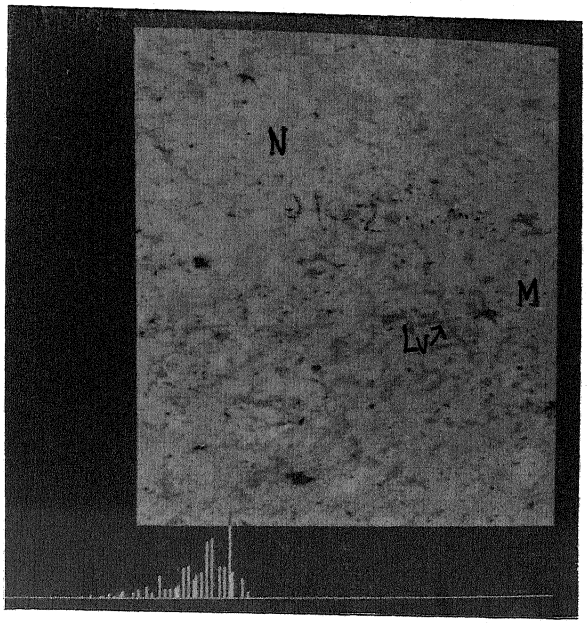

Fig.3.17 Linear stretching with histogram (Bhatapara-Tilda region). N = Nipania limestone; Lv = linear feature with vegetation; M = Moisture zone

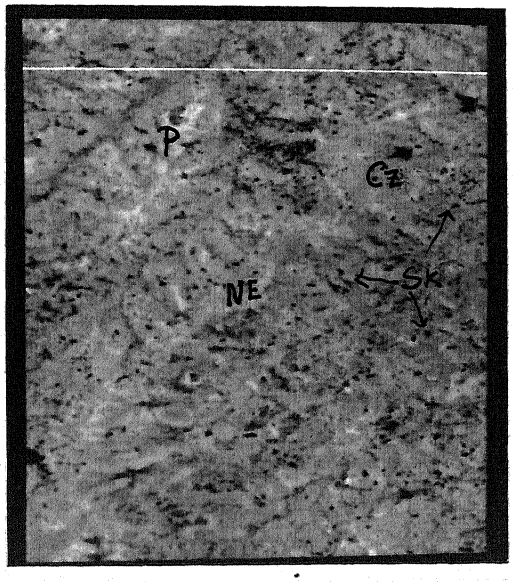

Fig.3.18 Linear stretching with histogram (Arjuni-Pendri region) NE = Newari limestone; P = Pendri limestone; Cz = Collapsed zone with vegetation; Sk = sinkhole

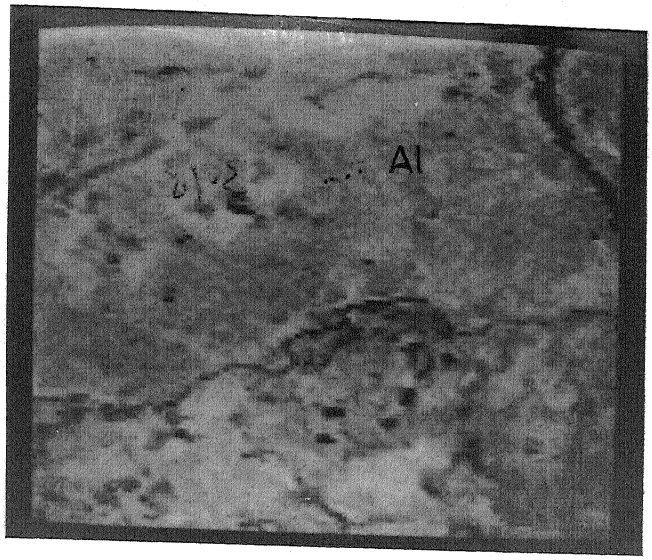

Fig.3.19 Linearly stretched and enhanced part of the Jamunia river (Rajpur region). Al= Alluvial tract

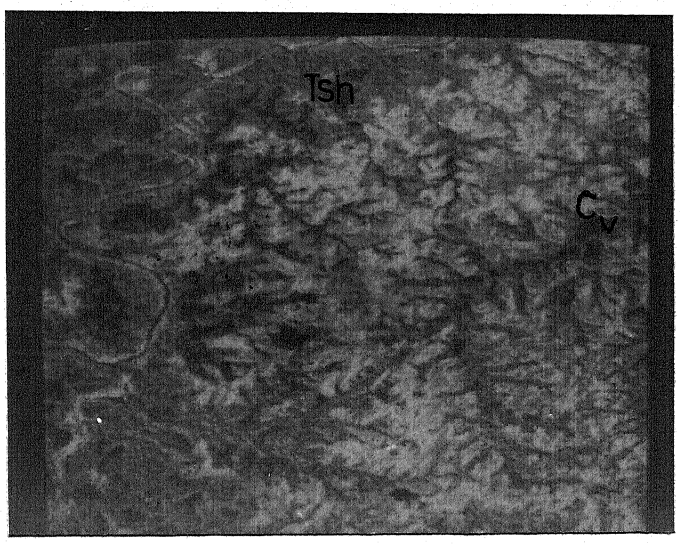

Fig.3.20 Selective stretching of part of the Jamunia river (Bhatapara-Tilda region); C_v = cavernous zone

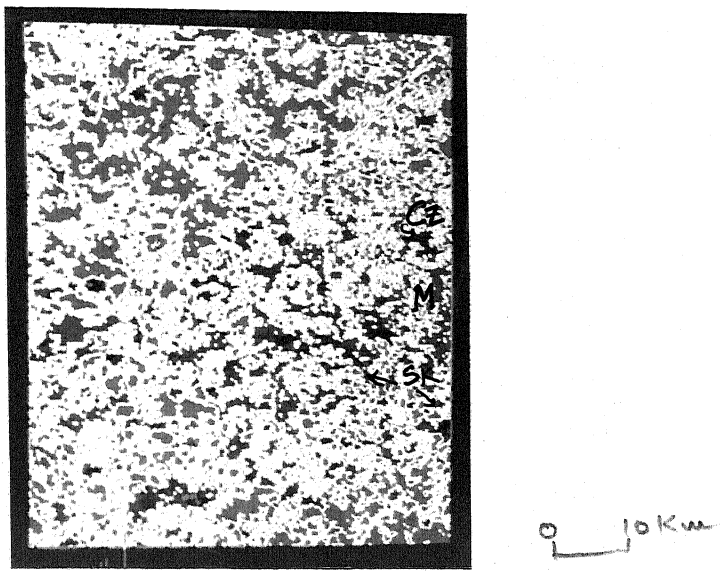

Fig.3.21 Edge enhancement section (Bhatapara-Tilda region).
Cz = Collapsed zone; Sk = Sinkhole;
M = Moisture-stress zone

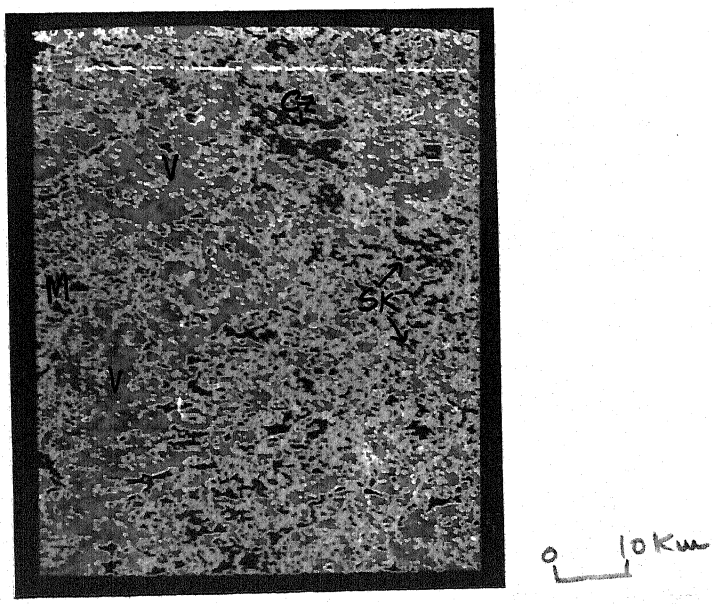

Fig.3.22 Edge enhancement section (Arjuni - Pendri region).
Red patches indicates dense vegetation (V) in fracture zones and dark patches indicate moisture zones (M) and sinkholes (Sk) and Collapsed zone(Cz)

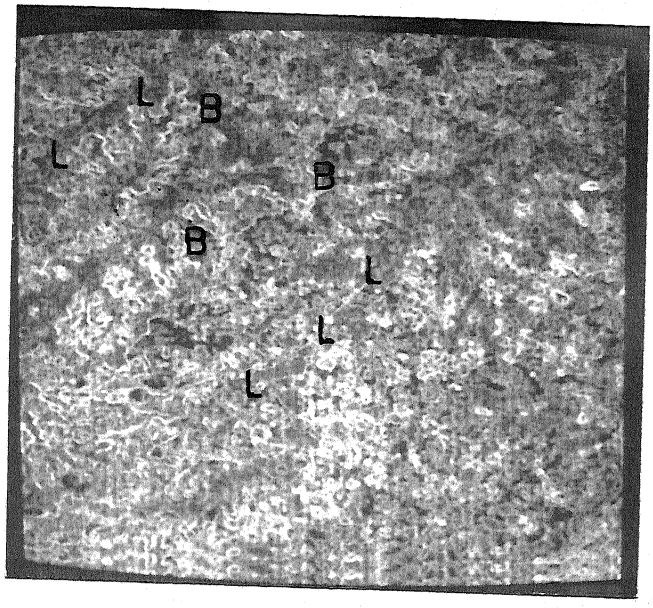

Fig.3.23 Edge enhancement section (Arjuni - Pend:

B = Limestone edged boundary; L-L = Line

Fig.3.24 Stretched and enhanced part of the Jamunia river (Rajpur-Arjuni region). F--F = Fracture zone; Cz = Collapsed zone

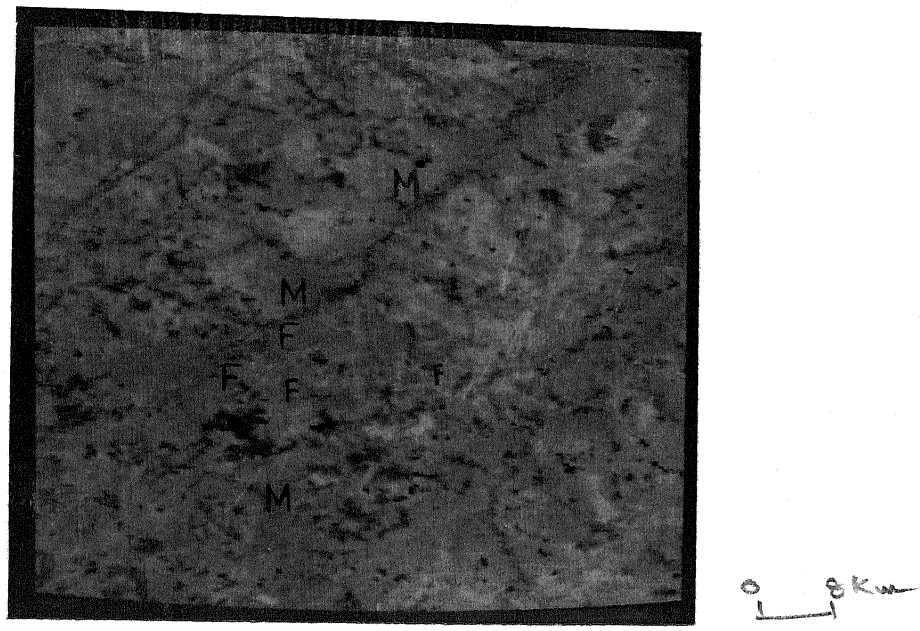

Fig.3.25 Stretched and enhanced part of the Jamunia river (Bhatapara-Tilda region). M = Moisture zone; F--F = Fracture zone

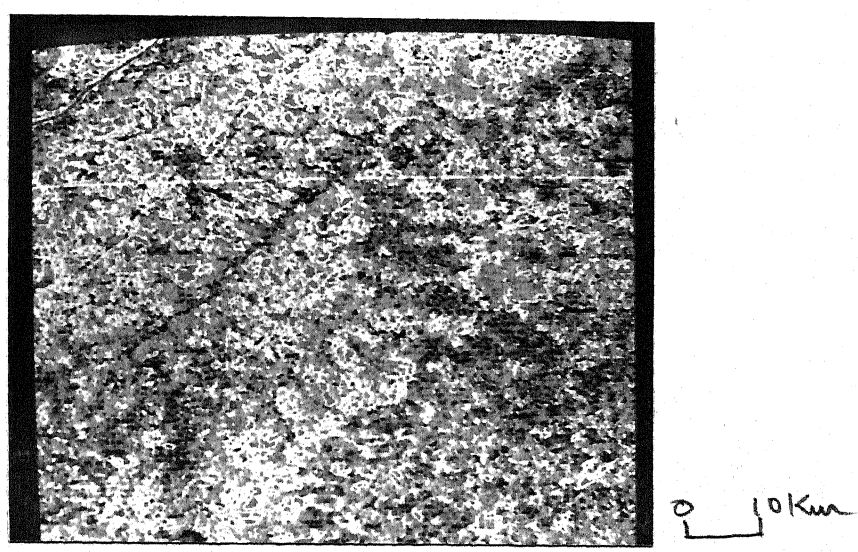

Fig.3.26 Thematic map representing various land cover types in the study area

Fig.3.27 Histogram equalization of the study area

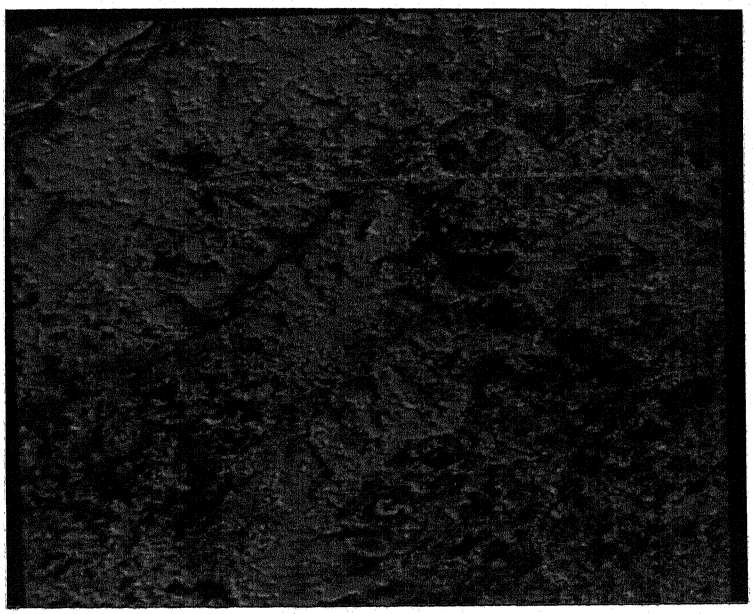

Fig.3.28 Histogram equalization with vegetational enhancement. All red patch areas represent vegetation

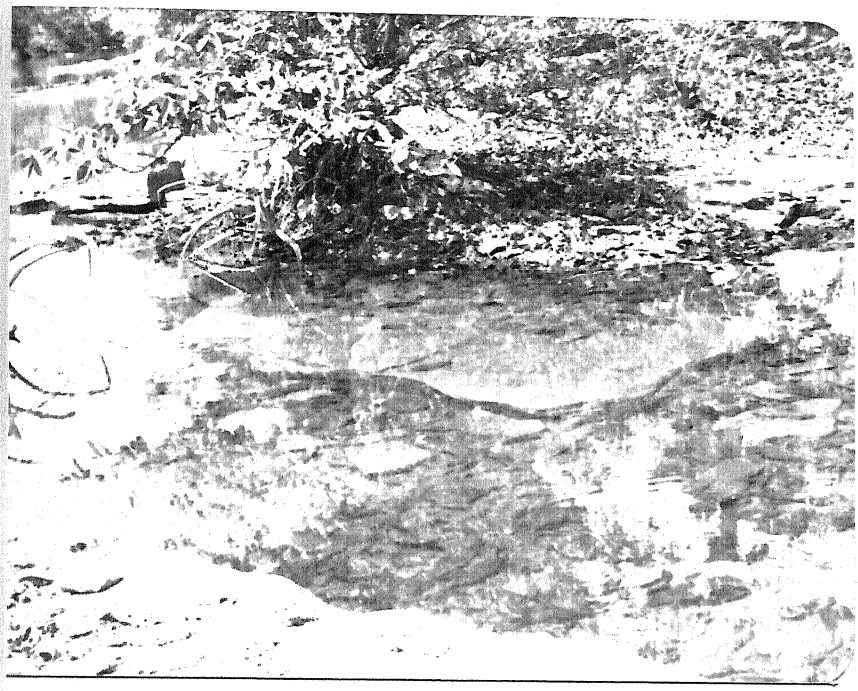

ur Shale in the course of Jamunia river near Murpar

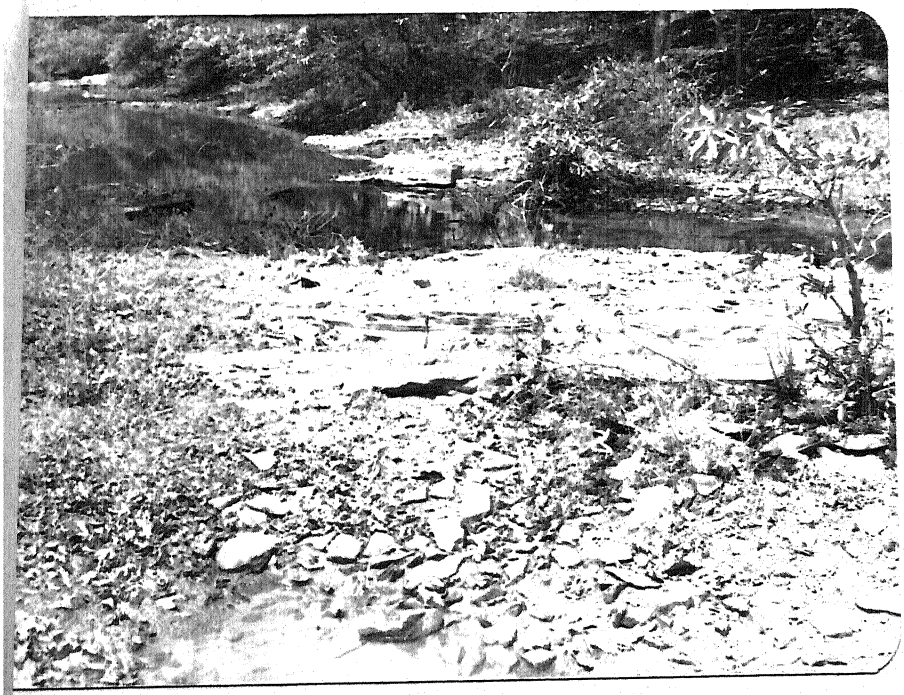

Raipur shale on the banks of Jamunia river Diggi

CHAPTER 4

DIGITAL IMAGE PROCESSING FOR MORPHOLOGY, DRAINAGE AND LAND USE

4.1 GENERAL

To study the morphology and drainage features, windowed noise-free images and pseudocoloured superimposed procedures were used. The terrain in the central portion of the Chhattisgarh basin has distinct and characteristic variations in terms of sinkholes, fracture zones and drainage. A study on regional scale of the fractured and collapsed zones in the limestone formations would facilitate the recognition of changes in the morphological units within the terrain. As the area (Fig.3.1) undertaken in present study being extensive and covered with vegetation over the limestone terrain, digital data of Landsat-4 has been chosen for analysis and interpretation. Different morphological units have been characterized by the changes in their reflectance values. In addition to the linear structural features, drainage characteristics are recognized on a regional scale. The processed picture data aid in the delineation of sinkholes and fracture zones within the limestone and to understand the nature of groundwater in terms of its proximity to the surface. In the present chapter, the analysis of the processed data has been carried out on the basis of which, the morphological and structural

features have been demarcated. Various sinkhole and collapsed zones have been mapped to indicate their association with areas of groundwater availability. An attempt has been made to determine the water table depth using reflectance values within the collapse zones filled with sediments as also the moisture zones.

Different techniques used in the present study have been described in the previous chapter. After checking all possible combinations, bands 1, 2 and 4 have been considered best for the present study.

The limestone and shale contacts have been clearly visible in the enhanced windowed data. Based on the tonal contrast, various morphological features have been identified along with distinct boundaries. Surface water bodies have been mapped using band-4. Areas with dense vegetative growth indicative of proximity to groundwater have been mapped using superimposition procedure. Ground checks have been carried out at various places for checking the interpretation. The results are presented in this chapter.

4.2 MORPHOLOGY

Hydrogeological deciphering is possible by studying the morphological features with characteristic relief. Since relief gives an idea about the distribution of surface water infiltration, recharge, discharge and also the flow of groundwater, study of the typical relief forms in a terrain

provide an understanding of the groundwater conditions of that terrain. Morphological units have been mapped on the basis of tone and erodability characteristics of the limestones.

The study area has been divided on the basis of morphological features into

(i) Upland tract

(ii) Valley tract

(iii) Moisture-stress areas

The upland area is characterized by its flat topography with thin soil cover. The valley tract exhibits sharp cutting nature throughout the central region. The moisture-stress zone is situated in the eastern and north-eastern part of the Jamunia river. To delineate the various morphological features of the study area, bands 2 and 4 as also the enhanced noise-free photographs along with pseudocoloured products have been used.

4.2.1 Upland Tract

This tract in general has flat topography and exhibits variation in tonal contrast in the imageries due to variations in soil texture and groundwater situation. When compared to the adjacent low lying areas, this tract is lighter in its tone due to its high reflectance. Within this tract, distinct differences in reflectance values enable a subdivision into two clear regions (designated as C_1 and C_2 in Figs.3.2 to 3.6 and 3.8 to 3.10). The tract between

Batapara and Hathbandh (C_1) could be recognized by its tone due to high reflectance values (ranging between 70-77) compared to the tract 'C_2'near Arjuni (ranging between 65-71). The tract 'C_2' is evidenced with frequent intermixing of upland and ravinous-like features and exhibits a wide variation in its erosional status, as in the areas around Arjuni and Mopar villages. For example in the tract around Arjuni, erosional features such as depressions and gullies with gently rounded cross sections (Figs.3.3 and 3.9) are distinctly visible. The fracture zones in the upland tract offer channels for surface water percolation to underground streams. The natural tanks, oval in shape, are indicative of the sinkholes with surface storage. Groundwater in this region is tapped through dug wells in fractured and jointed zones. The hydrogeological details of the same are presented in the subsequent chapter.

4.2.2 Valley Tract

This tract is characterized by its intense erosion due to solution action and associated erosional features such as gullies with intermittent ridges that distinctly stand out in relief. The ravinous gullies might have formed due to solution action along joints and fractures. The erosion action is maximum throughout the valley area. This erosion due to solution action continues its operation until groundwater is reached. Thus the depth of gullies in the

valley tract indicates the depth of groundwater. The deep valleys with a dry appearance can be seen clearly in the pseudocoloured figures (indicated as 'VL' in Fig.3.8). The area with the Banjari river channel is characterized by a wide flat terrain underlain by shale. The impervious nature is clearly indicated from the flow of surface water (as designated by 'W' in Fig.3.3). Field checks confirm such an observation.

4.2.3 Moisture-stress Areas

These areas have been delineated on the generated images on the basis of their dark tone (Figs.3.24 and 3.25) reflecting the presence of finer nature of the sediments with proximity to groundwater. For example, the irregular areas with dark tones around Nawapara and Kesili villages (Figs.3.11 and 3.14 as indicated by 'M') as well as around Arjuni are the moisture-stress areas which have also been confirmed through ground checks. Here the groundwater occurs in both confined and unconfined conditions. The coarser pediment zones that are prominent locations for good groundwater conditions, could be clearly indicated along the slopes of the upland tract. Surface water tanks and filled zones have been noticed on band-4 and pseudocoloured imageries (indicated by 'M' in Figs.3.9 and 3.12). Extensive vegetation in these areas reflects proximity of the groundwater. A number of collapsed zones have been mapped in the eastern part of Banjari river. One of such collapsed

zones with distinct oval outliers with water storage tank is identified and indicated in the Baloda Bazar area (indicated by 'CZ' in Figs.3.9 and 3.12). On the Western part of this ringed area, an irregular collapsed zone of a relatively older age has been identified with heavy vegetation (indicated by 'M' in Fig.3.12). Another ring-shaped unit has been located in the northern part of the imagery which might have been recently formed by intermixing of sinkholes with vegetation (indicated by 'H' in Fig.3.12). Dense vegetational areas were enhanced through histogram equalization and false colouring (Fig.3.2&) representing the areas of groundwater availability in the proximity. Tube wells in few of these localities have been operating with good yield. Field checks have confirmed dense vegetation in these areas. The hydrogeological aspects of these areas are detailed in the subsequent chapters.

4.3 DRAINAGE AND STRUCTURAL CONTROL

Drainage pattern plays an important role in influencing the hydrogeological situation of the limestone terrain. In general, drainage conforms to the regional structural trends. In the present work the structural control of the drainage pattern has been established on the basis of observations of the drainage network as related to the fractures and lineaments on the satellite imageries. The drainage pattern largely is of rectangular type. The Jamunia

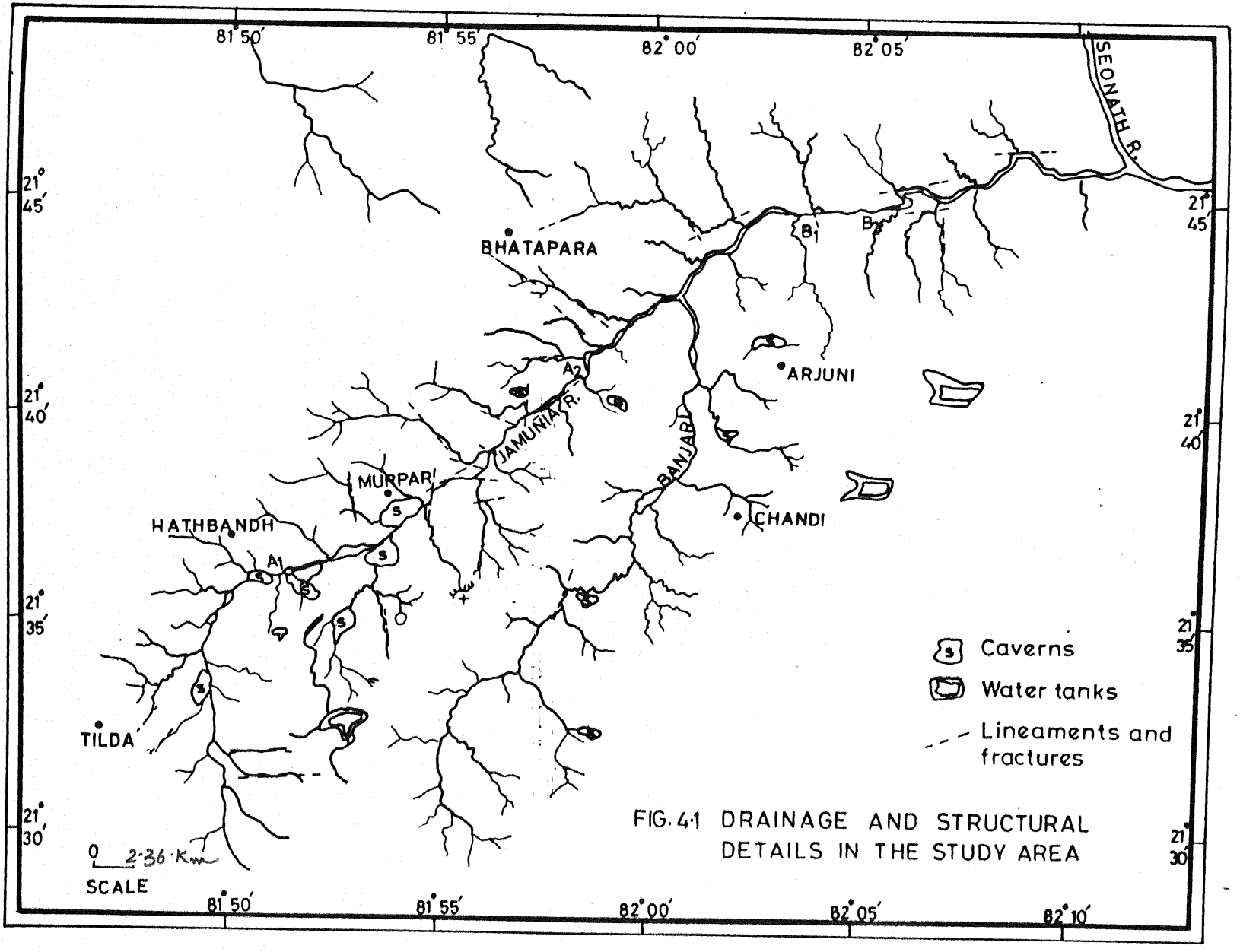

FIG. 4·1 DRAINAGE AND STRUCTURAL DETAILS IN THE STUDY AREA

river itself is flowing in a fracture zone trending NE-SW. Initially the river has a N-S trend which suddenly changes to east (Fig.3.8) following a fracture zone (indicated by 'F' in the Fig. 4.1). In this fracture region, considerable amount of water infilters, contributing to solution action. Consequently, caverns of various sizes have formed (indicated by 'S' in Fig.4.1) through which the water flows internally at the place indicated by 'A_1' in Fig.4.1, and emerges again at 'A_2' on the surface. Similar feature also been evidenced again at another place (indicated by 'B_1' in the Fig.4.1) infiltering through a fracture zone and subsequently emerging at B_2. In fact, all the streams contributing to the Jamunia river are controlled by regular fracture patterns. The drainage network in general is very coarse in texture with considerable amount of water infiltering through fractures and solution channels. Near Kesili and Nawapara, caverns of large size and sinkholes have been identified along the river (indicated by an arrow in Fig.3.8) reflecting the soluble nature of the limestone. In the eastern and southern parts of the river (Figs.3.6 and 3.12) surface water bodies, such as tanks are noticed as dark isolated spots in the terrain. Some of the tanks were connected to the natural drainage. The major part of the Jamunia river course appears to be controlled by these structural features. Present study revealed that the groundwater in these areas is under confined conditions.

4.4 IMAGE CLASSIFICATION

Supervised classification method, Bayes maximum likelihood classifier, has been used to classify various land use in the study area. The details of the classifier have been elaborately dealt in chapter 2. The statistical analysis of the training set of the classes given in Appendix III. The parameters calculated for all classes in four bands are, mean, variance-covariance matrix, inverse of variance - covariance matrix and correlation coefficients of all classes in four bands.

Once the above parameters are calculated for a training set, we may take reflectance values in all four bands of any unknown feature based on the logic described in chapter 2.

Initially training set itself is subjected to the classifier giving 40 samples for each class. Classes 1,3, and 5 have been classified 100 percent except class 2 which is 97.5 percent. The confusion matrix has given in the results showing the accuracy of the above mentioned classification. Infact before selecting the classes , the data has been checked with the numerical separation technique, which gives the idea about the overlapping. A divergence/transformed divergence matrix has been calculated to represent the separability within the classes. As can be seen from the results (Appendix III) all the classes mentioned above were

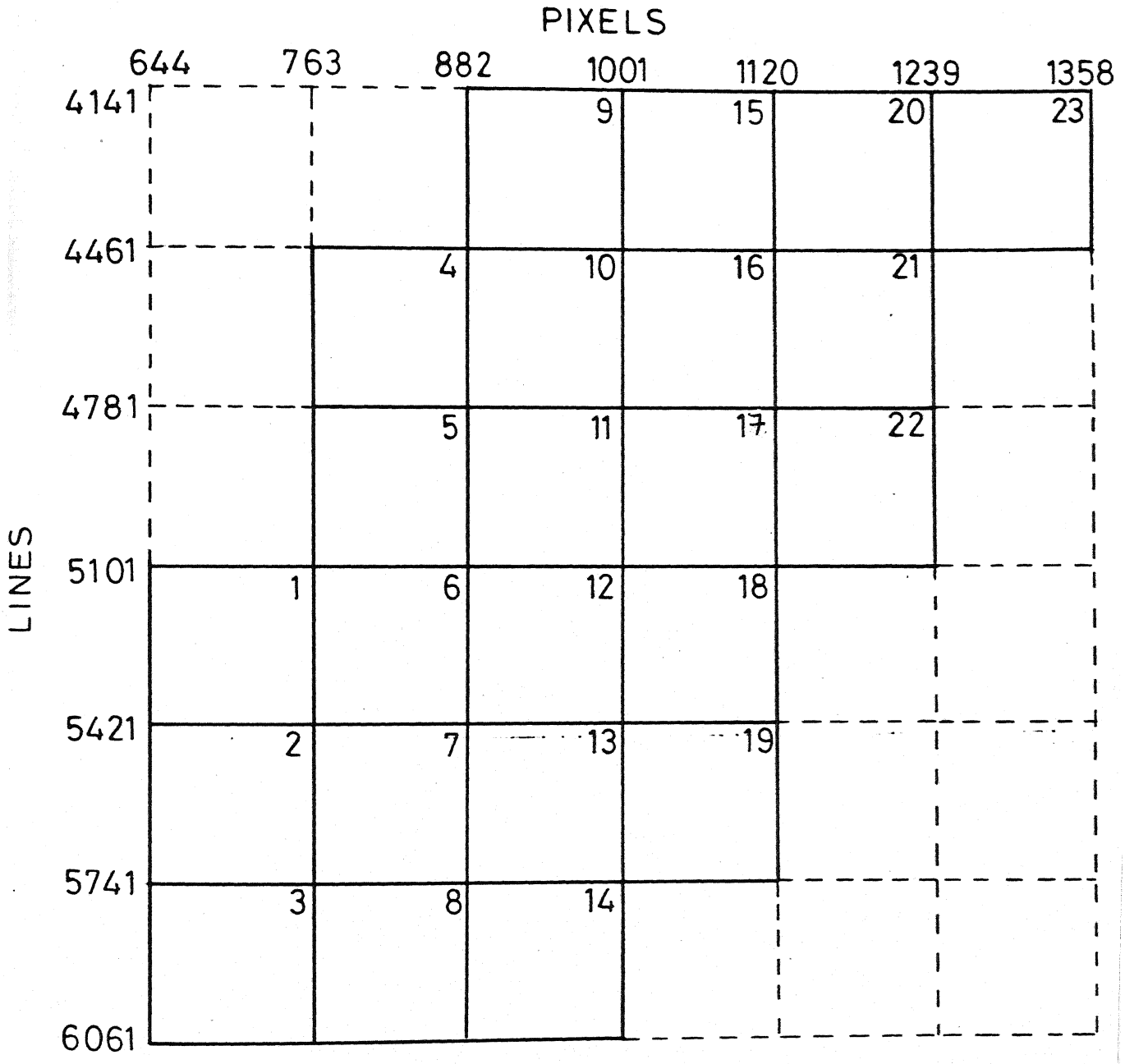

FIG. 4.2 INDEXING OF LINE PRINTER MOSAIC

(Each Unit Represents A Line Printer Map

Placed In The Pocket)

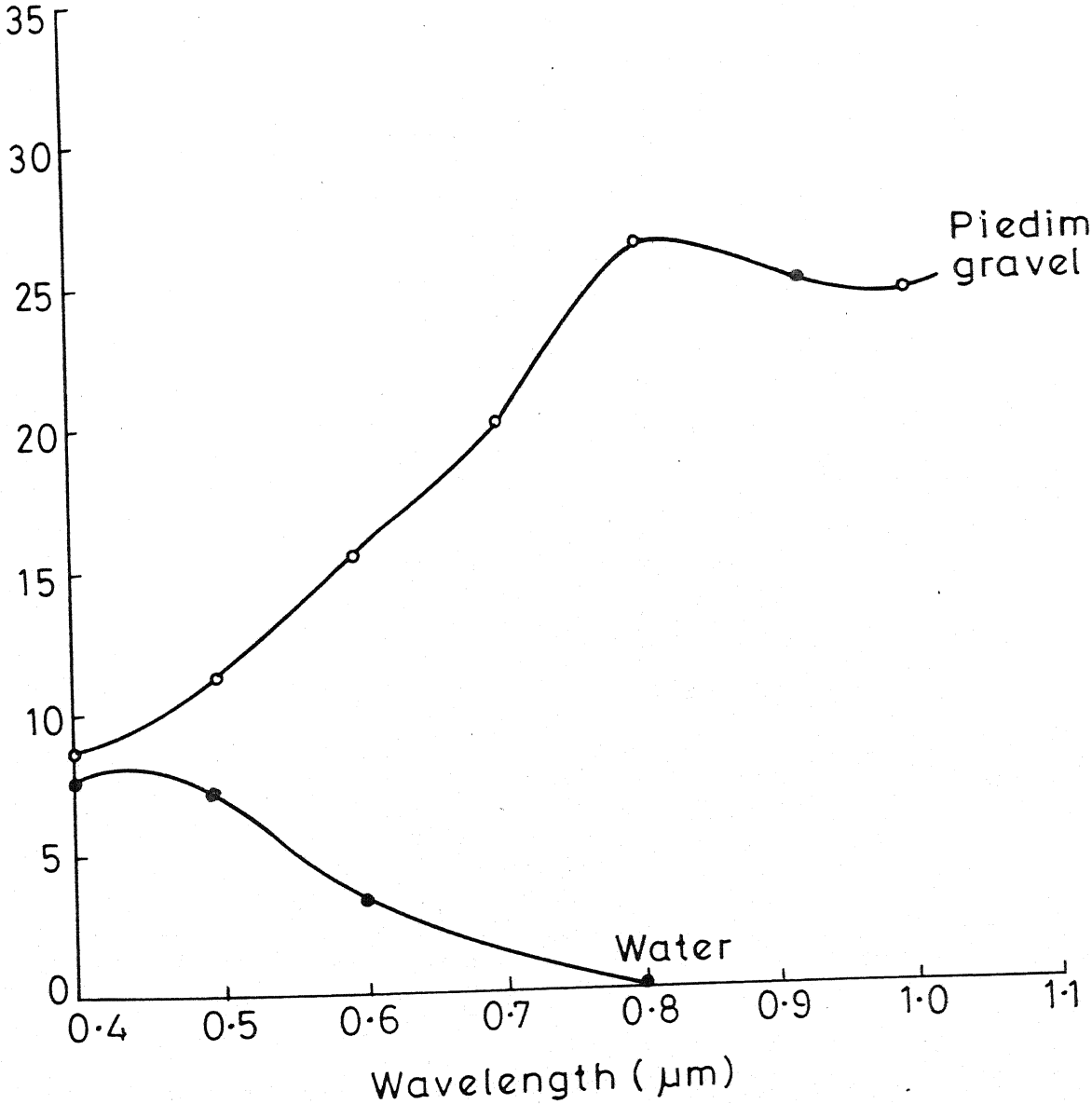

FIG. 4.3 REFLECTANCE CURVES

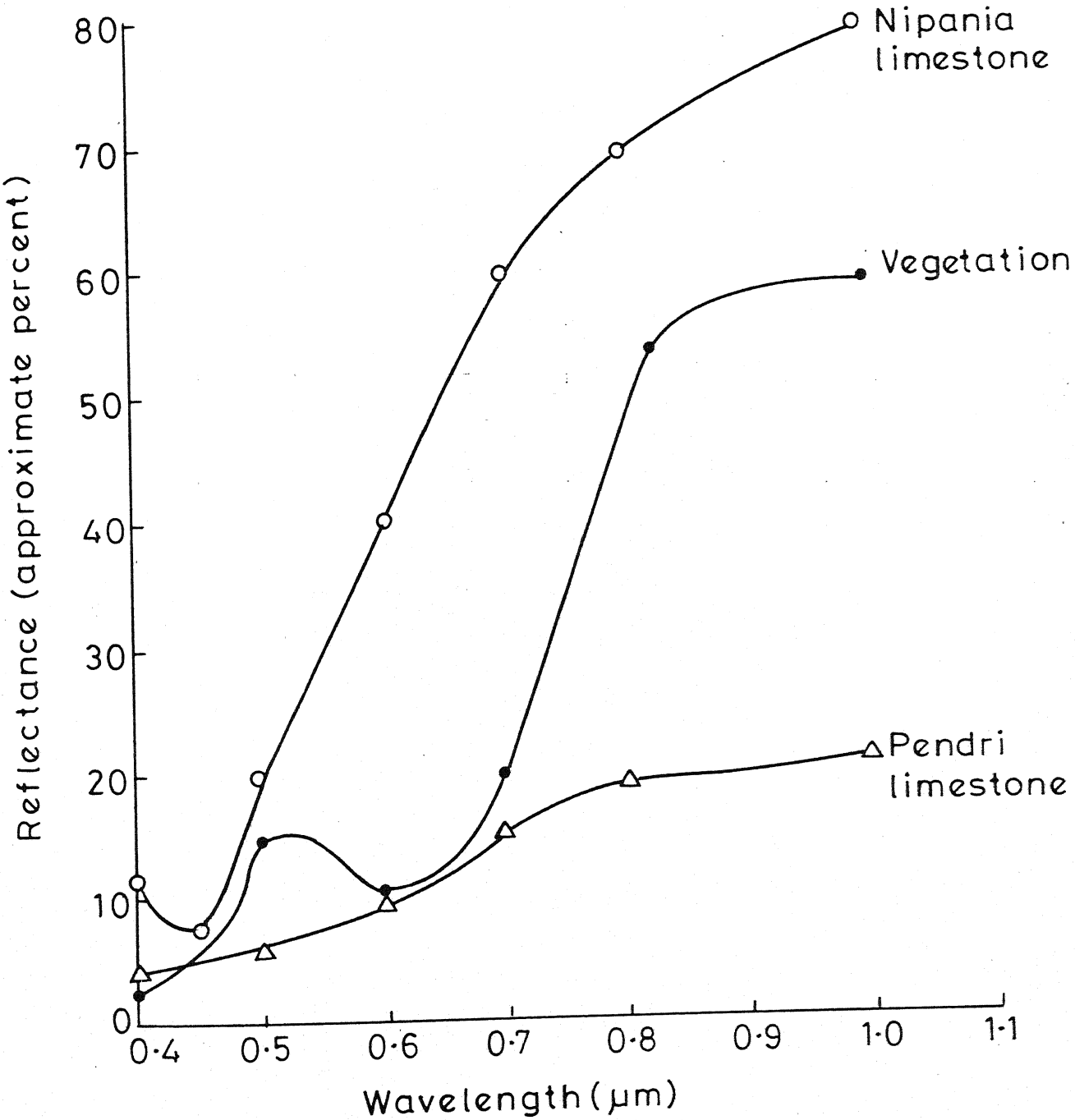

FIG. 4·4 REFLECTANCE CURVES FOR DIFFERENT LANDUSE

easily separable (e.g. classes 1,3,4 and 5 are almost near to 2000, but the class 2 has around 1850 which may be due to one misclassification shown in confusion matrix). Later the entire study area has been classified based on the same logic and a line printer map (Fig.4.2) has been produced to represent the classes. Spectral reflectance curves (Figs.4.3 and 4.4) have also been plotted for various land use of the study area.

CHAPTER 5

GROUNDWATER SITUATION AND AQUIFER CHARACTERISTICS

5.1 GENERAL

The carbonates in the central part of Chhattisgarh basin belong to fourth cycle (Schnitzer,1969) of the carbonate-shale sequence. These limestone formations have been demarcated as three distinct members namely Nipania, Pendri, and Newari members. A comprehensive hydrogeologic investigation of these limestone aquifers includes not only the distribution, structural features favourable for the recharge and storage of groundwater but also their performance characteristics as aquifers. The potential aquifer zones within the members together with all the associated structural features have been delineated on the basis of the remote sensing analysis as detailed in the previous chapters. Investigations have been carried out on groundwater situation and the seasonal fluctuations of water levels in the limestone aquifers. Systematic pumptests have been conducted in selected areas, delineated through enhancement procedures and the aquifer characteristics have been worked out. A brief study on the chemical quality of the water has also been undertaken to provide complete picture of the groundwater hydrogeology of the study area. The present chapter contains the details on all these aspects.

5.2 GROUNDWATER SITUATION

Primary porosity plays an important role in making the limestone formations as good aquifers. If the formation has little primary permeability with sluggish water circulation, it will be a poor aquifer. On the other hand if the rocks are in the zone of active circulation of water, they are usually cavernous and are likely to be good aquifers.

The carbonate rocks in the present area are of Raipur group, comprising of Chandi formation. The Chandi formation has been classified into three limestone members- (1) Nipania (2) Pendri and (3) Newari. Of the three members, the Newari member is less soluble being massive and devoid of joints. The recharge area for this member is in the eastern side where it has a gradational contact with Gunderdehi shale. Within this member in the area around Baloda Bazar on the northern side, collapsed zones with storage tanks were noticed, and these are formed by underground channeling from gradational contact. A collapsed zone with an irregular shape has been identified near Arjuni. This collapsed zone was later filled by recent alluvium which forms a potential source for groundwater occurrence within the member. The Pendri member is a soluble limestone. This formation is extensively jointed, fractured and has stromatolites. Shale intercalations are noticed towards the top surface of this member. Extensive solubility in this limestone on a wide

scale has been noticed along the fracture zones as well as along the contact of the stromatolites connected by carbonate mud. Sinkholes, potholes and collapsed zones are more prominent in this zone. Sinkhole distribution appears to have been controlled by weak zones associated with fractures. Surface drainage contributes to a substantial part of the recharge through fractures in the western and north-western region. As this member is more cavernous and has fractures and lineaments, it acts as a storage reservoir with high yield.

The Nipania limestone is coarse to medium-grained with mottled appearance. Fractures and lineaments are scantily distributed. This member, at a relatively higher elevation compared to the other members, has its recharge from monsoon. On the eastern side of the member, fracture zone helps in the recharge which contributes in the groundwater storage across the boundary to the Pendri limestone member. Sinkholes and collapsed zones are conspicuously absent in this member.

The limestone members in general are characterized by secondary porosity and permeability controlled by fractures and solution channels. Since dissolution is localized along the weak zones, such porosity and permeability is highly directional and strongly anisotropic. Using remote sensing techniques, the fracture traces and

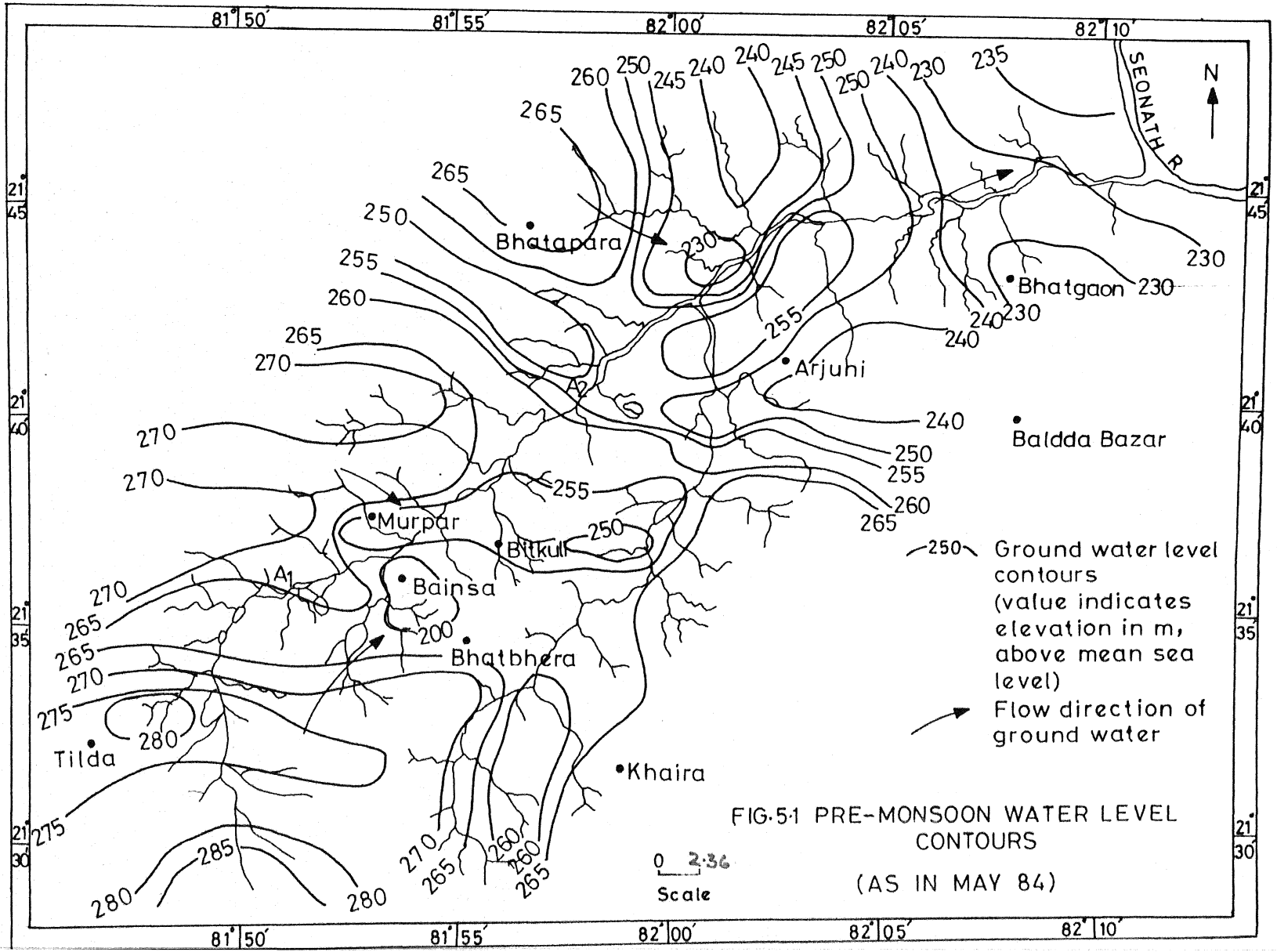

FIG·5·1 PRE-MONSOON WATER LEVEL CONTOURS

(AS IN MAY 84)

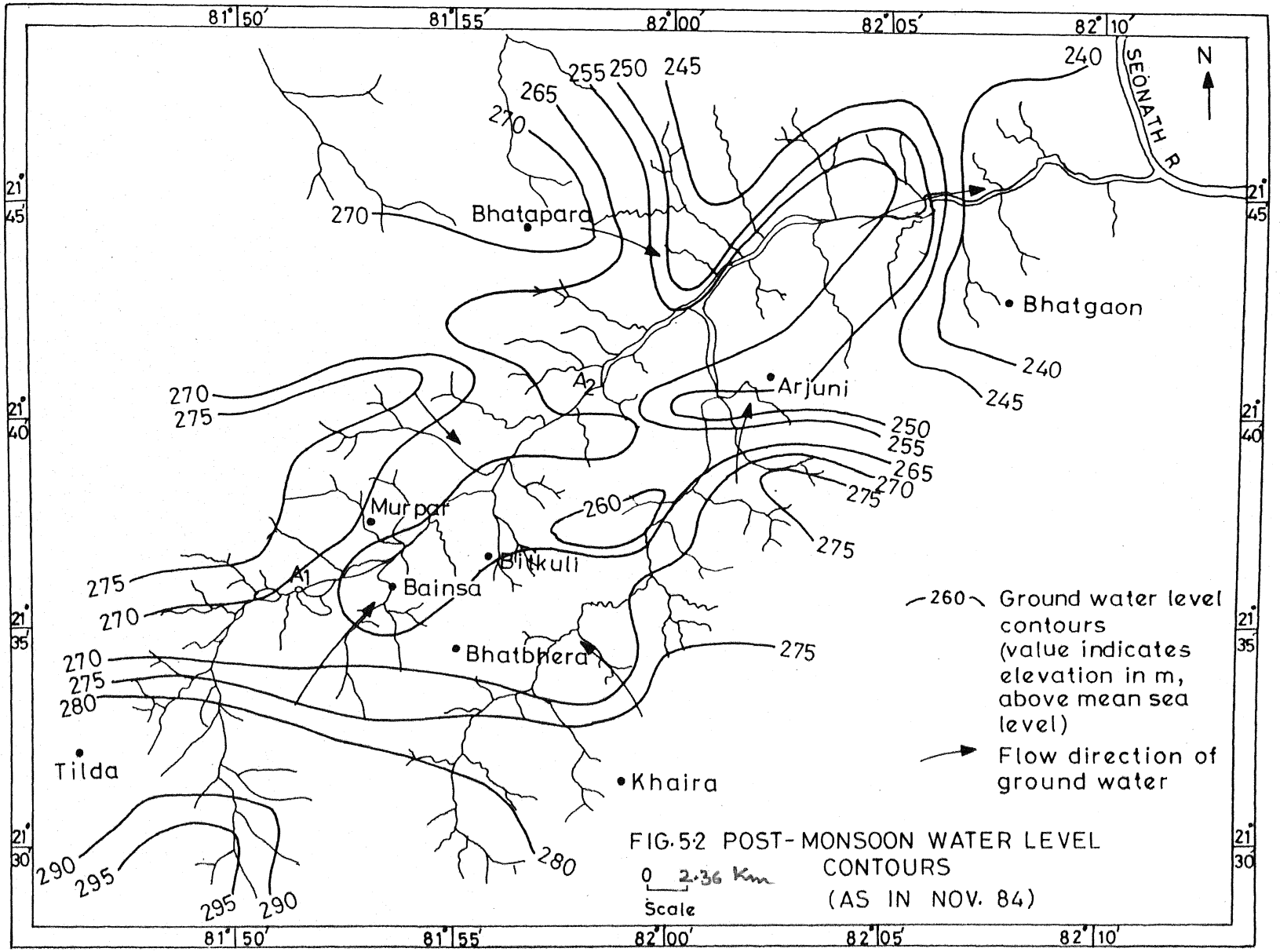

FIG. 5.2 POST-MONSOON WATER LEVEL CONTOURS (AS IN NOV. 84)

lineaments were delineated which act as a guide for locating the directional zones of porosity and permeability and hence could be used as a guide for locating the high capacity wells in these limestone members.

The main source of recharge to the groundwater in the study area is through precipitation and surface run-off. The surface run-off that approaches the sinkholes and other openings and channels in bed rock quickly replenishes the groundwater. It has been observed that the surface drainage as it enters the cavernous areas infilters to the subsurface as evidenced from sudden depletion of water in the channel (Fig.4.1-in the span from A_1 to A_2). The water again emerges into the channel as soon as the cavernous region is passed. This is clearly evidenced in Fig.3.9 where the channel on the northwestern corner has water (indicated by the lighter tone) while in the cavernous region (Fig.3.8) same channel in its upstream portion has no water. (as evidenced from its dark tone in the central part of the picture). The lithological and structural variations also control the depth to water level in the area. The movement of groundwater in carbonate rocks is complicated by variation of permeability within the limestones. To demarcate the recharge and discharge areas in the study area, water level maps (Figs.5.1 and 5.2) have been prepared for both pre-monsoon and post-monsoon periods. The arrows in these maps indicate the possible flow direction of the groundwater. The flow of water has gradient from west and

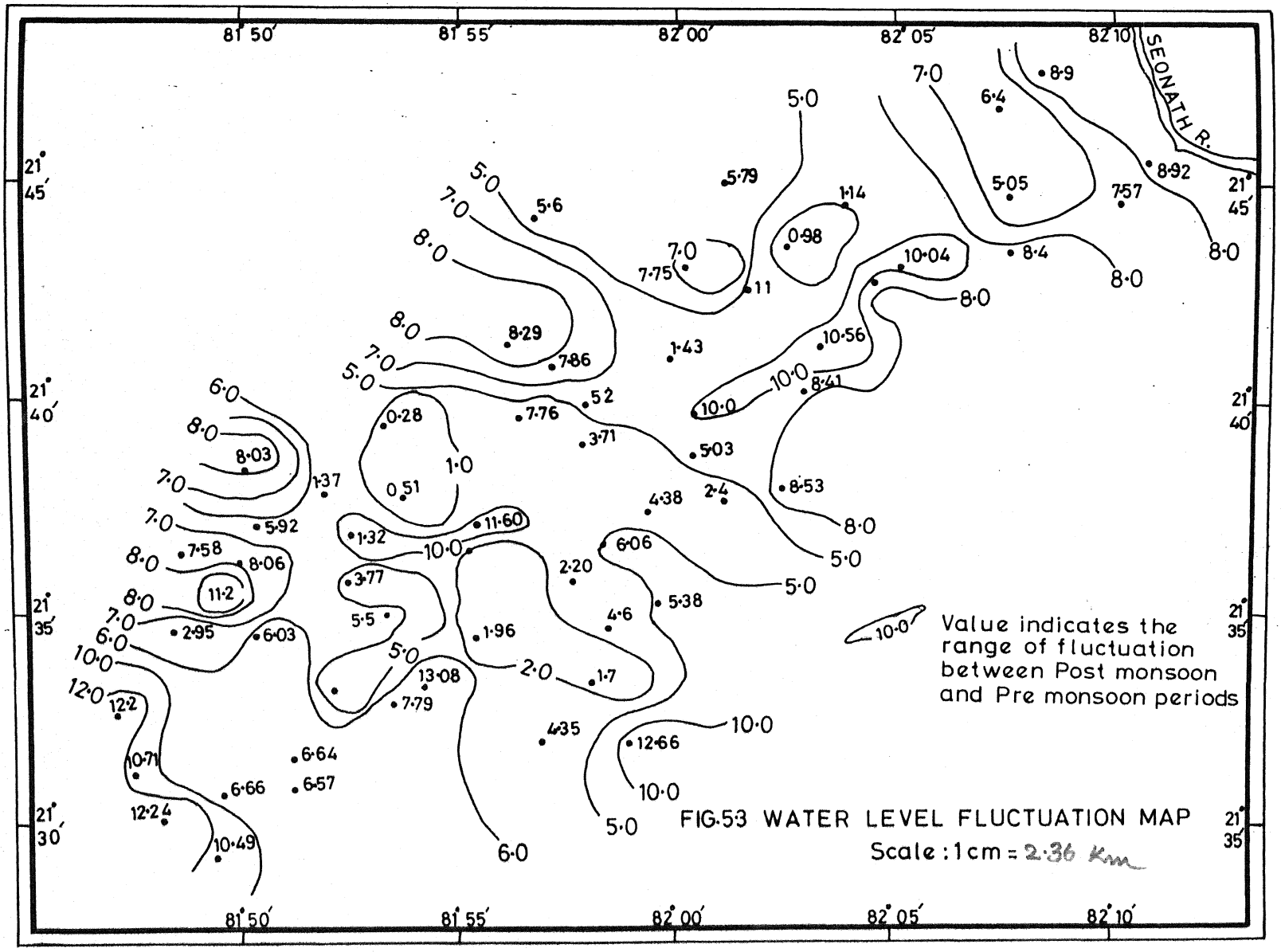

FIG.5.3 WATER LEVEL FLUCTUATION MAP

Scale : 1 cm = 2.36 Km

northwest and northern regions sloping toward the central region where the Pendri member is located. Water level fluctuation map (Fig.5.3) prepared on the basis of water level data in the pre-monsoon and post-monsoon periods has revealed maximum fluctuations wherever the sinkholes, caverns and collapsed zones are present. For example the fluctuations are maximum around Bitkuli, Arjuni and Jhipania and also within a substantial part of the central region where soluble and cavernous Pendri member is present. In general, the groundwater topography indicates a flow in the direction of river flow. However, there are extended patches (Figs. 5.1 and 5.2) where the groundwater slope appears to be very small indicating the likelihood of storage in caverns. Due to the presence of caverns acting as sinks, we cannot expect one to one correspondence between the groundwater topography and the river flow direction.

Concentrations in the groundwater samples from different locations together with the values of conductivity and pH are given in Appendix-IV. The general increase in the hardness in the direction of groundwater flow noticed can be attributed to the increased duration of the contact of water in caverns and filled zones within limestone member. In the recharge areas, the higher concentration of CO_2 and low dissolved solids content promotes dissolution of calcite and dolomite. The water in the study area in general can be

classified as weakly alkaline and soft to moderately hard. Existence of numerous ponds in the area appears to have a pronounced affect on chemical quality of groundwater in the wells. It has been observed that locations close to ponds show high HCO_3 and corresponding hardness as evidenced in Arjuni, Bhatapara and Bothidih villages.

5.3 METHODOLOGY OF PUMP TESTS

5.3.1 General

In the present work, aquifer evaluation has been carried out through pumptests on tube wells penetrating limestone aquifers in selected areas delineated by the author through remote sensing analysis, and time-drawdown as well as time-recovery data have been collected. As there is no observation well facility, all the pump tests were carried out in the abstraction well itself and the data has been analyzed by Theis, Jacob and Walton methods.

5.3.2 Analysis and Interpretation of Aquifer Tests

The hydraulic functions of an aquifer are to store and transmit water. The ability to store water is expressed by the storativity, S, defined as the volume of water that an aquifer releases from or takes into storage per unit surface area per unit change in the component of head normal to that surface. For water table aquifers, S is equivalent to specific yield of material, and its values range between 0.01 and 0.35; values for artesian aquifers range from 10^{-6} to 10^{-3} (Walton, 1964).

The ability to transmit water is expressed by transmissivity, T, defined as the rate of flow of water, at the prevailing temperature, through an unit width of the aquifer extending over the entire saturated thickness of the aquifer, under hydraulic gradient of 100 percent, which means 1 m drop in head over 1 m of flow distance. Transmissivity is numerically equal to the product of permeability of the material and the saturated thickness of the aquifer. In addition to the transmissivity, the storativity has also been calculated, using Walton's specific capacity equation, for the wells in the carbonate terrain.

All the test data analyzed have been obtained on the tube wells penetrating limestone and shale aquifers. Discharge from the wells has been measured with 90° V-notch or with piezometer depending upon the convenience and the facilities available in the field at individual well sites. The water level fluctuations during the drawdown and recovery periods have been monitored in the wells.

In the tests conducted, the static water level has been measured in the well in each case prior to the commencement of pumping operation. The drawdown measurements are made since the start of pumping at different time intervals during the pumping. These intervals have been chosen depending upon the pattern of variation in the drawdown in the well. Pumping has been carried out for

duration ranging from 250 min. to 6 hours, depending upon the availability of the wells. The recovery measurements were carried out on the cessation of pumping and the time intervals in recovery measurements are chosen to reflect the true pattern of variation of water levels during recovery period. Time-drawdown data have been interpreted using Jacob's straight line method and the recovery data by Theis (1935) method. To determine the storativity, Walton's specific capacity equation has been utilized.

5.3.3 Theis Non-equilibrium Formula

Theis (1935) derived an equation, the non-equilibrium or Theis formula, which describes spatio - temporal effects of pumping a well in an aquifer. When a well penetrating an aquifer is pumped at a constant rate, the influence of discharge extends outward with time. In the case of confined aquifer, the rate of decline of head multiplied by storage coefficient and summed over the area of influence equals the discharge. As the water is drawn from the storage, the head in an aquifer continues to decline for sufficient period of time and thus it is not possible for steady state flow to be attained.

The Theis non-equilibrium equation is written as

$$s = \frac{Q}{4 \pi T} \int_{u}^{\infty} \frac{e^{-u}}{u} du \qquad \ldots\ldots (5.1)$$

$$= \frac{Q}{4 \pi T} W(u)$$

Where

$$u = \frac{r^2 S}{4 T t}$$

and consequently

$$S = \frac{4 T t u}{r^2} \qquad \ldots\ (5.2)$$

s = drawdown, in m, measured in a piezometer at a distance 'r' from the abstraction well,

Q = constant well discharge in m^3/day,

S = storativity, dimensionless,

T = transmissivity of the aquifer in m^2/day,

and

t = time in days since pumping started.

The value of the integral expression in equation 5.1, also written as W(u) and read as "Well function of u," is given by an infinite series.

$$\int_u^\infty \frac{e^{-u}}{u}\, du$$

$$= W(u) = - 0.577216 - \log_e u + u - \frac{u^2}{2.2!} + \ldots \qquad (5.3)$$

Values of 'W(u)' for values of 'u' as tabulated in Wenzel (1942), are given by Ferris and others (1962). If the values

for W(u), Q and s are known, value of 'T' can be calculated from equation 5.1. However, to know W(u), both 's' and 'T' must be known, and in the equation 5.1, 'T' occurs both in the argument of the function and divisor of the exponential integral. Hence 'T' and 'S' can not be determined directly from this equation. However, a graphical method of superposition, popularly known as "type curve method", devised by Theis and described by Jacob (1940) is used to determine 'T' and 'S'.

From the equation 5.1 and 5.2 it follows that

$$\log s = \log W(u) + \log \frac{Q}{4 \pi T} \qquad \ldots\ldots (5.4)$$

$$\log t = \log \frac{1}{u} + \log \frac{r^2 S}{4 \pi T} \qquad (5.5)$$

Equation (5.5) has been arranged for having 1/u and t by Walton instead of u and r^2/t of Theis. For a constant discharge Q, the equations 5.4 and 5.5 show that W(u) is a function of (1/u) in the same way that 's' is a function of t. Therefore, it is possible to superimpose the data curve (s vs t plot) on double log sheet of the same modulus as type curve on the Walton's type curve (W(u) vs 1/u plot on double log sheet), keeping the corresponding axes of the graphs parallel to each other and in such a way that the data best fit the type curve. The match point coordinates W(u), 1/u, s and t are read from the respective graphs, which are used in

equations 5.1 and 5.2 to estimate the aquifer parameters T and S.

5.3.4 Jacob's Method

Jacob (1950) modified equation 5.1 to devise a straight line graphical method for the estimation of transmissivity and storativity. This method is based on the fact that when u becomes small (u<0.01) the sum of terms beyond three terms (Eqn. 5.3) is not significant and the equation 5.1 reduces to -

$$s = \frac{2.3\ Q}{4\ \pi\ T} \log \frac{2.25\ T\ t}{r^2\ S} \qquad \ldots\ldots\ (5.6)$$

This shows that a plot of drawdown against the logarithm of time after pumping started describes a straight line. The slope of the line is equal to $2.3\ Q/4\pi T$. For a pumped well, if the change in drawdown ($s=s_2 - s_1$) is taken over one log cycle of time ($\log_{10} t_2/t_1=1$), then the slope becomes

$$s = \frac{2.30\ Q}{4\ \pi\ T} \qquad \ldots\ (5.7)$$

and

$$T = \frac{2.30\ Q}{4\ \pi\ \Delta s} \qquad \ldots\ldots\ (5.8)$$

when s = 0, the equation 5.6 becomes

$$s = 0 = \frac{2.30\ Q}{4\ \pi\ T} \log \frac{2.25\ T\ t}{r^2 S} \qquad \ldots.(5.9)$$

or

$$\log_{10} 1 = \log_{10} \frac{2.25\ T\ t}{r^2 S} \qquad \ldots\ldots(5.10)$$

which gives

$$S = \frac{2.25\ T\ t}{r^2} \qquad \ldots\ldots (5.11)$$

where S,T, and r are previously defined and t is the time intercept; that is, the time at which drawdown (s) is zero. Equation 5.11 is used only with data obtained from observation well.

when $u = 0.01$, equation 5.1 gives

$$t = \frac{r^2\ S}{0.01 \times T} \qquad \ldots\ldots (5.12)$$

or

$$t = \frac{10^2 \times r^2\ S}{T} \qquad \ldots\ldots (5.13)$$

Equation 5.12 gives the time, in minutes, that must elapse before straight line method can be applied to pumping test data. This shows that t increases as r and S increase, and decreases with increasing T. For a constant value of S/T, t increases with r and for an abstraction well, where r is the radius of well, t is the smallest.

Using equation 5.12, the periods of time that must elapse before the straight line method can be applied to a pumped well of 7.6 Cm radius, for several assumed values of S

TABLE 5.1

MEMBER	LOCALITY	DEPTH OF WELL (m)	DISCHARGE m^3/DAY	TRANSMISSIVITY VALUES m^2/DAY			
				TIME DRAWDOWN	TIME RECOVERY	AVERAGE	
NIPANIA	BHATAPARA	67.07	468.78	100.63	114.61	106.62	1.509
NIPANIA	TILDA	60.00	545.04	121.71	124.69	123.20	1.330
NIPANIA	MURPAR	60.00	408.78	103.25	106.93	105.09	8.330
PENDRI	BITKULI	60.97	590.46	203.90	205.84	204.87	4.050
PENDRI	BAINSA	60.97	13626.00	1134.00	1176.98	1155.49	2.050
PENDRI	BHATBHERA	59.45	610.44	171.97	171.97	171.97	2.100
PENDRI	ARJUNI	60.97	772.14	144.99	153.69	149.34	3.050
NEWARI	KHAIRA	56.40	6540.48	704.17	717.10	710.63	6.404

and T were calculated (Appendix-V). This shows that except for five values, which are for combinations of T and S, rarely observed in the field, straight line method is applicable after a time period ranging from few seconds to 16 minutes of pumping. This indicates that the time-drawdown data from the pumped wells could be analyzed, using straight line method, to calculate the values of transmissivity.

5.3.5 Theis Recovery Method:

The recovery of water level in a well since the pumping is stopped is expressed in terms of residual drawdown s, which is the difference between the static water level and the actual water level measured at a certain time t since pumping stopped. The recovery method has an advantage in that, due to the constant rate of recharge 'Q' being equal to the mean rate of discharge 'Q' during pumping, the drawdown variations resulting from slight differences in the rate of discharge do not occur during recovery (Kruseman and Ridder, 1970). The residual drawdown, s', during the recovery period according to Theis(1935), given by:

$$s' = \frac{Q}{4 \pi T} \ln \frac{4 T t}{r^2 S} - \ln \frac{4 T t'}{r^2 S'} \quad \ldots\ldots (5.14)$$

where

s' = residual drawdown in m,

r = distance in m from pumped well to observation well

(if observations are recorded in the pumped well itself, r = r_w = effective radius of the pumped well)

S' = storativity during recovery, dimensionless,

S = storativity during pumping, dimensionless,

T = transmissivity in m^2/day,

t = time in days since pumping started,

t' = time in days since pumping stopped

and

Q = rate of recharge = rate of discharge, in m^3/day.

When S and S' are constant and equal and u = $(r^2S/4Tt)$ is sufficiently small, equation 5.14 can be written as

$$\triangle s' = \frac{2.30\ Q}{4\ \pi\ T} \log \frac{t}{t'} \qquad \ldots\ (5.15)$$

For the data obtained in observation well or in the abstraction well, s' vs t/t' is plotted on semilog paper (with t/t' on logarithmic scale) and a straight line is fitted through the plotted points. The slope of the straight line is given by $2.30Q/4\pi T$. The transmissivity (T) is obtained from the expression

$$T = \frac{2.30\ Q}{4\ \pi\ \triangle s'} \qquad \ldots\ (5.16)$$

where $\triangle s'$ is the drawdown for unit log cycle (of t/t') as measured on s' versus t/t' plots.

5.3.6 Specific Capacity Equation for Storativity Determination

Walton (1970) reported an expression for specific capacity as related to transmissivity (T) and storativity (S) for a well pumped at a constant rate in a homogenous isotropic non-leaky artesian aquifer infinite in aerial extent. According to him, the specific capacity can be written as

$$\frac{Q}{s} = \frac{T}{264\left[\log \frac{Tt}{2693\, r_w^2\, S}\right] - 65.5} \qquad .....(5.19)$$

where

Q/s = specific capacity, in gpm/ft,

Q = discharge in gpm,

s = drawdown, in feet,

T = transmissivity in gpd/ft,.

S = storativity, fraction,

r_w = normal radius of well in feet,

and

t = time after pumping started, in minutes.

If the following field units are taken,

Q/s in $m^3/day/m$

Q in m^3/day

s in m

T in m^2/day

r_w in m

t in days

then the equation 5.19 can be written as

$$\frac{Q}{s} = \frac{26.3 \times 10^{-7} \times T}{\log \frac{T\,t}{r^2_w\,S} - 7.71} \qquad \ldots (5.20)$$

Rearranging the terms,

$$\log \frac{1}{S} = \frac{26.3 \times 10^{-7} \times T \times S}{Q} + 7.71 - \log \frac{T\,t}{r^2_w} \qquad \ldots\ldots (5.21)$$

Thus the storativity of an aquifer can be obtained from specific capacity data. This procedure was adopted in the present study since no observation well facility was available. For this purpose, the values of Transmissivity (T) as obtained with Jacob's (1950) method have been used. Although such estimates are not very accurate these were useful in characterizing the nature of the aquifer.

5.4 PUMP TEST DATA ANALYSIS

Pumptests have been conducted on selected tube wells located in the productive aquifer zone delineated within the three limestone members. The transmissivity and storativity values were estimated on the basis of time-drawdown and time-recovery data.

Pumptest results on wells located within the delineated zone

5.4.1 Nipania member

1. Bhatapara

The well is situated near Bhatapara Railway station. This well with a diameter of 0.2 m penetrates to a depth of 67.07 m., through 42.60 m of aquifer horizon.

$Q = 468.78\ m^3$ / day

$t = 0.208$ days

Depth = 67.073 m

$\triangle s = 0.853$ m

$\triangle s' = 0.749$ m

(a) Jacob's Method using drawdown data, [Fig 5.4]

$$T = \frac{2.3 \times Q}{4 \pi \triangle s}$$

$$= \frac{2.3 \times 468.78}{4 \times \pi \times 0.853} = 100.63\ m^2/day$$

(b) Recovery test [Fig. 5.5]

$$T = \frac{2.3 \times Q}{4 \times \pi \times \triangle s'}$$

$$= \frac{2.3 \times 468.78}{4 \times \pi \times 0.749} = 114.61\ m^2/day$$

$T_{av} = 107.62\ m^2$ /day

(c) Storativity

$$\text{Log } \frac{1}{S} = \frac{26.3 \times 10^{-7} \times T \times s}{Q} + 7.71 - \log \frac{Tt}{r_w^2}$$

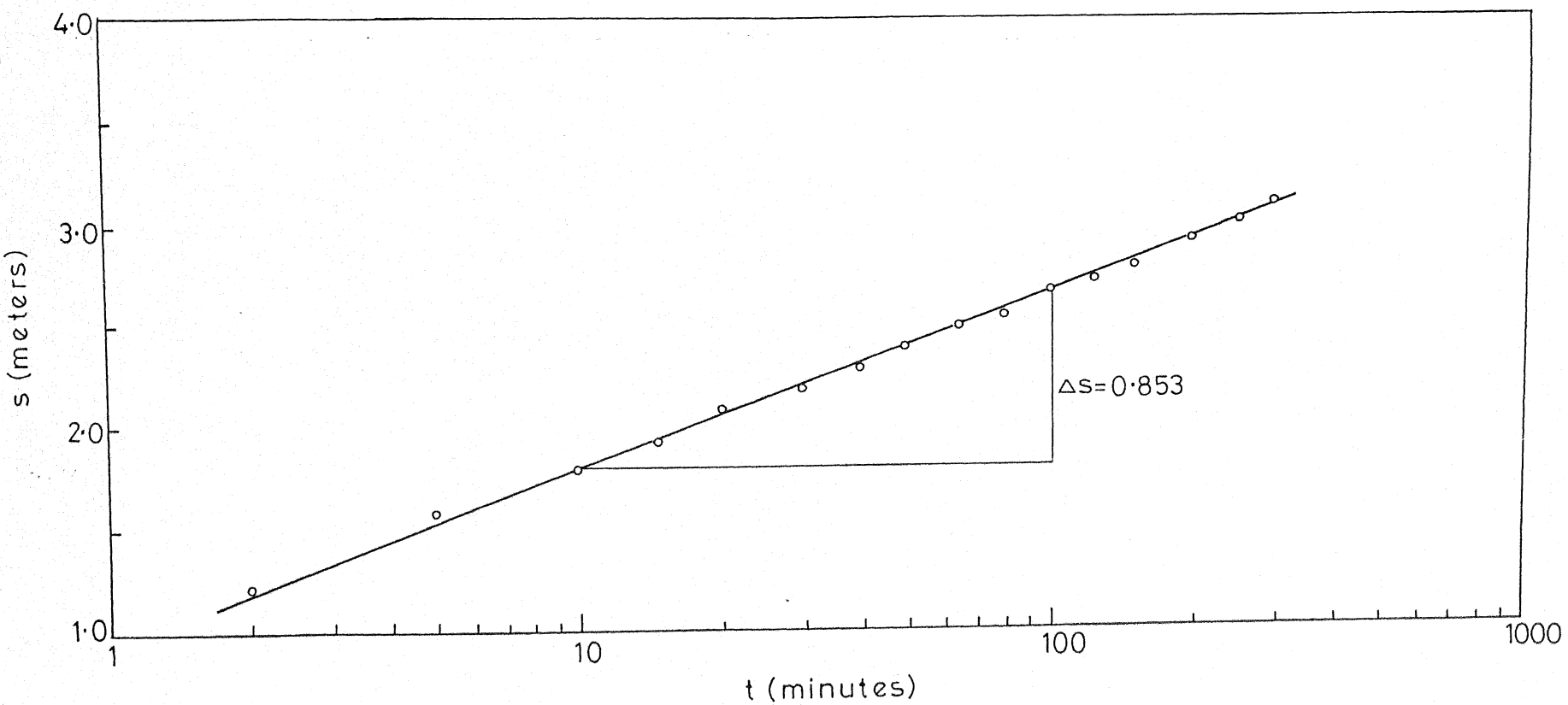

FIG. 5·4 TIME DRAWDOWN GRAPH FOR WELL AT BHATAPARA

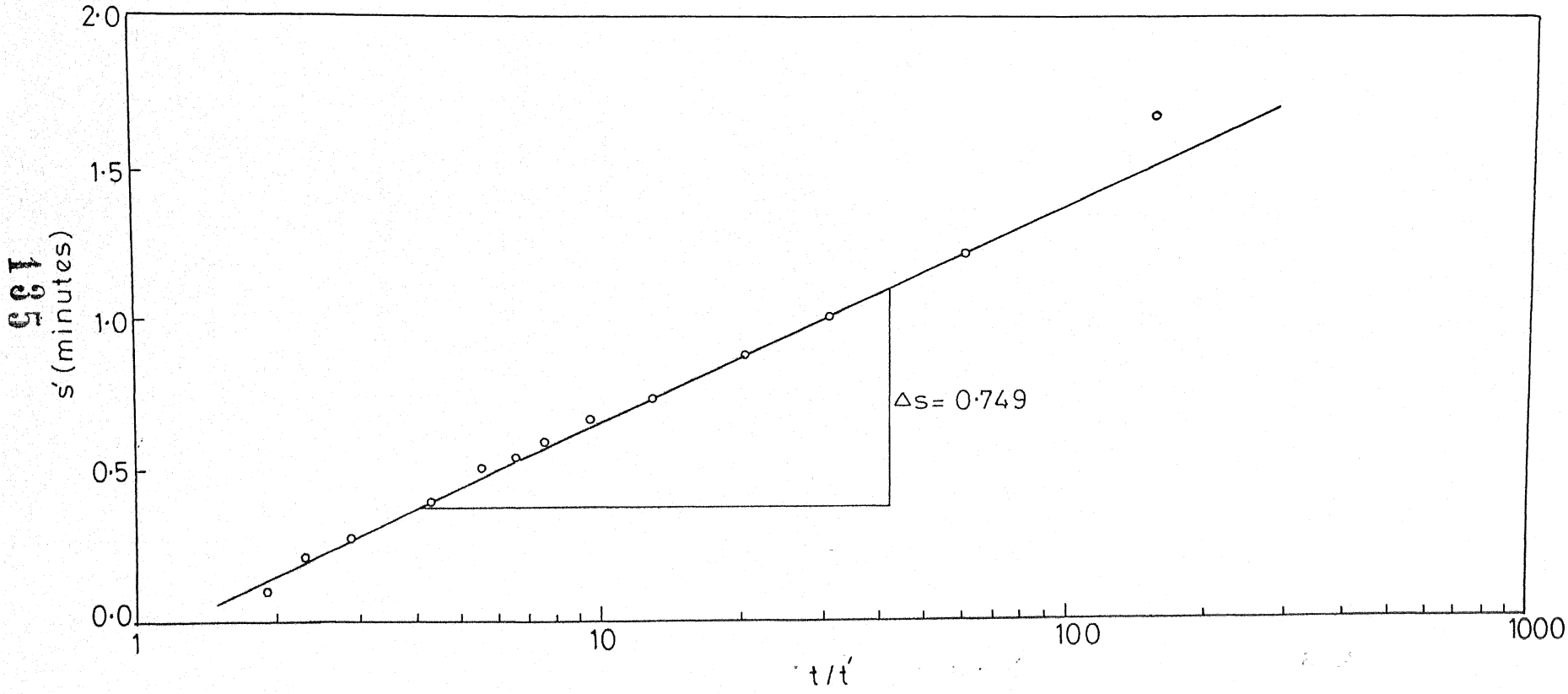

FIG.5.5 TIME-RECOVERY GRAPH FOR WELL AT BHATAPARA

$$= \frac{26.3X10^{-7}X107.62X1.75}{468.78} + 7.71 - \log \frac{107.62X0.208}{(0.203)^2}$$

$$\log \frac{1}{S} = 4.975$$

$$S = 1.059 \times 10^{-5}$$

2. Tilda

$Q = 545.04\ m^3$ /day

$t = 0.229$ days

Depth = 60 m

$r_w = 0.20$ m

$\triangle s = 0.82$ m

$\triangle s' = 0.80$ m

(a) Jacob's Method using drawdown data, [Fig.5.6]

$$T = \frac{2.3 \times Q}{4\ \pi \triangle s}$$

$$= \frac{2.3 \times 545.04}{4 \times \pi \times 0.82} = 121.71\ m^2/day$$

(b) Recovery test [Fig. 5.7]

$$T = \frac{2.3 \times Q}{4 \times \pi \times \triangle s'}$$

$$= \frac{2.3 \times 545.04}{4 \times \pi \times 0.80} = 124.69\ m^2/day$$

$T_{av} = 123.20\ m^2/day$

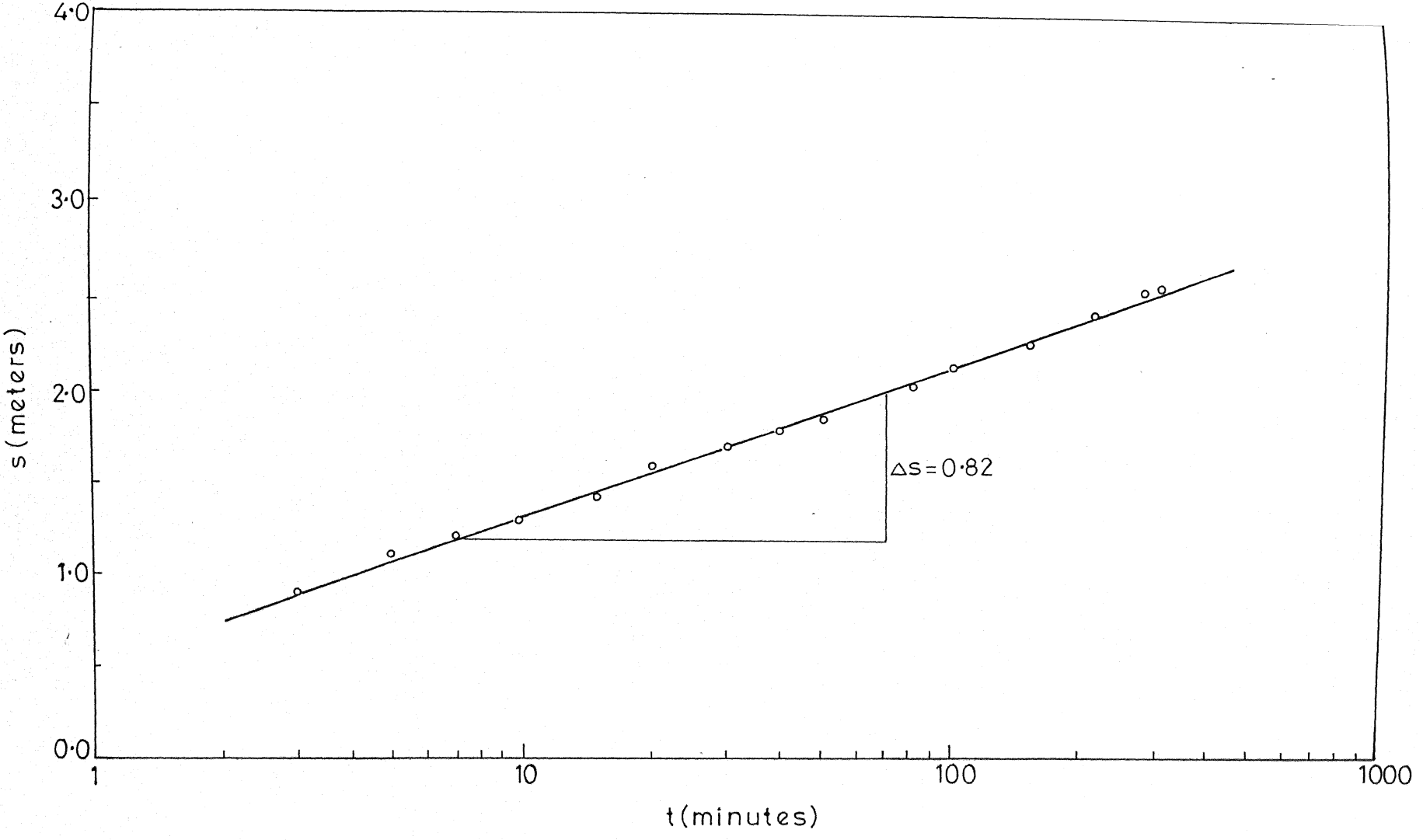

FIG. 5·6 TIME-DRAWDOWN GRAPH FOR WELL AT TILDA

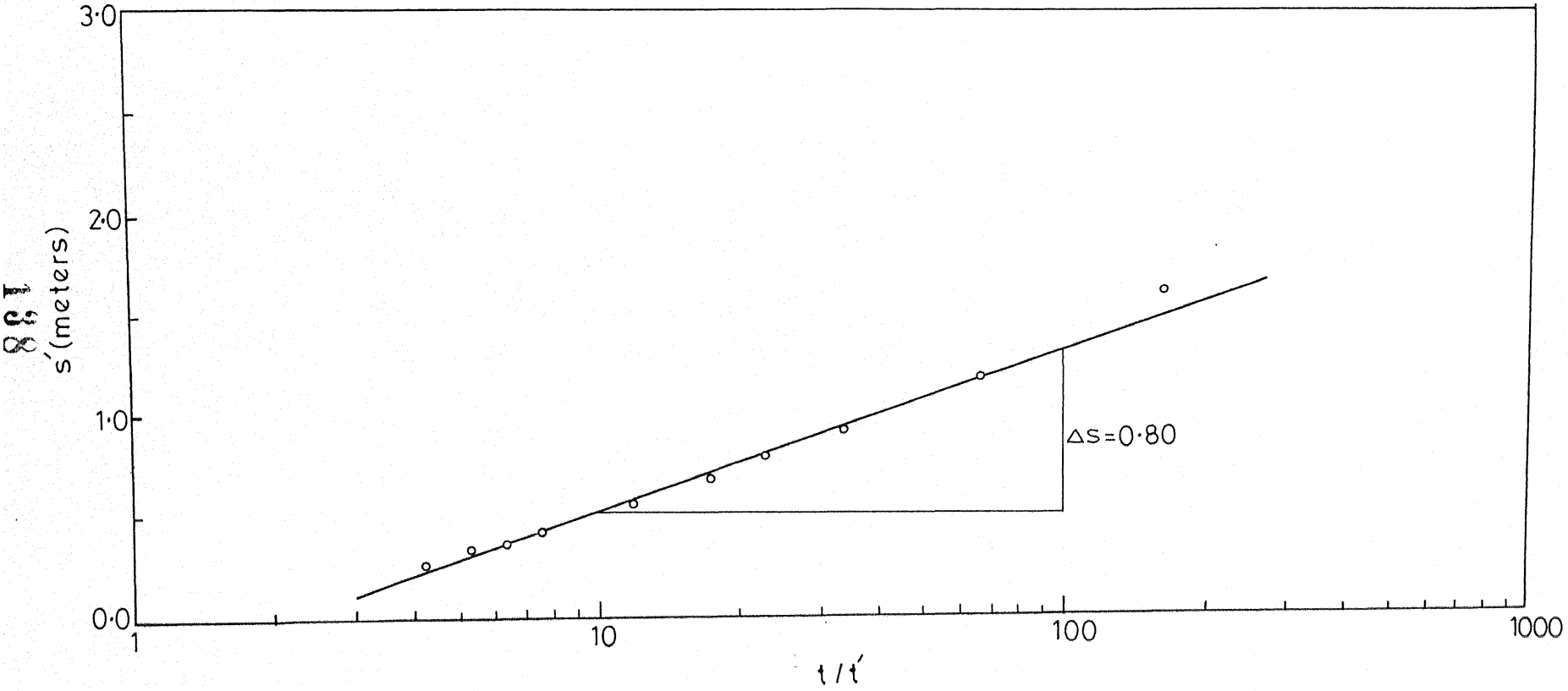

FIG.5·7 TIME RECOVERY GRAPH FOR WELL AT TILDA

(c) Storativity

$$\text{Log}\ \frac{1}{S} = \frac{26.3 \times 10^{-7} \times T \times s}{Q} + 7.71 - \log \frac{Tt}{r_w^2}$$

$$= \frac{26.3 \times 10^{-7} \times 123.2 \times 1.646}{545.04} + 7.71 - \log \frac{123.2 \times 0.229}{(0.203)^2}$$

$$\log \frac{1}{S} = 4.874$$

$$S = 1.33 \times 10^{-5}$$

3. Murpar

The well is located in the vicinity of the post office.

$Q = 408.48\ m^3$ /day

$t = 0.2569$ days

Depth = 60 m

$r_w = 0.15$ m

$\angle s = 0.725$ m

$\triangle s' = 0.70$

(a) Jacob's method using drawdown data, [Fig.5.8]

$$T = \frac{2.3 \times Q}{4\ \pi \angle s}$$

$$= \frac{2.3 \times 408.78}{4 \times \pi \times 0.725} = 103.25\ m^2/day$$

(b) Recovery test [Fig.5.9]

$$T = \frac{2.3 \times Q}{4 \times \pi \triangle s'}$$

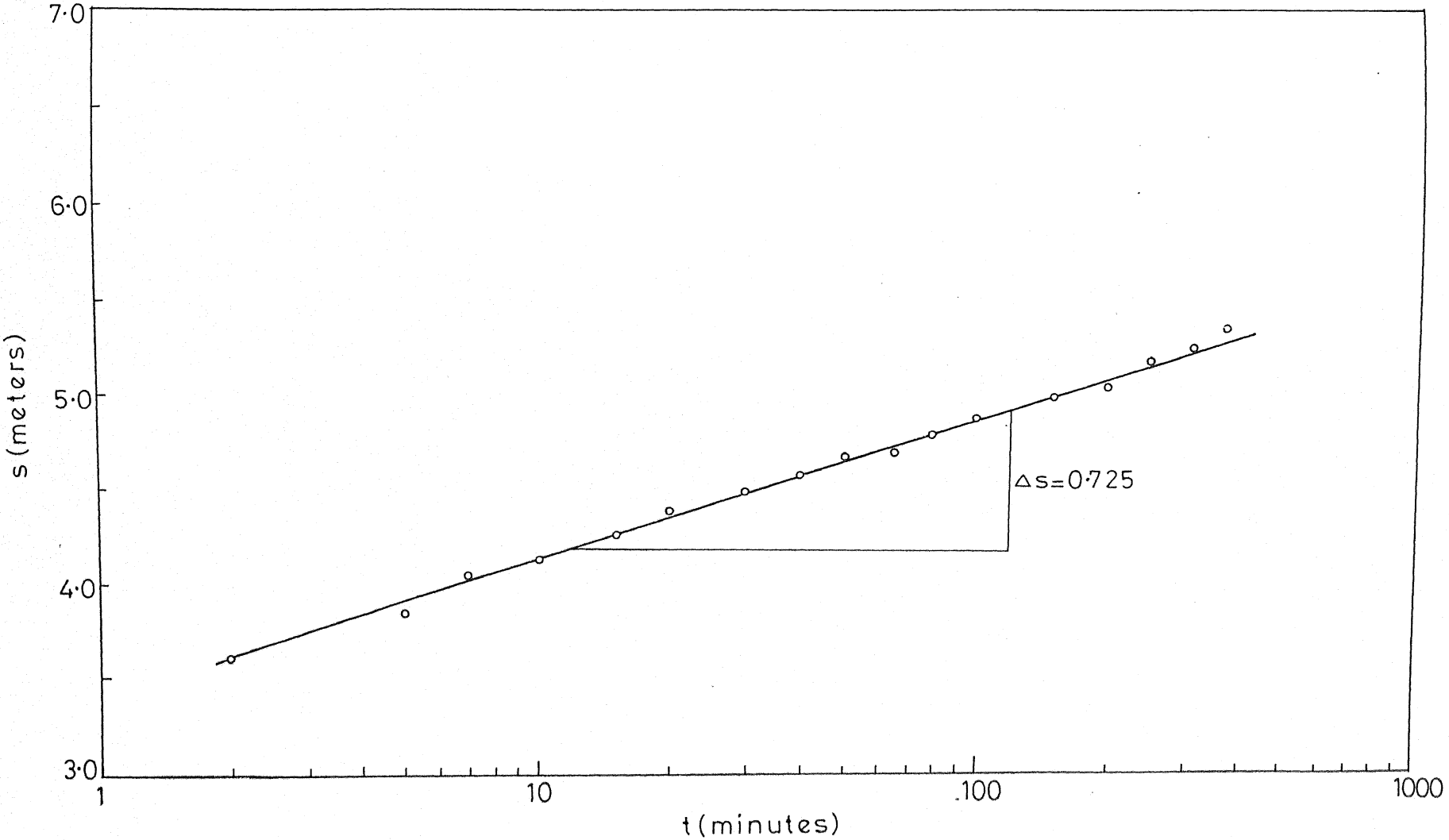

FIG. 5·8 TIME-DRAWDOWN GRAPH FOR WELL AT MURPAR

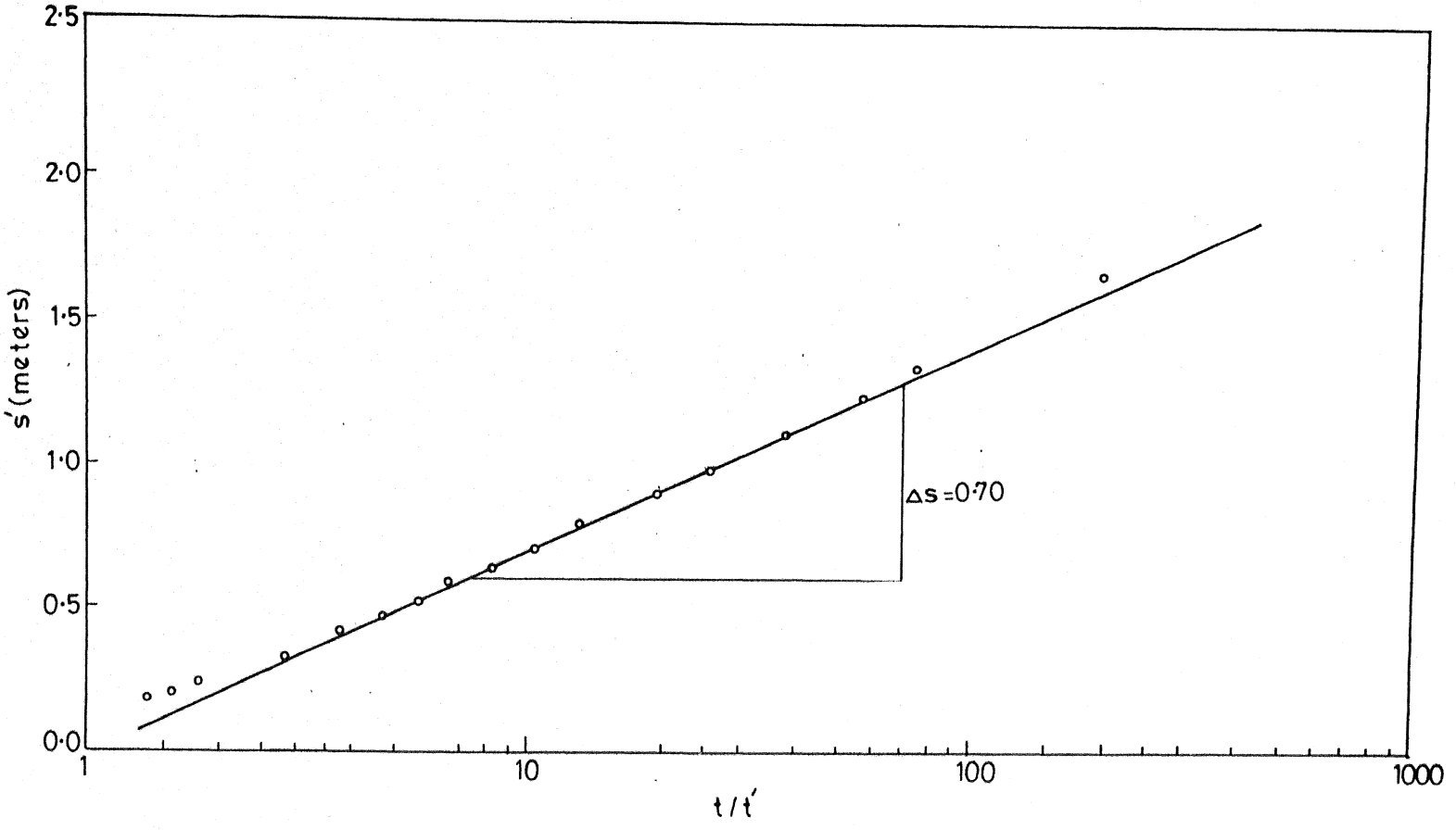

FIG. 5·9 TIME-RECOVERY GRAPH FOR WELL AT MURPAR

$$= \frac{2.3 \times 408.78}{4 \times \pi \times 0.70} = 106.93 \ m^2/day$$

$$T_{av} = 105.09 \ m^2/day$$

(c) Storativity

$$\text{Log} \frac{1}{S} = \frac{26.3 \times 10^{-7} \times T \times s}{Q} + 7.71 - \log \frac{Tt}{r_w^2}$$

$$= \frac{26.3 \times 10^{-7} \times 105.09 \times 1.75}{408.78} + 7.71 - \log \frac{105.09 \times 0.2569}{(0.15)^2}$$

$$\log \frac{1}{S} = 3.0798$$

$$S = 8.33 \times 10^{-4}$$

5.4.2 Pendri Member

In this member four pumping sites were taken in for analysis.

1. Bitkuli

$Q = 590.46 \ m^3$ /day

$t = 0.229$ days

$r_w = 0.15$

Depth = 60.97 m

$\triangle s = 0.53$ m

$\triangle s' = 0.525$ m

length of the slotted pipe = 7 m

(a) Jacob's Method using drawdown data, [Fig.5.10]

$$T = \frac{2.3 \times Q}{4 \pi \triangle s}$$

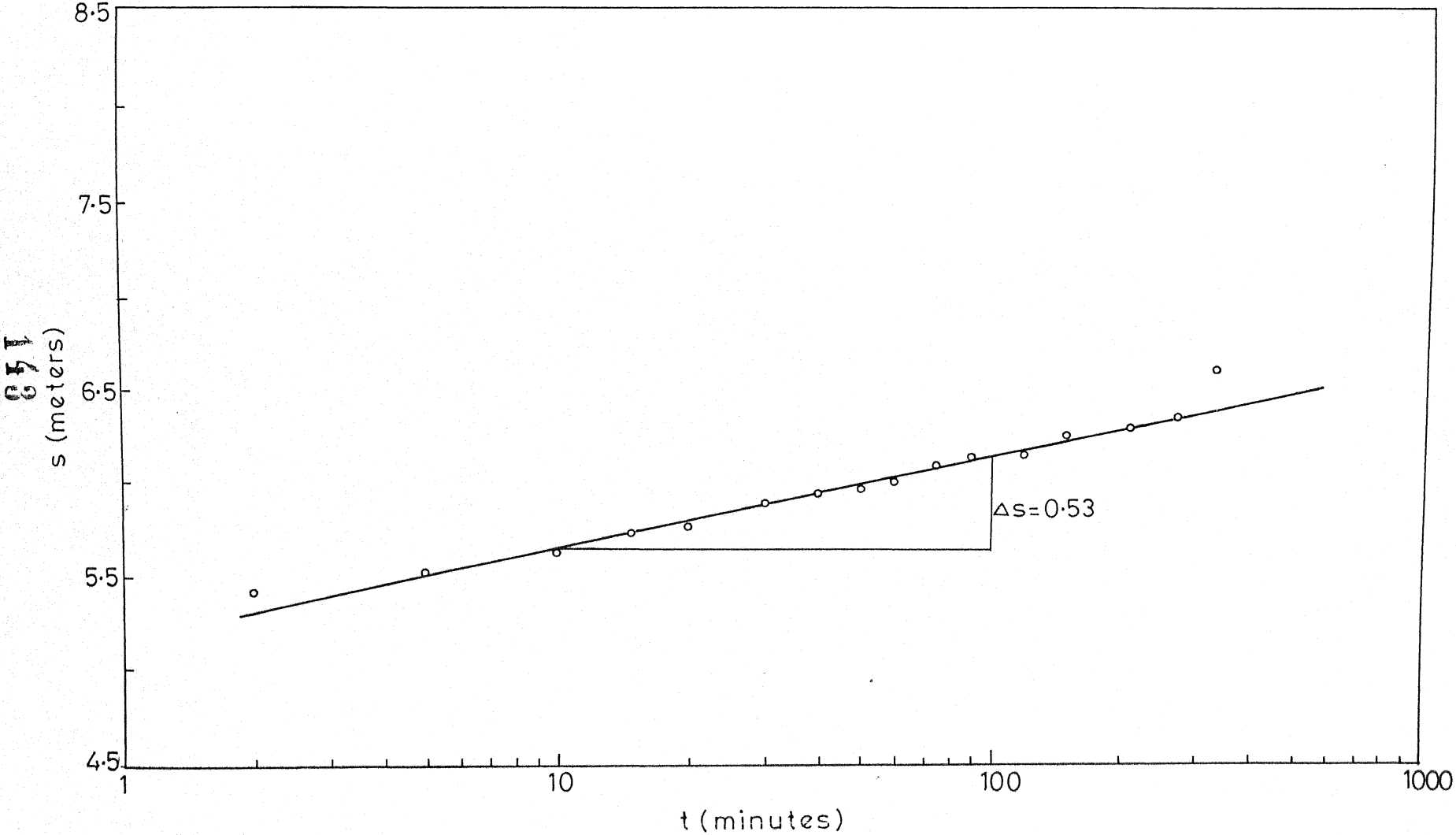

FIG. 5·10 TIME - DRAWDOWN GRAPH FOR WELL AT BITKULI

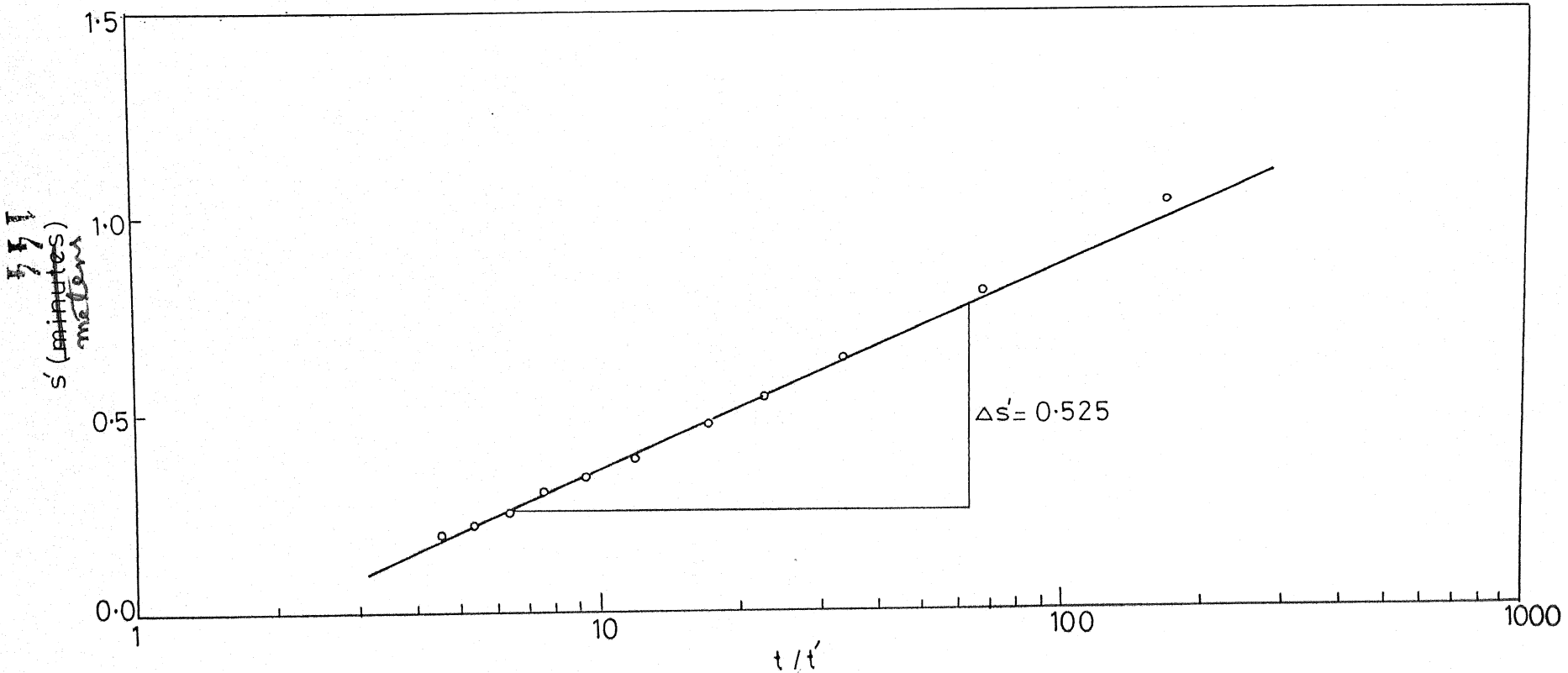

FIG. 5·11 TIME RECOVERY GRAPH FOR WELL AT BITKULI

$$= \frac{2.3 \times 590.46}{4 \times \pi \times 0.53} = 203.90 \text{ m}^2/\text{day}$$

(b) Recovery test [Fig.5.11]

$$T = \frac{2.3 \times Q}{4 \times \pi \times \triangle s'}$$

$$= \frac{2.3 \times 590.46}{4 \times \pi \times 0.525} = 205.849 \text{ m}^2/\text{ day}$$

$T_{av} = 204.874 \text{ m}^2/\text{day}$

(c) Storativity

$$\text{Log } \frac{1}{S} = \frac{26.3 \times 10^{-7} \times T \times s}{Q} + 7.71 - \log \frac{Tt}{r_w^2}$$

$$= \frac{26.3 \times 10^{-7} \times 204.874 \times 1.25}{590.46} + 7.71 - \log \frac{204.874 \times 0.229}{(0.15)^2}$$

$$\log \frac{1}{S} = 4.39$$

$$S = 4.05 \times 10^{-5}$$

2. Bainsa

$Q = 13626 \text{ m}^3/\text{day}$

$t = 0.25$ days

Depth = 60.9 m

$r_w = 0.15$ m

$\triangle s = 2.2$ m

$\triangle s' = 2.12$ m

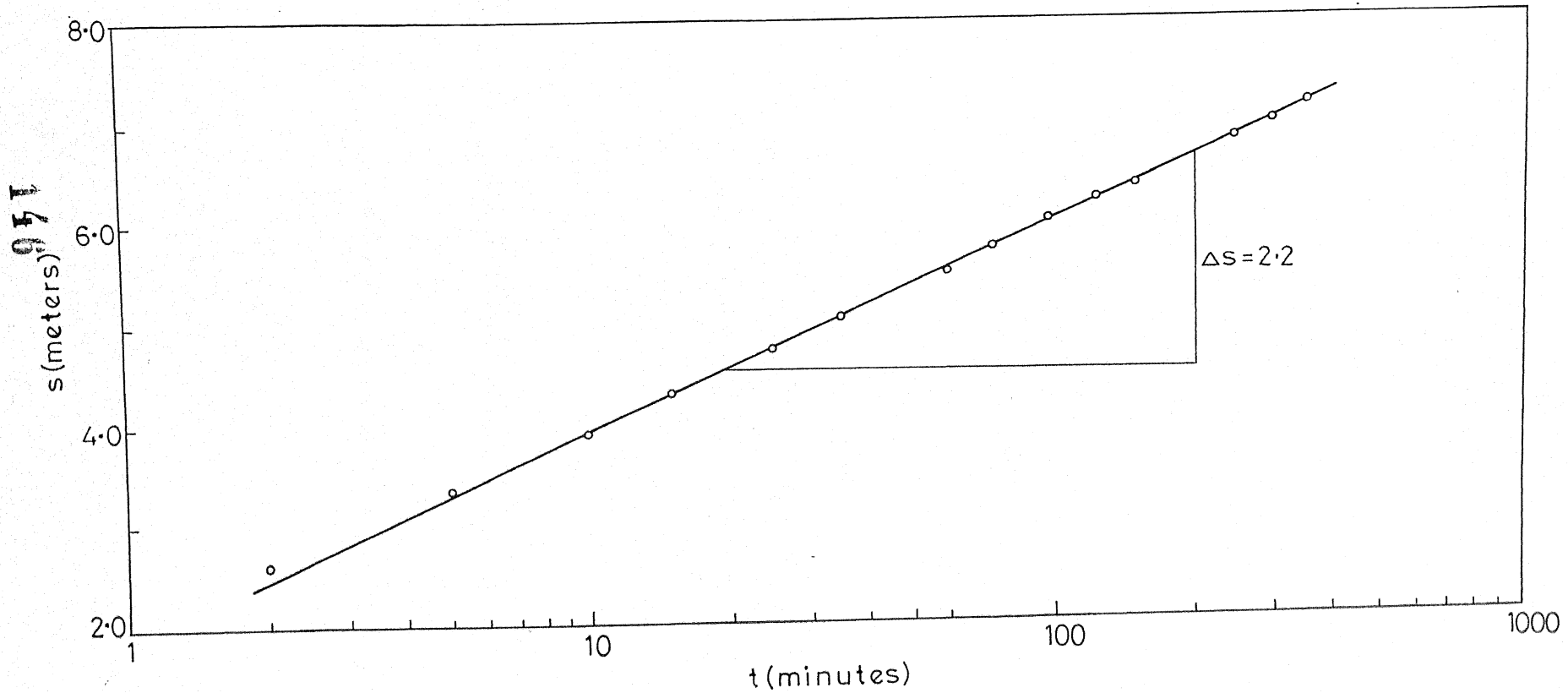

FIG. 5·12 TIME - DRAWDOWN GRAPH FOR WELL AT BAINSA

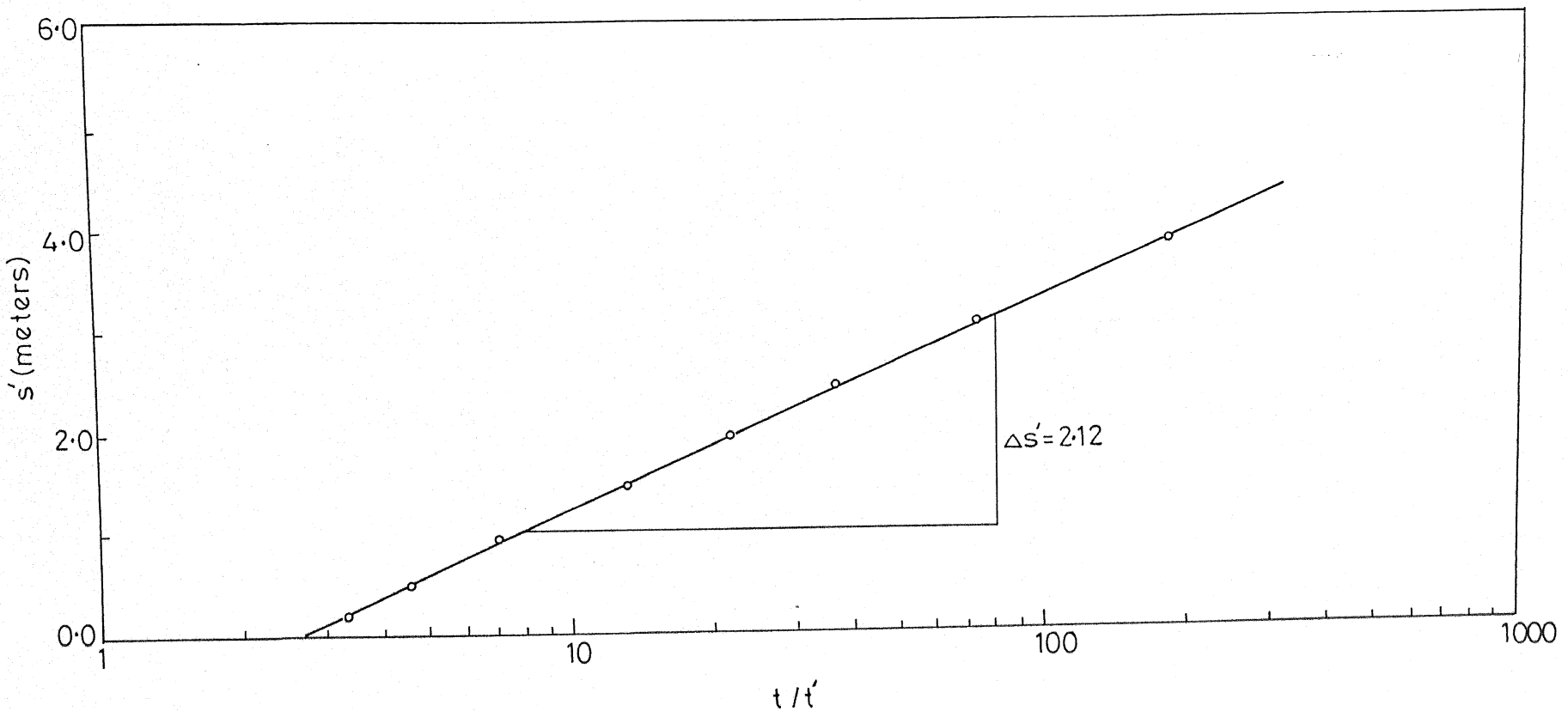

FIG. 5·13 TIME-RECOVERY GRAPH FOR WELL AT BAINSA

(a) Jacob's Method using drawdown data, [Fig.5.12]

$$T = \frac{2.3 \times Q}{4 \pi \triangle s}$$

$$= \frac{2.3 \times 13626}{4 \times \pi \times 2.2} = 1134 \text{ m}^2/\text{day}$$

(b) Recovery test [Fig.5.13]

$$T = \frac{2.3 \times Q}{4 \times \pi \times \triangle s'}$$

$$= \frac{2.3 \times 13626}{4 \times \pi \times 2.12} = 1176.98 \text{ m}^2/\text{ day}$$

T_{av} = 1155.49 m² /day

(c) Storativity

$$\text{Log } \frac{1}{S} = \frac{26.3 \times 10^{-7} \times T \times s}{Q} + 7.71 - \log \frac{Tt}{r_w^2}$$

$$= \frac{26.3 \times 10^{-7} \times 1155.49 \times 4.42}{13626} + 7.71 - \log \frac{1155.49 \times 0.25}{(0.15)^2}$$

$$\log \frac{1}{S} = 3.60$$

$$S = 2.50 \times 10^{-4}$$

3. Bhatbhera

$Q = 610.44 \text{ m}^3$ /day

t = 0.26 days

Depth = 59.45 m

r_w = 0.20 m

$\triangle s$ = 0.65 m

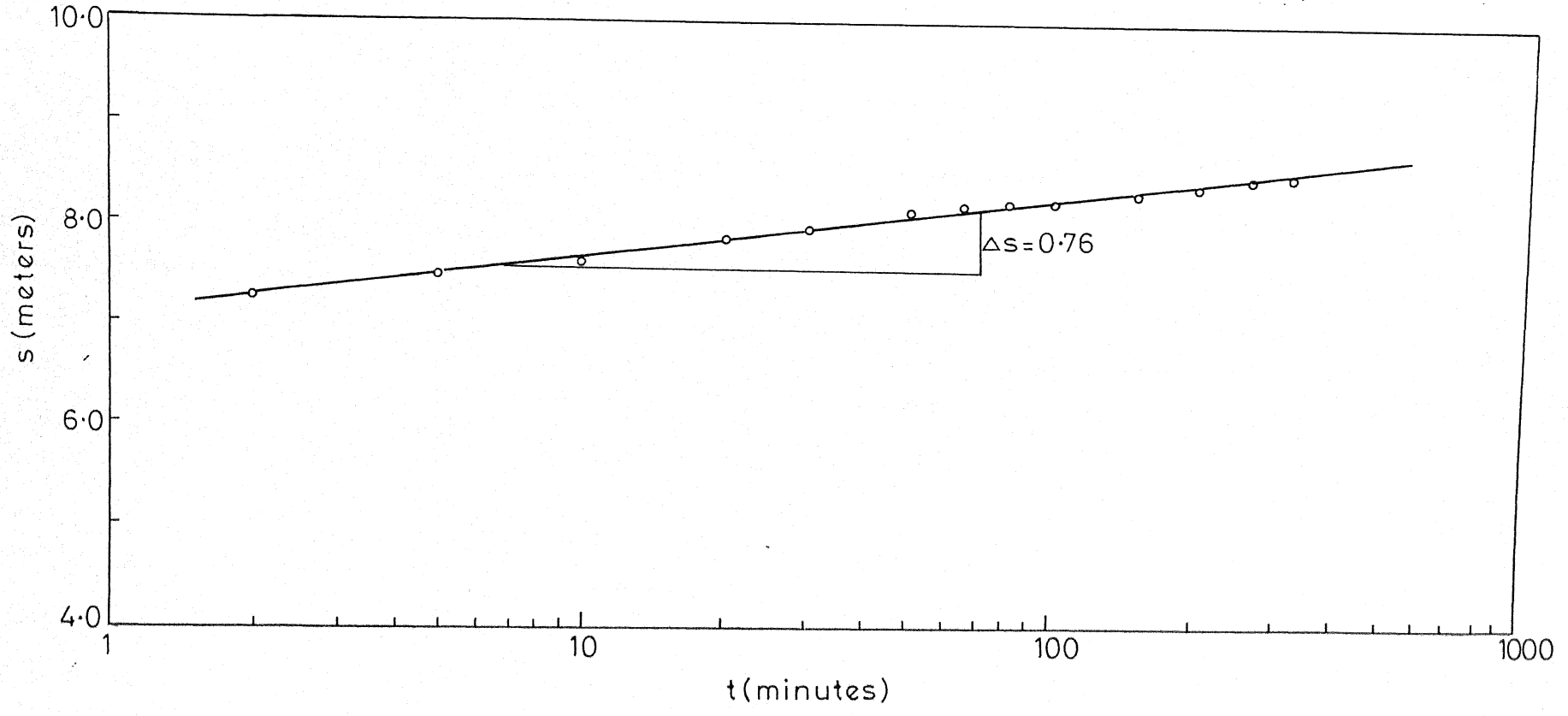

FIG. 5·14 TIME-DRAWDOWN GRAPH FOR WELL AT BHATBHERA

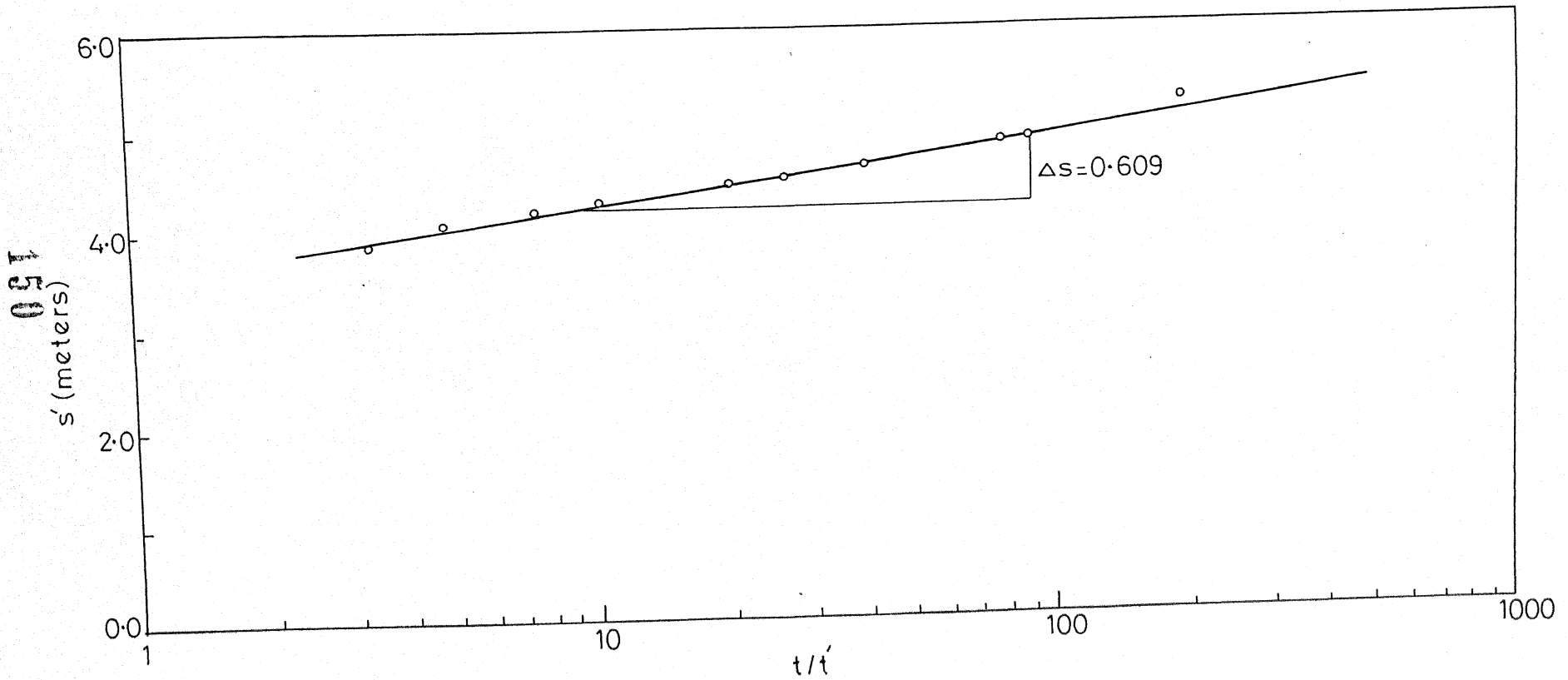

FIG. 5·15 TIME-RECOVERY GRAPH FOR WELL AT BHATBHERA

$\triangle s' = 0.65$ m

(a) Jacob's Method using drawdown data, [Fig.5.14]

$$T = \frac{2.3 \times Q}{4 \pi \triangle s}$$

$$= \frac{2.3 \times 610.44}{4 \times \pi \times 0.65} = 171.97 \text{ m}^2/\text{day}$$

(b) Recovery test [Fig.5.15]

$$T = \frac{2.3 \times Q}{4 \times \pi \times \triangle s'}$$

$$= \frac{2.3 \times 610.44}{4 \times \pi \times 0.65} = 171.97 \text{ m}^2/\text{day}$$

$T_{av} = 171.97$ m^2 /day

(c) Storativity

$$\text{Log } \frac{1}{S} = \frac{26.3 \times 10^{-7} \times T \times s}{Q} + 7.71 - \log \frac{Tt}{r_w^2}$$

$$= \frac{26.3 \times 10^{-7} \times 171.97 \times 1.53}{610.44} + 7.71 - \log \frac{171.97 \times 0.26}{(0.203)^2}$$

$$\log \frac{1}{S} = 4.67$$

$$S = 2.1 \times 10^{-5}$$

4. Arjuni

$Q = 772.14\ m^3/day$

$t = 0.236$ days

Depth = 60.97 m

$r_w = 0.15$ m

$\triangle s = 0.975$ m

$\triangle s' = 0.92$ m

(a) Jacob's Method using drawdown data, [Fig.5.16]

$$T = \frac{2.3 \times Q}{4 \pi \triangle s}$$

$$= \frac{2.3 \times 772.14}{4 \times \pi \times 0.975} = 144.99\ m^2/day$$

(b) Recovery test, [Fig.5.17]

$$T = \frac{2.3 \times Q}{4 \pi\ s'}$$

$$= \frac{2.3 \times 772.14}{4 \times \pi \times 0.92} = 153.69\ m^2/day$$

$T_{av} = 149.34\ m^2/day$

(c) Storativity

$$\text{Log}\ \frac{1}{S} = \frac{26.3 \times 10^{-7} \times T \times s}{Q} + 7.71 - \log \frac{Tt}{r_w^2}$$

$$= \frac{26.3 \times 10^{-7} \times 149.34 \times 1.75}{772.14} + 7.71 - \log \frac{149.34 \times 0.236}{(0.152)^2}$$

$$\log \frac{1}{S} = 4.515$$

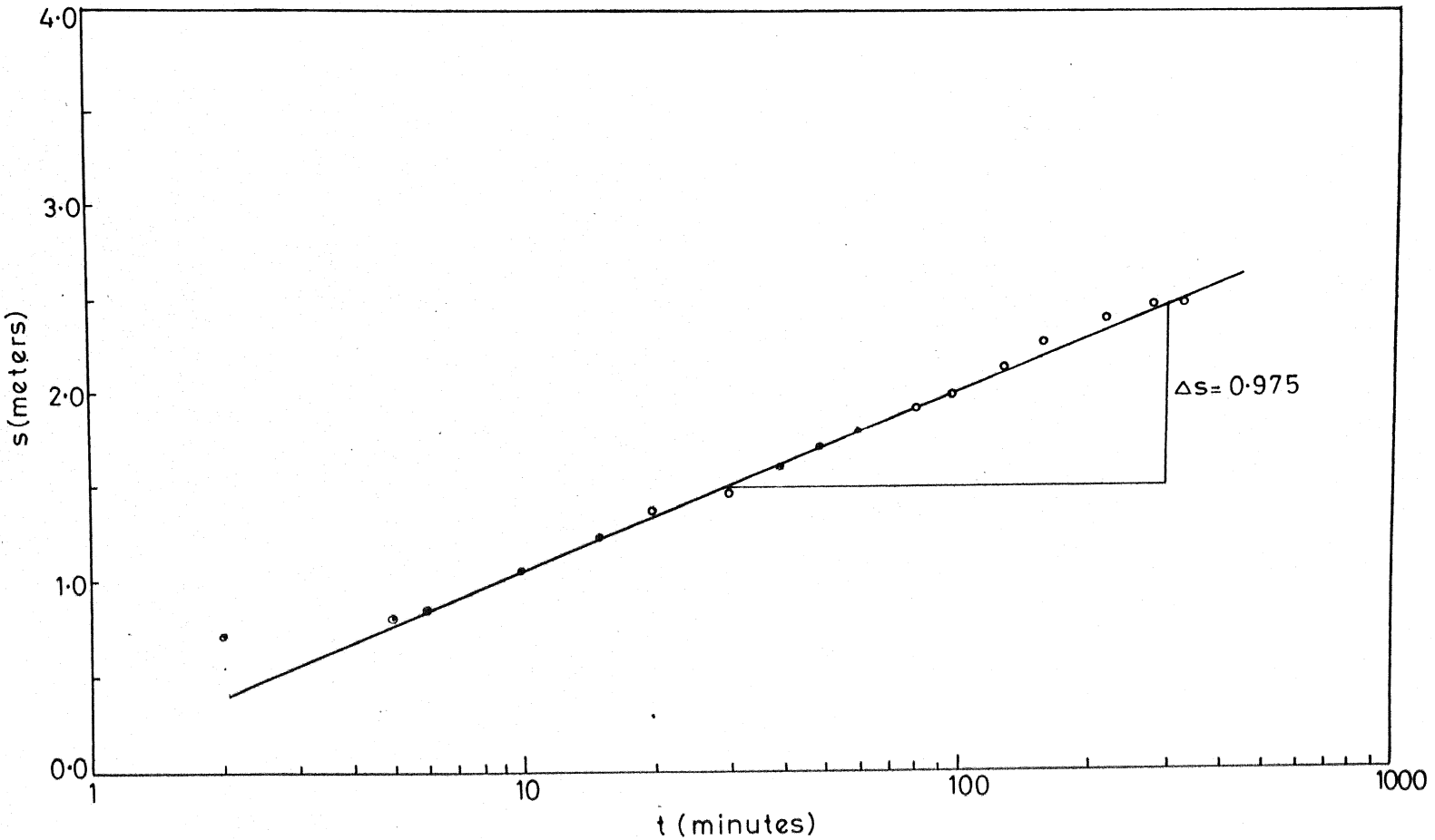

FIG·5·16 TIME DRAWDOWN GRAPH FOR WELL AT ARJUNI

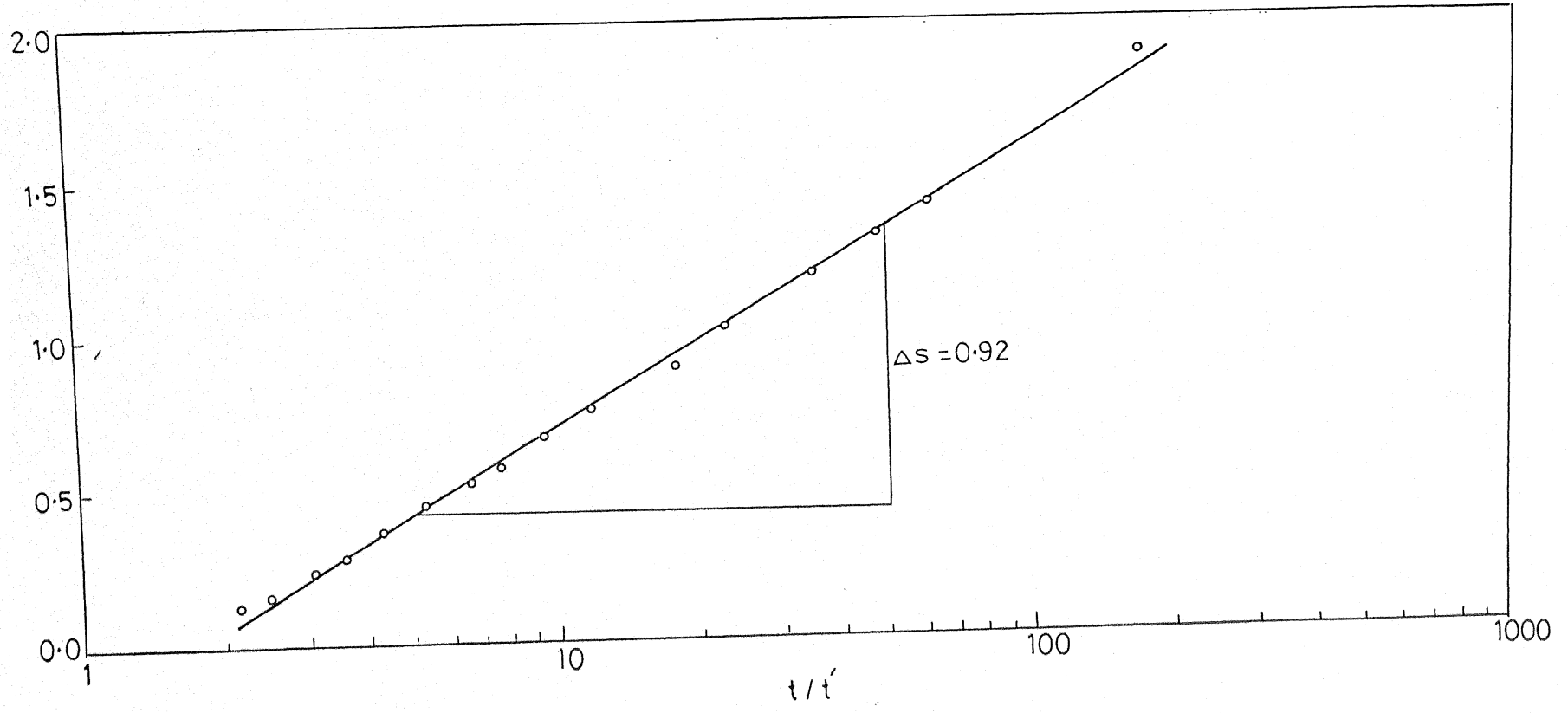

FIG.5·17 TIME RECOVERY GRAPH FOR A WELL AT ARJUNI

$S = 3.05 \times 10^{-5}$

5.4.3 Newari Member

1. Khaira

$Q = 6540.48\ m^3/day$

$t = 0.104$ days

Depth = 56.40 m

$r_w = 0.15$ m

$\triangle s = 1.7$ m

$\triangle s' = 1.67$ m

(a) Jacob's Method using drawdown data, [Fig.5.18]

$$T = \frac{2.3 \times Q}{4 \pi \triangle s}$$

$$= \frac{2.3 \times 6540.48}{4 \times \pi \times 1.70} = 704.17\ m^2/day$$

(b) Recovery test, [Fig.5.19]

$$T = \frac{2.3 \times Q}{4 \pi \triangle s'}$$

$$= \frac{2.3 \times 6540.48}{4 \times \pi \times 1.67} = 717.1\ m^2/day$$

$T_{av} = 710.63\ m^2/day$

(c) Storativity

$$\text{Log}\ \frac{1}{S} = \frac{26.3 \times 10^{-7} \times T \times s}{Q} + 7.71 - \log \frac{Tt}{r_w^2}$$

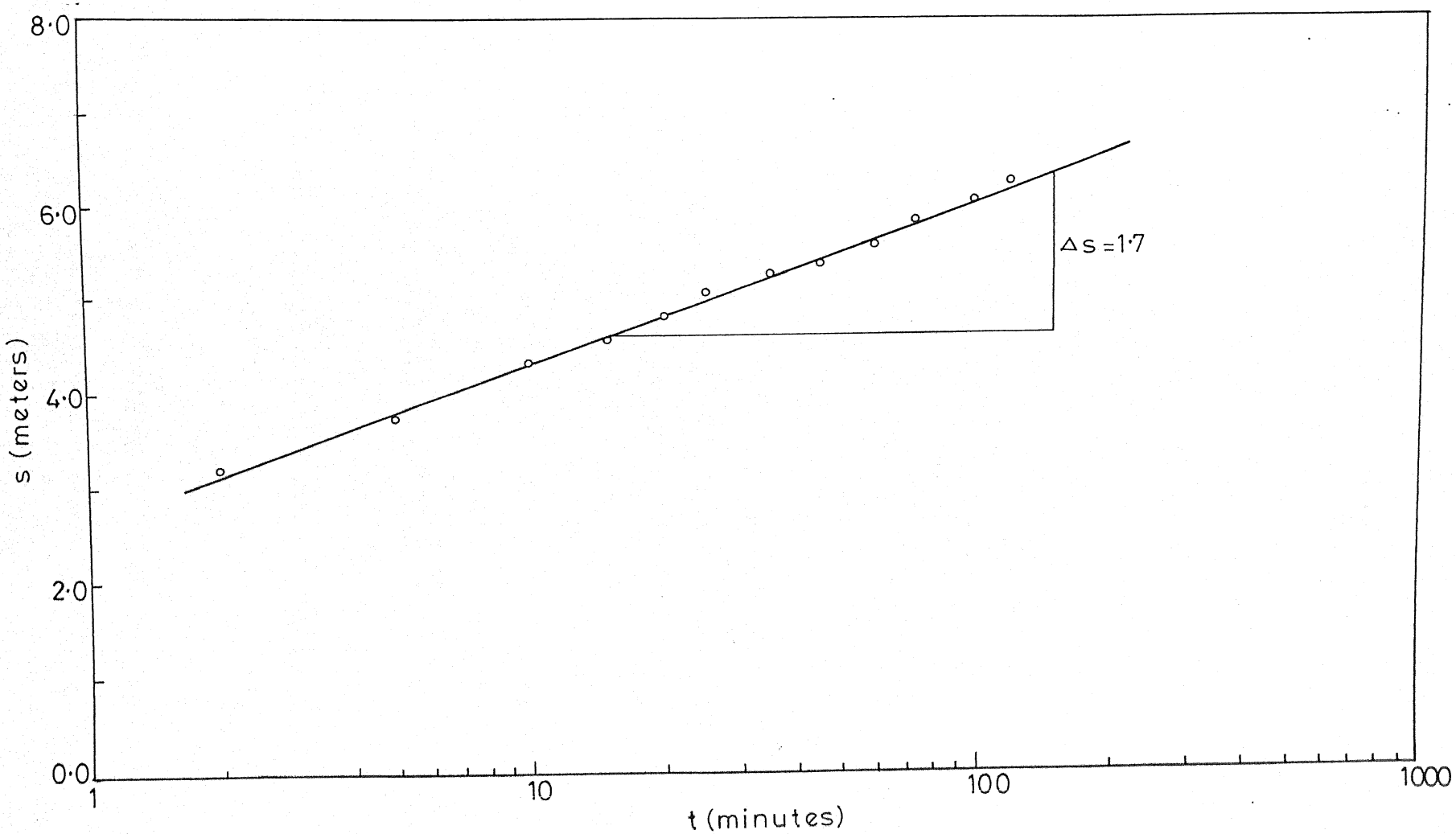

FIG. 5·18 TIME DRAWDOWN GRAPH FOR WELL KHAIRA

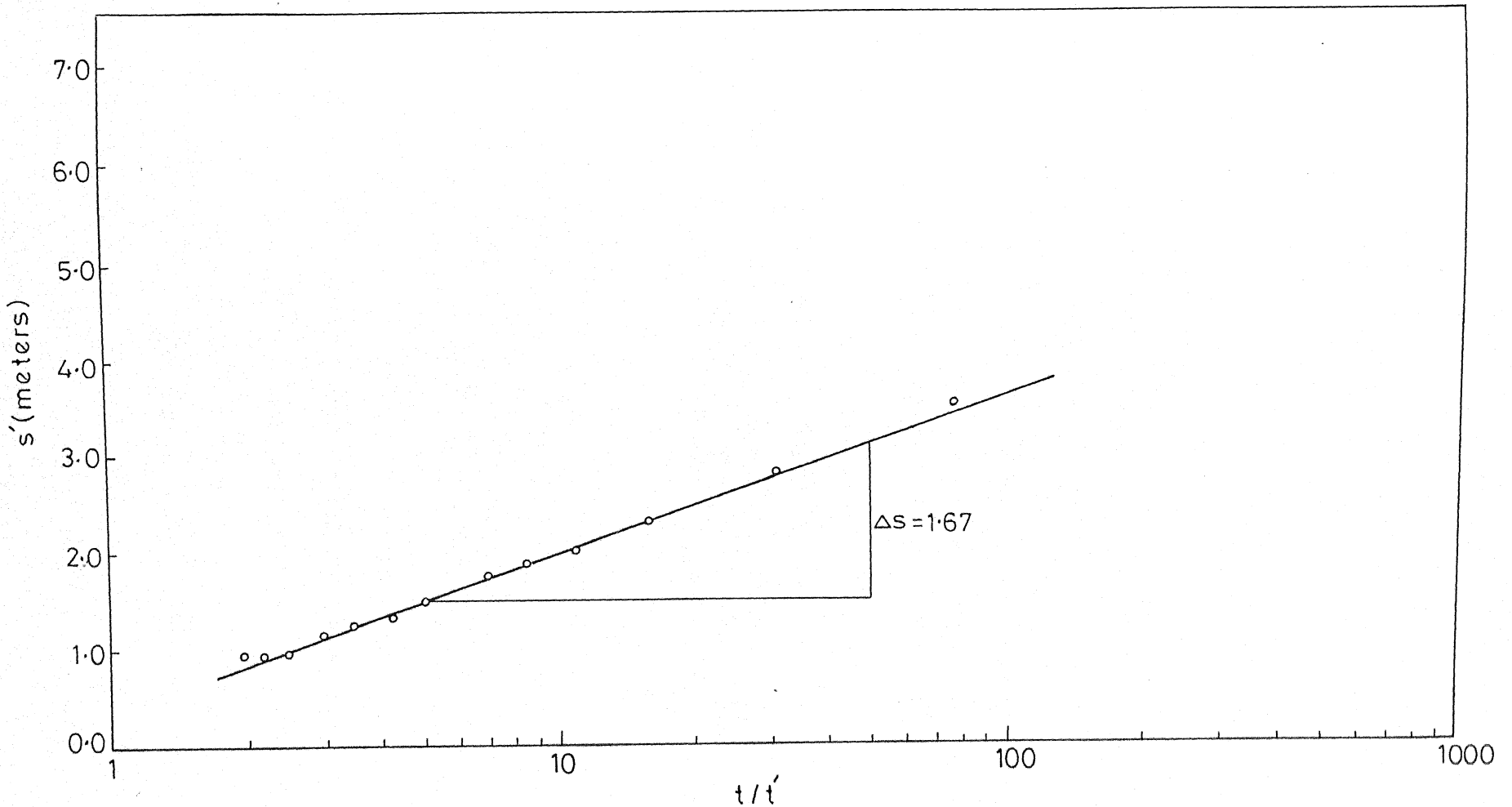

FIG·5·19 TIME RECOVERY GRAPH FOR WELL AT KHAIRA

$$= \frac{26.3X10^{-7}X710.63X1.75}{6540.48} + 7.71 - \log \frac{710.63X0.104}{(0.15)^2}$$

$$\log \frac{1}{S} = 4.193$$

$$S = 6.404 \times 10^{-5}$$

5.4.4 Performance Characteristics of the Wells Located Outside the Delineated Zone

To enable comparison of the performance of the formations as aquifers, tests have also been conducted on five wells located outside the identified zones. The transmissivity estimates are as follows :

		Transmissivity (T) m^2/day		
Member	Well location	Time-drawdown	Time-recovery	Average
NIPANIA	KUKRACHUDA	51.3	56.3	53.8
NIPANIA	DHURRABANDH	58.8	64.6	61.7
PENDRI	PURENA	65.0	69.0	67.0
NEWARI	BHATGAON	141.0	149.0	145.0

As can we seen from the results, the Pendri member has registered high transmissivity values (of around 1100 m^2/day) in the Bainsa area. It may be indicated that the digital processing and subsequent ground checks have revealed that the limestone member in the area to be closely fractured and highly cavernous (Fig.6.1). The transmissivity estimates in

the other three localities within this member range between 144 and 204 m^2/day. Present investigations revealed prominence of fractures in the localities. In contrast, the transmissivity value for Pendri member registered at Purena is around 61 m^2/day. This locality is out side the delineated zone and has relatively compact limestone devoid of cavities and fractures.

For the three wells in the Nipania formation within the delineated zone the transmissivity estimates are in the same range of around 100 to 110 m^2/day. However, outside this zone, the formation has registered comparatively lower values of transmissivity of around 53 m^2/day in the Kukrachunda area and around 61 m^2/day in the Dhurrabandh area.

In the Newari formation, while the transmissivity estimate was around 704 m^2/day in the Khaira area, the value drastically is low (of around 145 m^2/day) around Bhatgaon due to the compact natures of the limestone. The storativity values in all the cases are in the range for confined aquifers.

CHAPTER 6

SUMMARY AND CONCLUSIONS

In the carbonate terrains, delineation of aquifer zones involves recognition and mapping in detail of the various features such as the fracture zones, sinkholes, caverns and collapsed zones, that aid in the ability of formation not only to store water but also to transmit the same. Lithology plays an important role in the selective dissolution of the formation resulting in solution features. Since many years, visual interpretation of the imageries in remote sensing has been carried out in delineating the morphological and structural features. Thermal infrared imageries have also been used in the visual interpretation . However, digital image processing enables an accurate interpretation as the digital data is involved. A combination of image processing techniques using MSS data has facilitated a clear demarcation of the structural and morphological features in the karstified zones. While band ratioing gives the effects of slope change within the valley region, stretching improves the overall resolution to enable a better interpretation. Edge enhancement with proper filter provides not only the enhancement but also creates an edge for all the subdued caverns and collapsed zones in a carbonate terrain. Selective stretching results in the enhancement of a particular area of interest, in the present case caverns have

been enhanced through this technique. All these techniques have been utilized in locating aquifer zones within the limestone terrain.

Central part of the Chhattisgarh basin is taken up as a case study for the application of methodology for digital image processing developed by the author during the course of the present work. Located in Madhya Pradesh, the study area covers parts of Raipur, Baloda Bazar and Bilaspur districts. The formations in the area belong to the Raipur series. This series essentially, is a repetitive sequence of limestone and shale with 5 cycles occurring in the basin. A sub-tidal to tidal environment has been inferred for the deposition of these sediments (Schnitzer,1974). The formation of the shale has been attributed to release of fine mud through minor uplift of landmass by epirogenic forces. Predominance of limestone in the sequence is indicative of prevalence of warm temperatures and chemical weathering in the provenance. Variations in the lithology of shales revealed changes in the oxidizing and reducing conditions in environment during deposition. The formations within the study area pertain to the third and fourth cycles. The Gunderdehi shale (of the third cycle) is overlain by the limestone members (Newari, Pendri and Nipania) and the Tarenga shale belonging to the 4th cycle. The Pendri and Newari limestones are stromatolitic. Variations in lithology

in these limestone members have facilitated recognition of the same on the images. Hitherto, no systematic classification of this carbonate terrain has been attempted by the earlier workers in terms of morphological features, drainage characteristics and the distribution of the aquifer zones.

In the present work the data on tape from Landsat-4 was windowed on OMEGA system and this data has been converted into Dec mode for image classification. Initially the window data when viewed on PDP 11/24 system was found to possess a skew effect as consequence of which the generated picture of the area did not match with the toposheet of the same area. This skewness effect, due to Earth's rotation has been corrected using nearest neighbourhood method. Software necessary for all corrections has been developed in present work. The corrected window data has been processed through several steps of image processing in sequence. Band ratioing was adopted as a first step and it has been found that, of all band combinations , the ratio of bands 2 and 4 yields better results in enhancing the slope of the river valleys. In the pseudocoloured technique, the corrected window of the band data has been pseudocoloured by intensifying the hue of the colour, which gives better results of surfacial feature identification. Tonal contrast is obtained for variations of reflectance all over the terrain. The sinkholes appeared hazy in the ratio pictures. Stretching has been done on the ratio

picture data (based on the distribution of the reflectance values) to obtain better resolution of the features. The technique involves plotting histogram for the data initially covering range 1.0 - 2.5 (reflectance values) which has been later stretched to the entire dynamic medium. This has resulted in the improvement of the intensity and enhancement of the sinkholes which were otherwise observed to be hazy in the initial ratio pictures. Further enhancement of caverns was achieved by subjecting the data to selective stretching with the help of the reflectance value ranges of the cavernous areas. The study area has been classified on the basis of tonal characteristics into three major morphological units- the upland tract, the valley tract and the alluvial tract. The upland tract is characterized by its flat topography. This tract has been further subdivided into two units, based on the variation in reflectance values. The valley tract is characterized by typical pattern of gully erosion as a consequence of the dissolution of limestone. The alluvial tract, situated in the northeast corner of the area, is characterized by a gray tonal contrast.

The edge enhancement technique used in the present study has facilitated the delineation of the edges of collapsed and sinkhole-prone zones. For this, the noise has been smoothened through a correction using 3 by 3 filter initially. However, since this procedure has not yielded all

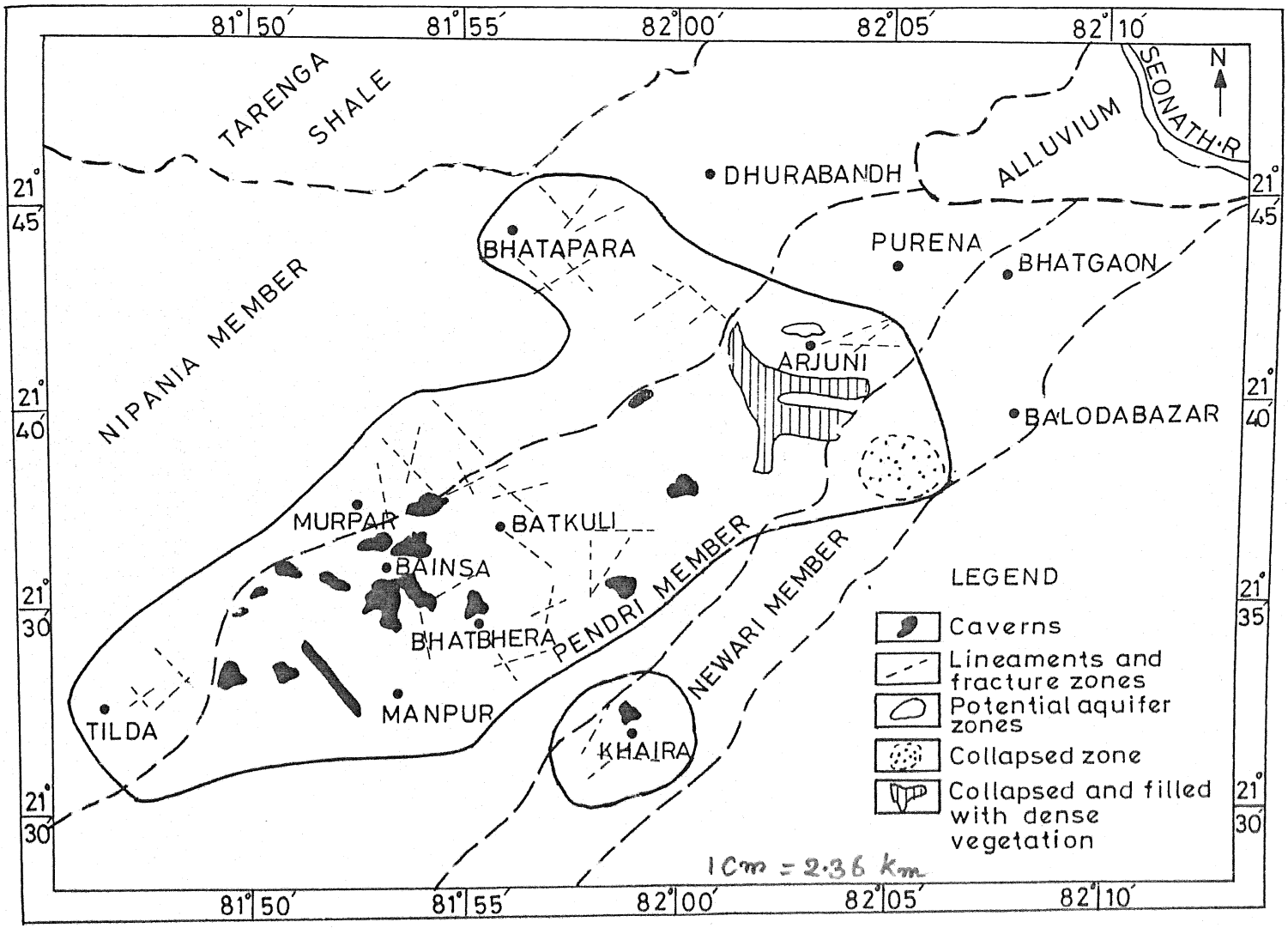

FIG·6·1 MAP INDICATING POTENTIAL AQUIFER ZONES DELINEATED THROUGH IMAGE PROCESSING IN THE STUDY AREA

the details, a 5 by 5 filter was developed by the author which has provided sharp boundaries wherever the reflectance values change suddenly. This technique has enabled distinct demarcation of the collapsed zones in the study area. Subsequently the same data has been subjected to convolution operation with gradient filter. This procedure has helped in highlighting all the lineaments. Detailed mathematical treatment of the procedures has been presented together with the relevant soft ware developed by the author. The 5 by 5 filter has also been used in enhancing the dense vegetational areas within the study region through histogram equalization of the window data.

Image classification is done by taking the a priori probability of features into consideration. The data has been checked with a numerical separation technique using the training data set and a line printer map of the study area was prepared.

Within the limestone terrain, productive aquifer zones [Fig.6.1] have been delineated in the study area using the image processing techniques. Pumptests have been conducted on a few wells located in the three limestone members within this zone and the estimates of transmissivity and storativity were obtained on the basis of time-drawdown and time-recovery data. The very low values of storativity in the range of 10^{-3} to 10^{-6} reflect the confined nature of the aquifer. The Pendri limestone has registered high

transmissivity values ranging between 200 and 1155 m^2/day within the aquifer zone depending on the presence of the fractures, sinkholes and the cavernous features. In the localities where the fractures are present but caverns are not seen as in Nipania and Newari members , the transmissivity is around 124 to 700 m^2/day. Pumptests carried out on wells located outside the delineated aquifer zone within these three limestone members have revealed relatively low transmissivity values of the order 53 to 61 m^2/day. Thus the productive aquifer zone, as delineated on the basis of digital image processing in the present work has been proved for ground water development, through aquifer evaluation tests.

Water level contour maps for pre-monsoon and post-monsoon periods have enabled the identification of recharge areas. The general flow pattern is towards the center of the study area where the caverns and sinkholes in the Pendri member act as storage spaces for groundwater. The quality of groundwater has been observed to vary in flow direction. The TDS content and the hardness have registered an increase in the flow direction.

REFERENCES

Adyalkar,P.G., and Phadtare,P.N., 1972. Karstic limestones in parts of Raipur District, M.P., and their groundwater possibilities. Jour. Geol. Soc. of India.,Vol.13, No. 4, pp 382 - 387

Adyalkar,P.G., and Ramana,K., 1980. Karstic limestones: Mode of development and evaluation of aquifer characteristics. Quart. Jour. Geol., Min. and Met. Soc. of India., Vol.52, NO.2, pp 43-55

Balakrishnan,P., 1986. Issues in water resources development management and the role of remote sensing. ISRO, Technical report, NNRMS-TR 67-87, 194p.

Baldev Sahai, Sood,R.K., and Sharma, S.C., 1983. Groundwater exploration in Saurashtra. National Natural Resources Management System. pp II-10.1 to II-10.15

Baldev Sahai, Sood, R.K., and Sharma, S.C., 1982. Application of Landsat imageries in groundwater investigations in semi-arid hard rock region of the state of Gujarat, (India). Proc. Int. Symp. on Remote sensing of environment, First thematic conference: Remote sensing of arid and semi arid lands. Cairo, Egypt, Vol.20 pp 709-718.

Bernstein,R.,1976. Digital image processing of Earth observation sensor data. IBM Jour. Res. and Dev. vol.20, pp 40-57

Benny,A.H., 1983. Automatic relocation of ground control points in Landsat Imagery. Int.Jour.of Remote Sensing, Vol.4, pp 335-342.

Cocker, A.E., Marshal,R., and Thomson, N.S., 1970. Application of computer processed multispectral data to the discrimination of land collapse (sinkhole) prone areas in Florida. Poc. 6th Int. Symp. Remote Sensing Environment, Ann Arbor., Michigan, pp 65-70

Chaturvedi, R.S., and Bhattacharya, Kamal, P., Krishnamurty,J and sunder Raman,N., 1983. Integrating remote sensing techniques in groundwater exploration -A typical case study from Bundelkhand region in Uttar Pradesh. Proc. Nat. Symp. on Remote Sensing in Development and Management of Water Resources. pp 267-276

Crawford, A.R., 1969. India, Ceylon and Pakistan: New age data and comparison with Antarctica. Nature, London, pp 380-381

Crawford,A.R., and Compston,W., 1973. The age of Cuddapah and Kurnool systems, South India. Jour. Geol. Soc. Aust., Vol. 19(4), pp 453-464

Dutt,N.V.B.S., 1964. A suggested succession of the Purana formations of the southern part of Chhattisgarh, M.P. Records. Geol. Surv. of India, Vol. 93, Pt.2., pp 143-148

Gonzalez R.C., and Wintz,P., 1977. Digital image processing. Addison - Wesley, Reading, Massachusetts. 420p

Jacob,C.E.,1956. Flow of groundwater, Engineering Hydraulics; John Wiley and Sons, New York, 346p

Kim,C.E.,and Strintzis,M.G.,1980. High speed multidimensional Convolution. IEEE Transactions on Pattern Analysis and Machine Intelligence, Vol 2., pp 269-273

Kreuzer,H., et.al., 1977. K/Ar dates of two glauconites from the Chandarpur-series (Chhattisgarh, India): On stratigrphic status of the late Precambrian basins in central India; Geol. Jb. B-28, pp.23-36.

Lamoreaux,P.E.and Wilson,B., 1984 Guide to the hydrogeology of carbonate rocks. UNESCO, 345P

Lillesand,T.M. and Kieffer, R.W., 1979. Remote sensing and image interpretation., Wiley, New York. 612p

Moore, G.K., 1980. Groundwater application of remote sensing. U.S.G.S Open File Report 82-240, Eros Data Center, 55p

Murti,K.S., 1978a. Sedimentary structures from central part of the Chhattisgarh basin. Symp. on Purana Formations of Peninsular India. Center of Advanced study in Geology, University of Sagar, M.P. pp 268-275.

Murti,K.S., 1978b. A study of stromatolites of Chhattisgarh basin. Symp. on Purana Formations of Peninsular India. Center of Advance Study in Geology,

University of Sagar, Sagar, M.P., pp 276-281.

Murti,K.S., 1980. Pattern of sedimentation in the Southern part of the Chhattisgarh basin. Unpublished Ph.D Thesis, Sagar University, Sagar, 334p

Murti,K.S., 1987. Stratigraphy and sedimentation in Chhattisgarh basin. Memoir Geol. Surv. of India. pp 239-260

Nefedov,K.E., and Popova,T.A., 1969. Deciphering of groundwater from aerial photographs. Grdrometeorologichescoe press, Leningrad. 191p

Niblack,N., 1986. An Introduction to digital image processing: Printice-Hall International (UK) Ltd. 215p

Pascoe,E.H., 1963. A Manual of geology of India and Burma. Published by controller of Publications, Govt. of India, Delhi, 3rd ed. Vol.1, 484p

Pathak, B.D., 1983. Survey of Remote Sensing application in groundwater development in India. National Natural Resources Management System, Proce. of National Seminar, Hyderabad, pp II -2.1-2.22

Rampal,K.K., 1978. Text book of photogrammetry, IBH & Oxford Publishers. 300p

Rampal,K.K., 1985. Determination of Water table depths using remotely sensed data. Final Report, IIT, Kanpur, 130p

Robinove,C.J., 1965. Infrared photography and imagery in water research. Jour.of Amer. Wat. Wor. Asso. vol 57(7), pp834 - 840.

Robinove,C.J., 1966. Remote sensor applications in hydrology.

Proc. of the 4th symp. on Remote Sensing Environment, Michigan Univ., Ann. Arbor, Michigan

Sarkar,S.N., 1972. Present status of the Precambrian geochronology of peninsular India. 24th Int. Geol. Cong., Montreal, Canada, sec.1: Precambr. Geol. pp 260-272

Santosh Kumar,S., and Thiruvengalachari,S., 1981 Satellite Sensing for extraction of groundwater Resources Information. Proc.of the 5th Inter. Symp. on Remote Sensing of Environment, Vol-1, pp 569-617

Schnitzer, W.A., 1969. Zur stratigraphic and lithologic des nordiichen Chhattisgarh beckens (Zentral - Indian) unter besonderer berucksichtingung von ulgenriff Komplexenz dt. geol., Ges. 1966., 118, pp 290-295

Schnitzer,W.A., 1971. Das jungorakambrium Indians "(Purana-System)", Earlanger, Geol. Abs. 85 44p

Sharma, S.K., et.al., 1983. Groundwater targeting in Chittoor region - A remote sensing perspective. National Natural Resources Management system. Proc. of National seminar, Hyderabad, pp II-1.1 to 1.27

Siegal,B.S., and Gillespie,A.R., 1980. Remote sensing in geology. John Wiley & Sons, New York, 702p

Slater,P.N.,1979. A re-examination of the Landsat MSS. Photogrammetric engineering and Remote Sensing. Vol.45, pp 1479-1485

Stephenson,D.A., and Souto-Maior,J., 1971. Application of remote sensing to hydrogeology. Remote Sensing

Program Progress Report.,University of Wisconsin.

Swain, P.H., and Davis, S.M., 1978. Remote sensing: The quantitative approach, McGraw Hill, New York , 730p

Swain,P.H., 1972. Pattern recognition: A basis for remote sensing data analysis: LARS, Purdue Univ., Information note 111572

Thillaigovindarajan, Saleem Sontosh Kumar, and M. Jayaraman, 1980. Evaluation of hydrogeological condition in southern part of Tamil Nudu using Remote Sensing techniques. National Natural Resources Management System, Proce. of National seminar, Hyderbad pp II- pp II- 27.1 - 27.20.

Walton, W.C., 1962. Selected analytical methods for well and aquifer evaluation. Illinois State Water surv. Bull., no.49, 81p.

Walton, W.C., 1970. Groundwater resource evaluation., McGraw-Hill, New York, 664p

APPENDIX I

EVALUATION OF REMOTE SENSORS AS HYDROLOGIC TOOLS

(ROBINOV 1968)

Remote-Sensor System	General Comments on Potential value and use of Remote-Sensor System for Hydrologic Studies
Panchromatic Photography	Panchromatic photography is the most widely used remote sensing technique because of its availability and relatively low cost. Interpretive techniques are well developed and formal training of its use is available.
Multispectral Photography	Multispectral photography interpretation requires a background of spectral signature studies of terrain and water features that have not yet been made. Data returns from multispectral systems may be so voluminous that they can not be readily interpreted. Little work has been done on interpretation for hydrologic purposes.

Infrared Photography	Infrared photography is primarily of value in mapping drainage features and shorelines. The water is always black in positive print. Some vege-tation characteristics are discernible. Its most valuable use is as an adjunct to, but not a replacement for, standard aerial photography.
Colour Photography	Colour photography, in spite of its built-in spectral redundancy, promises to be a major tool of hydrologist in many special fields and is suffic-iently better for recognition of significant hydrologic features that it may replace panchromatic photo-graphy for many uses. The interpr-etation capability of the potential operational hydrologic users of colour photography must be greatly increased. Methods for spectral and density extraction of data are being developed.
Colour Infrared	Colour-infrared photography may be superior to standard phtography in some respects. It shows differences in

vegetation more clearly and provides a slightly higher contrast on water surfaces. Its general superiority to standard colour photography has yet to be proved but it may be highly useful and its worthy of much additional research.

Infrared Radiometry

Infrared radiometry is very useful for sequential measurements of changes in land and water surface temperatures because it is a simple measurement technique and data reduction is simpler than for infrared imagery. Radiometry is routinely used for periodic surveys of near shore oceanic areas.

Infrared Imagery

Infrared imagery has shown its value as a tool for measuring water surface temperature and as a means of qualitatively differentiating some terrestrial features. The lack of a simple means of determining emissivity hampers its quantitative usefulness. Analytical techniques for proper use of the reduced data need to be developed.

Radar Imagery	Side-looking airborne radar has an all weather capability for coverage of large areas. Its ability to penetrate foliage and accentuate topographic features enhances its value. Water surfaces are excellent reflectors of microwaves, resulting in a uniform black-tone image. For these reasons stream drainage systems and water surfaces are easy to identify. The black-tone precludes measuring the physical, chemical or biologic characteristics of water. Radar may be of value in terrain analysis for ground water exploration.
Microwave Radiometry and Imagery	Passive-microwave sensors measure the brightness temperature of terrain and water surfaces. Spatial resolution is lower than infrared systems but radiance is directly proportional to temperature. Probably will find greatest application in oceanic and snow-field mapping.

APPENDIX II

FEATURES THAT ARE IMPORTANT FOR MAPPING CONSOLIDATED ROCK AQUIFERS ON LANDSAT MSS IMAGES (FROM MOORE,1982)

ROCK TYPE :

1. Landform; topographic relief; erosional characteristics.
2. Outcrop pattern--banded pattern for sedimentary rocks;lobate outline for basalt flows; arcuate or faulted boundaries for igneous intrusions.
3. Drainage pattern and drainage texture (density).
4. Fracture type and symmetry (as indicated by lineaments).
5. Topographic position; steepness of slope; presence or absence of erosional terraces on hillsides.
6. Shape of ridgeline and plateau edge.
7. Type and density of vegetation cover; landuse.
8. Presence of sinkholes (visible only where occupied by water or distinctive vegetation).
9. Tone or hue; image texture.

FOLDS :

1. Ridge and valley topography; mountain, dome, and elliptical hill; short, parallel and intersecting ridge crests with V-shaped sections (complexly folded metamorphic rocks); cuesta or hogback.
2. Flatirons on dip slope and irregular topography on back

slope; parallel to dendritic drainage on dip slope and angulate or trellis drainage on back slope; uniform distribution of vegetation on dip slope and vegetation banding parallel to ridge crests on back slope.

3. Banded out crop pattern not related to topography. U-shaped to V-shaped map pattern of these ridges.
4. Trellis, radial, annular, or centripetal drainage pattern; partly developed pattern of these types.
5. Major deflection in stream channel; change in meander wavelength or change from meandering to straight or braided channel.
6. Assymmetric drainage; channel not centered between drainage divides.

LINEAMENTS :

1. Continuous and linear stream channel or valley; discontinuous but straight and aligned valleys, draws, swags, and gaps.
2. Elongate or aligned lakes,large sinkholes, and valvanoes.
3. Identical or opposite deflections (such as doglegs) in adjacent stream channels or valleys; alignment of nearby tributaries and tributary junctions.
4. Elongate or aligned patterns of natural vegetation; thin strip of relatively open (may be right-of-way) or dense vegetation.
5. Alignment of dark or light soil tones.

APPENDIX–III

Statistics for class 1 Water

Band :	1	2	3	4
Mean	34.83	15.95	14.38	12.32
Variance	96.30	65.84	261.06	24.07
Minimum	18	4	0	2
Maximum	58	30	56	20

Variance Covariance matrix

Band 1	96.30			
Band 2	55.17	65.84		
Band 3	73.94	66.43	261.06	
Band 4	14.14	19.20	37.18	24.07

Inverse Variance Covariance matrix

Band 1	0.02			
Band 2	-0.02	0.04		
Band 3	-0.00	-0.00	0.01	
Band 4	0.00	-0.02	-0.01	0.06

Correlation coefficients

Band 1	1.00			
Band 2	0.69	1.00		
Band 3	0.47	0.51	1.00	
Band 4	0.29	0.48	0.47	1.00

Statistics for class 2 Valley fill

band :	1	2	3	4
mean	47.60	32.45	37.58	28.35
variance	150.09	369.23	127.17	21.82
minimum	26	9	18	20
maximum	71	61	65	39

Variance Covariance matrix

band 1	150.09			
band 2	199.52	369.23		
band 3	37.11	57.94	127.17	
band 4	22.40	23.81	-3.90	21.82

Inverse Variance Covariance matrix

band 1	0.02			
band 2	-0.01	0.01		
band 3	-0.00	-0.00	0.01	
band 4	-0.01	0.00	0.00	0.06

Correlation coefficients

band 1	1.00			
band 2	0.81	1.00		
band 3	0.27	0.27	1.00	
band 4	0.39	0.27	-0.07	1.00

Statistics for class 3 Moisture - Stream areas

band :	1	2	3	4
mean	43.83	33.03	47.00	45.63
variance	21.12	30.74	55.08	15.63
minimum	36	24	36	38
maximum	55	47	68	50

Variance Covariance matrix

band 1	21.12			
band 2	5.41	30.74		
band 3	-0.23	8.33	55.08	
band 4	-8.56	2.37	17.10	15.63

Inverse Variance Covariance matrix

band 1	0.08			
band 2	-0.01	0.04		
band 3	-0.02	-0.00	0.03	
band 4	0.06	-0.01	-0.04	0.15

Correlation coefficients

band 1	1.00			
band 2	0.21	1.00		
band 3	-0.01	0.29	1.00	
band 4	-0.47	0.11	0.58	1.00

Statistics for class 4 Vegetation

Band :	1	2	3	4
Mean	46.50	39.53	58.03	58.77
Variance	43.64	62.36	30.23	10.38
Minimum	36	24	46	51
Maximum	59	57	73	64

Variance Covariance matrix

Band 1	43.64			
Band 2	30.83	62.36		
Band 3	16.35	25.81	30.23	
Band 4	-2.53	6.76	10.19	10.38

Inverse Variance Covariance matrix

Band 1	0.04			
Band 2	-0.02	0.03		
Band 3	-0.02	-0.02	0.06	
Band 4	0.03	-0.01	-0.07	0.17

Correlation coefficients

Band 1	1.00			
Band 2	0.59	1.00		
Band 3	0.45	0.59	1.00	
Band 4	-0.02	0.27	0.57	1.00

Statistics for class 5 Limestone

Band :	1	2	3	4
Mean	53.10	62.90	82.12	76.10
Variance	68.86	200.19	87.96	17.02
Minimum	34	21	59	68
Maximum	69	79	95	86

Variance Covariance matrix

Band 1	68.86			
Band 2	60.75	200.19		
Band 3	40.71	101.04	87.96	
Band 4	11.50	27.06	29.55	17.02

Inverse Variance Covariance matrix

Band 1	0.02			
Band 2	-0.00	0.01		
Band 3	-0.01	-0.02	0.06	
Band 4	0.00	0.01	-0.07	0.15

Correlation coefficients

Band 1	1.00			
Band 2	0.52	1.00		
Band 3	0.52	0.76	1.00	
Band 4	0.34	0.46	0.76	1.00

HISTOGRAMS FOR DIFFERENT CLASSES IN FOUR BANDS

Class identification number 1 Band sequence number 1

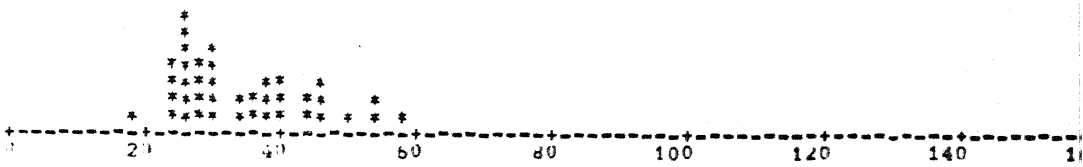

Class identification number 1 Band sequence number 2

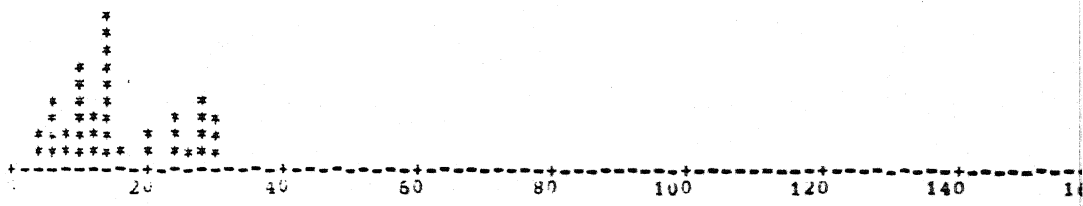

Class identification number 1 Band sequence number 3

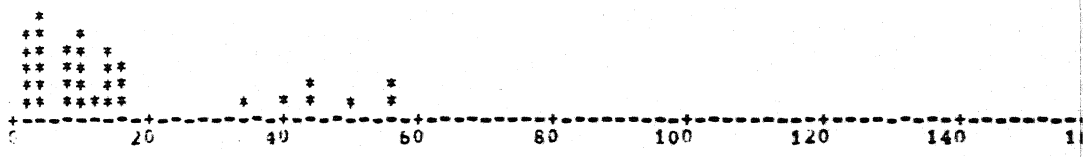

Class identification number 1 Band sequence number 4

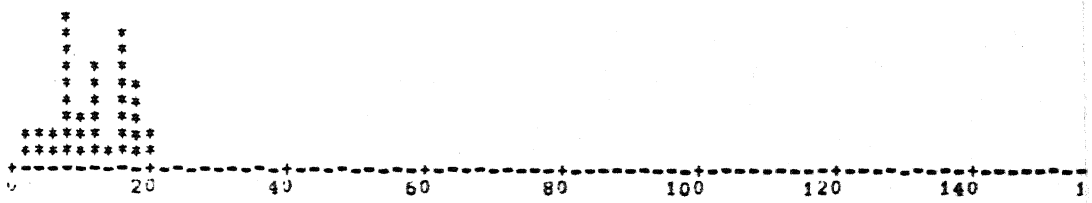

Class identification number 2 Band sequence number 1

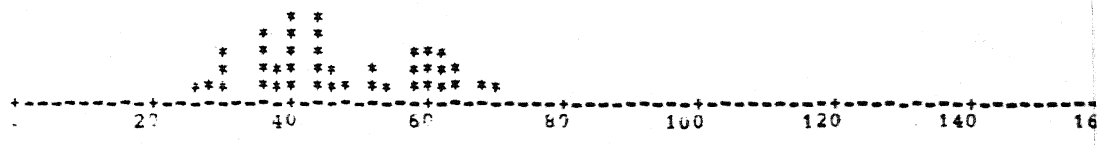

Class identification number 2 Band sequence number 2

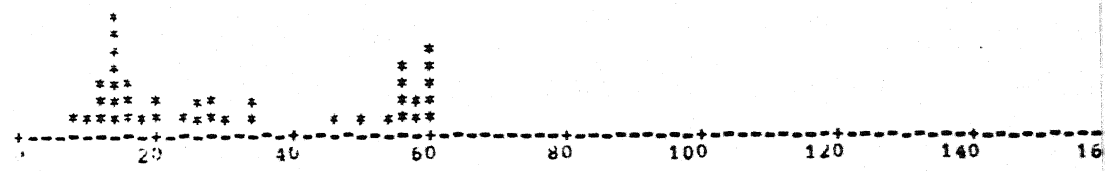

lass identification number 2 Band sequence number 3

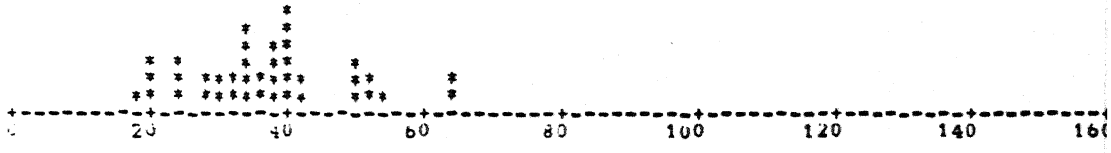

lass identification number 2 Band sequence number 4

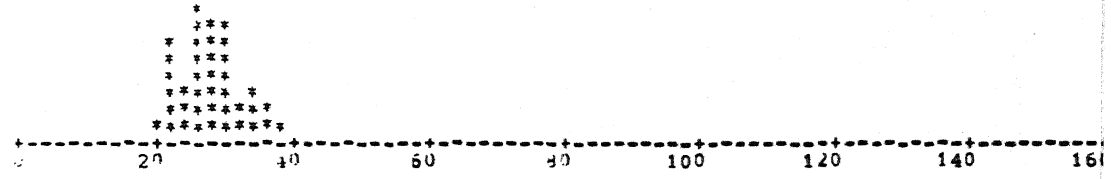

lass identification number 3 Band sequence number 1

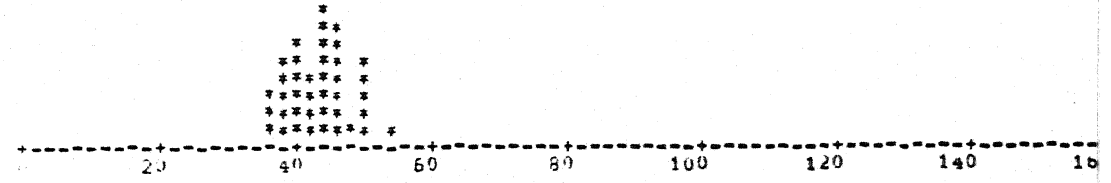

Class identification number 3 Band sequence number 2

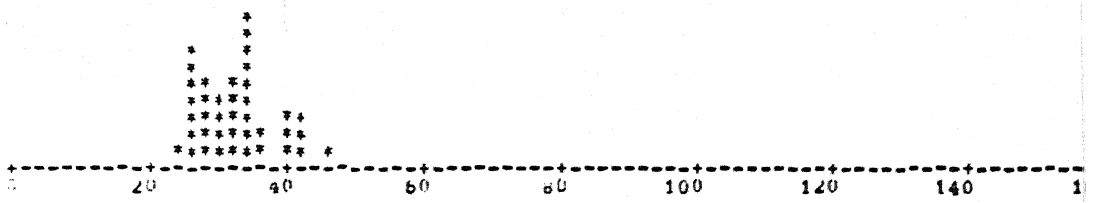

Class identification number 3 Band sequence number 3

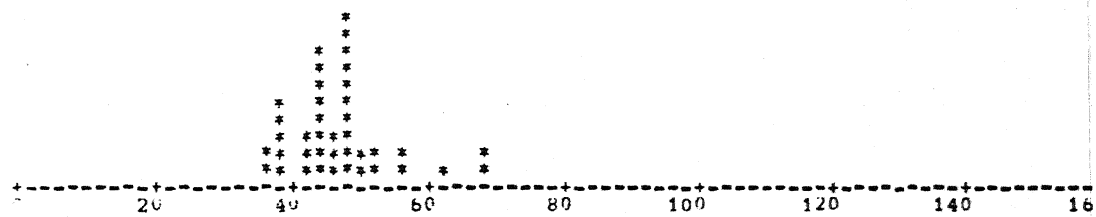

Class identification number 3 Band sequence number 4

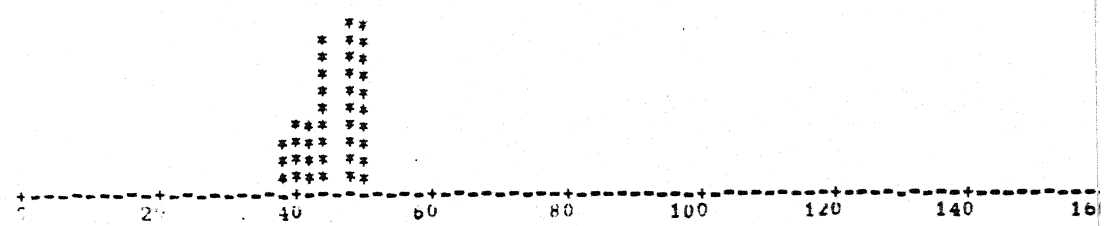

Class identification number 4 Band sequence number 1

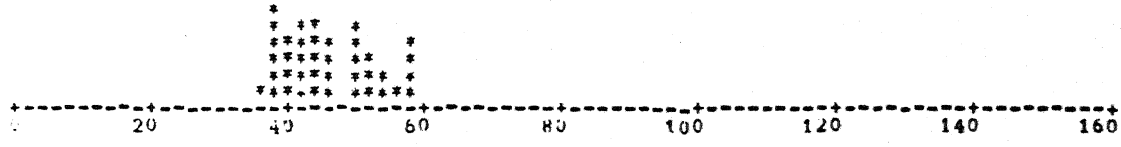

Class identification number 4 Band sequence number 2

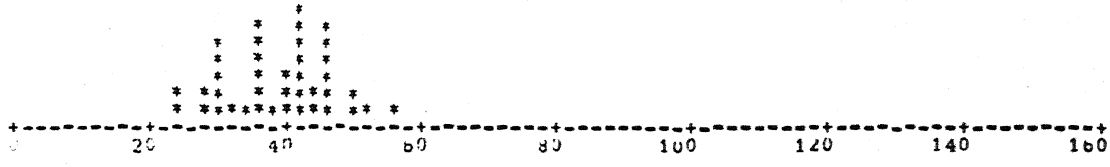

Class identification number 4 Band sequence number 3

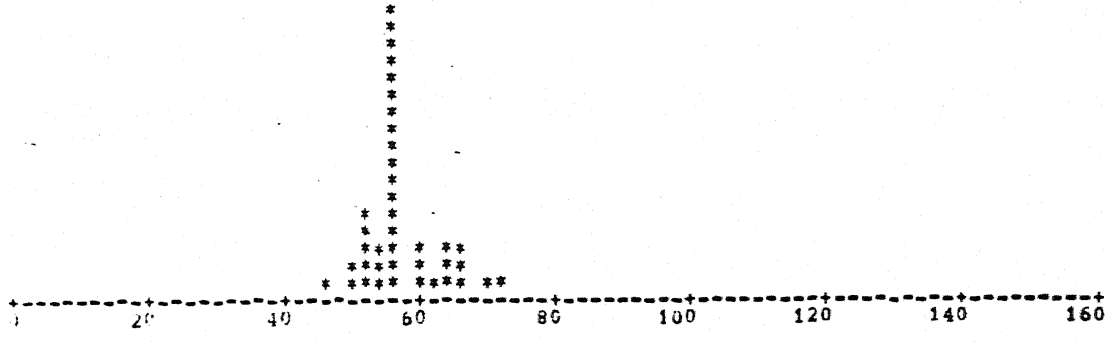

Class identification number 4 Band sequence number 4

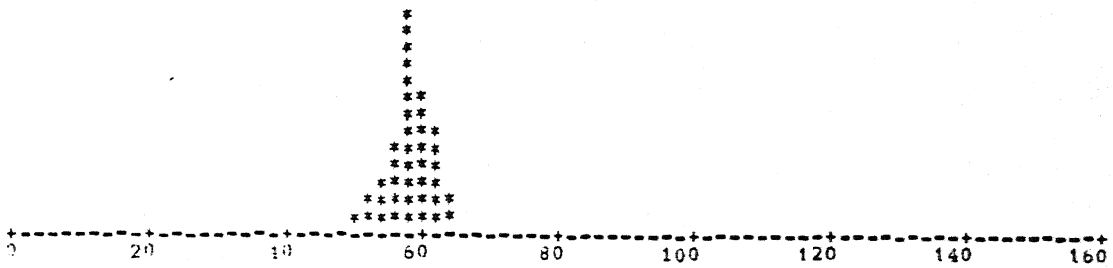

Class identification number 5 Band sequence number 1

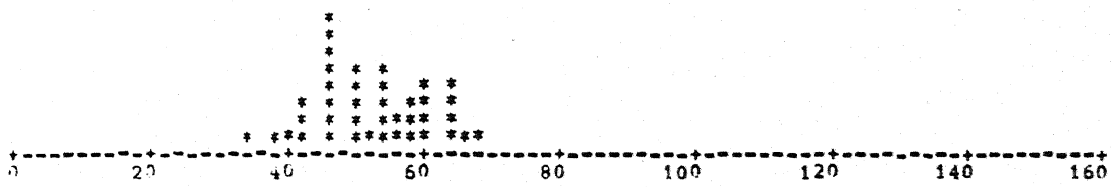

Class identification number 5 Band sequnce number 2

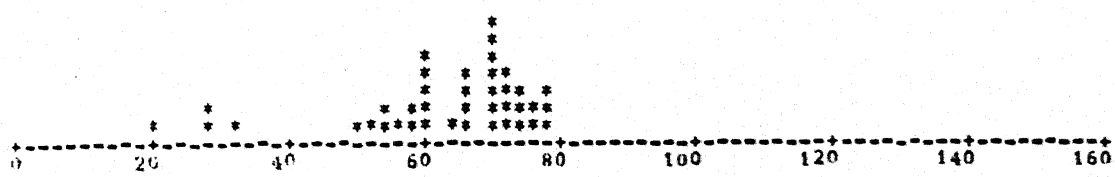

Class identification number 5 Band sequence number 3

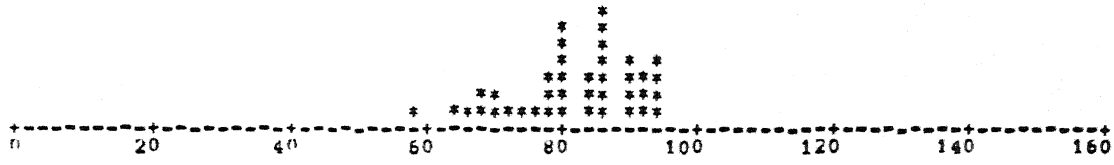

Class identification number 5 Band sequence number 4

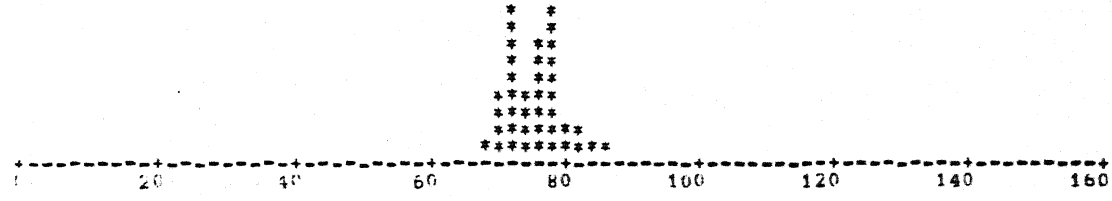

1

Confusion Matrix for training data set

	Class 1	Class 2	Class 3	Class 4	Class 5
Class 1	40	0	0	0	0
Class 2	1	39	0	0	0
Class 3	0	0	40	0	0
Class 4	0	0	0	40	0
Class 5	0	0	0	0	40

DIVERGENCE/TRANSFORMED DIVERGENCE

	CLASS 1	CLASS 2	CLASS 3	CLASS 4	CLASS 5
CLASS 1	0.00 0.00				
CLASS 2	18.69 1809.16	0.00 0.00			
CLASS 3	93.23 1999.98	35.16 1975.32	0.00 0.00		
CLASS 4	165.53 2000.00	89.74 1999.97	20.27 1841.28	0.00 0.00	
CLASS 5	239.78 2000.00	177.43 2000.00	93.53 1999.98	27.18 1933.06	0.00 0.00

APPENDIX–IV

TIME IN MINUTES THAT MUST ELAPSE FOR STRAIGHT-LINE METHOD TO BE APPLICABLE (After S.H. SIDDIQUI)

		TIME IN MINUTES FOR r_w = 0.076 m				
T m^2/day	S	10^{-4}	10^{-2}	10^{-1}	0.2	0.4
0.1242		1.250	125.24	1252.40	2504.70	5009.60
1.2420		0.125	12.52	125.23	250.47	500.95
6.2100		0.025	2.50	25.04	50.09	100.19
12.4200		0.012	1.25	12.52	25.04	50.09
62.1000		2.50×10^{-3}	0.25	2.50	5.00	10.01
124.200		1.25×10^{-3}	0.12	1.25	2.50	5.00

CHEMICAL ANLYSIS-RESULTS OF WATER SAMPLES

SNO. LOCALITY	pH	BICARBONATE HCO_3 ppm	TOTAL hardness as $CaCo_3$	Ca ppm	Mg ppm	Cl ppm	Na ppm	TDS ppm	Na absorption Ratio	Specific conductance mohs at 25°C
1. Aujuni	7.2	315.00	405.00	60.00	62.22	185.0	133.0	1152	2.6	1800.00
2. Bhatpara	7.8	355.00	325.00	52.00	47.58	120.0	181.0	1151	4.2	1800.00
3. Bhothidih	7.2	400.00	465.00	40.00	80.66	122.5	145.0	1152	2.7	1800.00
4. Maldi	7.6	260.00	265.00	82.00	14.64	72.5	7.0	576	0.17	900.00
5. Rawan	7.5	260.00	215.00	22.00	39.09	50.0	2.5	499	0.07	780.00
6. Tarenga	8.0	250.00	230.00	44.00	29.28	50.0	28.5	576	0.68	900.00
7. Jamuria	8.1	220.00	145.00	50.00	4.88	17.5	1.0	384	0.03	600.00
8. Shivanath	8.2	190.00	105.00	36.00	3.66	20.0	9.5	345	0.38	540.00
9. Kesada	7.8	225.00	175.00	36.0	20.74	15.0	4.0	345	0.12	540.00

```
**********************************************************
* This Program converts the latitudes and  longitudes *
* of a given point on the Earth's surface to its line *
* number  and  pixel  number  on  the  imagery  after *
* conversion to conical orthomorphic coordinates. The *
* constants  in this program are valid only  for  the *
* Chhattisgarh area.                                  *
**********************************************************
  IMPLICIT DOUBLE PRECISION(A-H,K-Z)
  DIMENSION LAT(150),LONG(150),LATRAD(150)
  LONG0=81.0
  LAT0=21.0*3.1415926/180.0
  A=6377277.6
  ELLIP=1.0/300.8
  ELLIP=ELLIP*ELLIP
  SIN=DSIN(LAT0)
  SINSQ=SIN*SIN
  DENOM=1.0-ELLIP*SINSQ
  N0=A/DSQRT(DENOM)
  R0=N0*((1.0-ELLIP)/DENOM)
  P=N0*(DCOS(LAT0)/DSIN(LAT0))
  RM=DSQRT(R0*N0)
  WRITE(22,18)
  READ(21,*)II
  DO 100 I=1,II
  READ(21,*)DEG1,MIN1,SEC1,DEG2,MIN2,SEC2
  LAT(I)=DEG2+MIN2/60.0+SEC2/3600.0
  LONG(I)=DEG1+MIN1/60.0+SEC1/3600.0
  LATRAD(I)=LAT(I)*3.1415926/180.0
  LONGDF=LONG(I)-LONG0
  GAMMA=LONGDF*SIN
  GAMMA=GAMMA*3.1415926/180.0
  M=RM*(LATRAD(I)-LAT0)
  M1=M**3/(6.0*R0*N0)
  TAN=DSIN(LAT0)/DCOS(LAT0)
  M2=M1*(M*TAN/(4.0*N0))
  M11=M+M1+M2
  X=(P-M11)*DSIN(GAMMA)
```

```
GAMMA=GAMMA/2.0
Y=M11+X*(DSIN(GAMMA)/DCOS(GAMMA))
A1=      -15.37834371515483
B1=       54.28787394037448
C1=X -     75235.19856468876090
A2=      -76.71755874202162
B2=      -10.81379684548759
C2=Y -    184572.45036062989400
X1=(B2*C1-B1*C2)/(A1*B2-A2*B1)
ILIN=X1+0.5
ILIN1=ILIN*4
Y2=(A2*C1-A1*C2)/(A2*B1-A1*B2)
IPIX=Y2+0.5
WRITE(22,1001)LAT(I),LONG(I),ILIN,IPIX,ILIN1
FORMAT(7X,60(1H-)//9X,'LATITUDE',6X,'LONGITUDE',4X,'LINE NO',
13X,'PIXEL NO',3X,'RECORD NO',//7X,60(1H-)/)
FORMAT(6X,F12.8,3X,F12.8,4X,I4,6X,I4,7X,I4)
CONTINUE
FORMAT(5X,'LATITUDE=',F23.16,5X,'LONGITUDES=',F23.16/)
FORMAT(5X,79(1H=)//3X,'LATITUDE',5X,'LONGITUDE',//5X,79(1H-)/)
STOP
END
```

```
C       ************************************************************
        *                                                          *
        *           INTERACTIVE  PROGRAM FOR HISTOGRAM             *
        *  Reads a full-resolution (256 in) histogram from the     *
        *  selected image refresh memory, then plots the results   *
        *  in the selected overlay plane, enabling overlay         *
        *  visibility. The process may be repeated indefinitely.   *
        *                                                          *
        *   BY:C.D.MURTY                          Date:24-5-85     *
        ************************************************************
C
        EXTERNAL IAOVLY, ICSR, IBPMA, IOPOP
C
        DIMENSION HIST(256), IHIST(256), ICHAR(1000)
C
        EQUIVALENCE (HIST(1), ICHAR(1)), (IHIST(1), ICHAR(513))
C
        JAOVLY = IADDR (IAOVLY)
        JCR = IADDR (ICSR)
        JBPMA = IADDR (IBPMA)
        JOPOP = IADDR (IOPOP)
C
        CALL IP5INI
C
        CALL SETUP
        CALL IPOKE (JOPOP, "41503)
        DO 10 I = 1, 1000
             ICHAR(I) = 0
 10     CONTINUE
        ENCODE (7, 900, ICHAR(1))
 900    FORMAT ('CHANNEL')
        ENCODE 7, 910, ICHAR(121))
 910    FORMAT ('MAXIMUM')
        CALL BLKMOV (ICHAR, IAOVLY, 1000)
        CALL IPOKE (JCSR, IOR (IPEEK (JCSR), "20000))
 20     TYPE 1000
 1000   FORMAT ('$Channel to be histogrammed (0 - 4): ')
        ACCEPT 1010, NCHAN
 1010   FORMAT (I1)
        IF (NCHAN .GT. 4) GO TO 20
        MHS = 2**NCHAN
 30     TYPE 1020
 1020   FORMAT ('$Channel for plot,bit plane: ')
        ACCEPT 1030, IPLCH, IBIT
 1030   FORMAT (2I2)
```

```
      IF (IPLCH .LT. 0 .OR. IPLCH .GT. 4) GO TO 30
      IF (IBIT .LT. 0 .OR. IBIT .GT. 7) GO TO 30
      IF (IPLCH .EQ. 4) CALL OVLINI
      MPLCH = 2**IPLCH
      MBIT = 2**IBIT
      NBIT = MBIT
      CALL OUTNBL (MPLCH)
      IF (MOD (IPLCH, 2) .EQ. 1) NBIT = ISWAB (NBIT)
      IF (MOD (IPLCH, 4) .LE. 1) CALL IPOKE (JBPMA, NBIT)
      IF (MOD (IPLCH, 4) .GE. 2) CALL IPOKE (JBPMA  2, NBIT)
      CALL FMOPER
      CALL GTHSTA (MHS, HIST)
      RMAX = 0.0
      DO 40 I = 1, 256
           IF (HIST(I) .GT. RMAX) RMAX = HIST(I)
40    CONTINUE
      SCALE = 511.99/RMAX
      DO 50 I = 1, 256
           IHIST(I) = SCALE*HIST(I)
50    CONTINUE
      DO 60 I = 1, 256
           IX = (I - 1)*2
           CALL VECTOR (IPLCH, IX, 0, IX, IHIST(I), MBIT, MBIT)
60    CONTINUE
      CALL IPOKE (JCSR, IOR (IPEEK (JCSR), "40))
      ENODE (1, 1010, ICHAR(769)) NCHAN
      ENCODE (8, 920, ICHAR(770)) RMAX
920   FORMAT (1X,F7.0)
      CALL IPOKEB (JAOVLY + 83, ICHAR(769))
      CALL BLKMVA (ICHAR(770), JAOVLY + 320, 4)
      GO TO 20
      END


*****************************************************************
*         SUBROUTINE GTHSTA (MEMORY, HIST)                      *
*****************************************************************
      DIMNNSION HIST(256), IHIST(512)
      MEMSEL = MEMORY
      CALL RDHSTA (MEMSEL, IHIST)
      DO 10 I = 1, 256
           K = I*2
           J = K - 1
           IF (IHIST(J) .LT. 0) GO TO 5
           HIST(I) = 65536.0*IHIST(K) + IHIST(J)
           GO TO 10
5          HIST(I) = 65536.0*(IHIST(K) + 1) + IHIST(J)
```

```
10      CONTINUE
        RETURN
        END
```

```
C*****************************************************************
C                                                                *
c         INTERACTIVE PROGRAM FOR BAND RATIOING                  *
C          (Using some System routines)                          *
C    (1) the memory channel containing the dividend,             *
c    (2) the memory channel containing the divisor and           *
C    (3) the  memory channel in  which  the  remainder  will     *
C        appear.                                                 *
C    The quotient overwrites the the dividend.                   *
C                                                                *
C     BY  :  C.D.MURTY                          DATE:24.5.86     *
C*****************************************************************
C
            EXTERNAL ITSTOP, IOPOP, IODPSH
            CALL IP5INI ! Set up mapping to IP-5000
            JTSTOP = IADDR (ITSTOP)
            JOPOP = IADDR (IOPOP)
            JODPSH = IADDR (IODPSH)
 1          TYPE 1010
 1010       FORMAT ('$Channels for dividend, divisor,
            remainder: ')
            ACCEPT 1020, MSQ, IDV, IRM
 1020       FORMAT (3I2)
            IF (MSQ .LT. 0 .OR. MSQ .GT. 3) GO TO 1
            IF (IDV .LT. 0 .OR. IDV .GT. 3) GO TO 1
            IF (IRM .LT. 0 .OR. IRM .GT. 3) GO TO 1
            IF (MSQ .EQ. IDV .OR. MSQ .EQ. IRM) GO TO 1
            IF (IDV .EQ. IRM) GO TO 1
            MSQ2 = 2**MSQ
            IDV2 = 2**IDV
            IRM2 = 2**IRM
            CALL SETUP
            CALL INSEL (MSQ2, 2, 0)
            CALL IPOKE (JTSTOP, "20)
            CALL IPOKE (JOPOP, "41503)
            CALL IPOKE (JODPSH, IRM2*"400 + "331)
            CALL OUTNBL (IRM2 + MSQ2)
            CALL FMOPER
            CALL INSEL (IRM2, 10, MSQ2, 4, IDV2, 1, 34)
            CALL IPOKE (JTSTOP, "2006)
            CALL IPOKE (JOPOP, "50106)
            CALL IPOKE (JODPSH, IRM2*"400 + "331)
            CALL OUTNBL (MSQ2 + IRM2)
            DO 10 ISTEP = 1, 7
            CALL FMOPER
 1          CONTINUE
            CALL IPOKE (JODPSH, IRM2*"400)
```

```
CALL FMOPER
STOP
END
```

```
00100   C*************************************************************
00200   C                                                             C
00300   C   THIS PROGRAM USES 5X5 CONVOLUTION  OPERATOR  FOR        C
00400   C   FINDING EDGES ON IMAGE DATA STORED IN SPECIFIED          C
00500   C   CHANNEL.IT CALLS SUBROUTINE 'CONVOL' FOR PERFORMING     C
00600   C   CONVOLUTION.                                            C
00700   C                                                             C
00800   C   AUTHOR:C.D.MURTY              DATE:15-JAN-1987          C
00900   C*************************************************************
01000
01100           EXTERNAL ICSR,ICBCRG,IMAGE,ITSTOP,IPPOP,IODPSH
01200           DIMENSION FACTOR(5,5)
01300           IMPLICIT INTEGER(A-Z)
01400           DATA FACTOR/1,0,2,0,1,0,4,2,4,0,2,2,-36,2,2,0.4,
                            2,4,0,1,0,2,0,1/
01500           CALL IP5INI
01600           CALL SETUP
01700           TYPE 1030
01800   1030    FORMAT('$SOURCE CHANNEL:')
01900           ACCEPT *,SCHAN
02000           TYPE 1040
02100   1040    FORMAT('$TARGET CHANNEL:')
02200           ACCEPT *,TCHAN
02300           CALL CONVOL(FACTOR,2**SCHAN,2**TCHAN)
02400           STOP
02500           END
02600   C-------------------------------------------------------------
02700   C       SUBROUTINE CONVOL                                     C
02800   C-------------------------------------------------------------
02900           SUBROUTINE CONVOL(FACTOR,ISOUR2,ITARG2)
03000           DIMENSION FACTOR(5,5),ITT(256)
03100           IMPLICIT INTEGER (A-Z)
03200           LOCAL IPOS
03300           EXTERNAL IPOP,IODPSH,ITSTOP
03400           DATA ITT/256*0/
03500           JOPOP=IADDR(IOPOP)
03600           JODPSH=IADDR(IODPSH)
03700           JTSTOP=IADDR(ITSTOP)
03800           CALL SETUP
03900           CALL ZEROM(ITARG2)
04000           CALL NBLITT(ISOUR2,2)
04100           CALL INSEL(ISOUR2,4,ITARG2,8,0)
04200           CALL IPOKE(JODPSH,"400*ITAG2+"300)
04300           CALL OUTNBL(ITARG2)
04400           DO 80 I=1,5
```

```
04500            DO 70 J=1,5
04600            IF(FACTOR(I,J).EQ.0.0)GOTO 70
04700            IXSHFT=I-5
04800            IYSHFT=J-5
04900            AFAC=IABS(FACTOR(I,J))
05000            IPOS=.FALSE.
05100            IF(FACTOR(I,J).GE.0.0)IPOS=.TRUE.
05200            DO 30 K=1,256
05300            ITT(K)=ISHFT(K-1,-5)
05400    30      CONTINUE
05500            CALL READY
05600            CALL SCRLZM(ISOUR2,IXSHFT,IYSHFT)
05700            CALL LOADIT(ISOUR2,ITT)
05800            IF(IPOS)CALL IPOKE(JOPOP,"54531)
05900            IF(.NOT.IPOS)CALL IPOKE(JOPOP,"43106)
06000            DO 60 ITIME=1,AFAC
06100            CALL FMOPER
06200    60      CONTINUE
06300    70      CONTINUE
06400    80      CONTINUE
06500            DO 90 I=1,128
06600            ITT(I)=(I-1)
06700    90      CONTINUE
06800            DO 100 I=129,256
07100            ITT(I)=(257-I)
07200    100     CONTINUE
07300            CALL READY
07400            CALL LOADIT(ITARG2,ITT)
07500            CALL NBLITT(ITARG2,2)
07600            CALL IPOKE(JOPOPP,"47517)
07700            CALL FMOPER
07800            CALL SCRLZM(ISOUR2,0,0)
07900            RETURN
08000            END
```